Development of an Engagement Mechanism for a Dual Functional Clutch Pack for Limited Slip Differential

Mohamad Bara, Yaman Zatar

Division of Sustainable Energy Systems | Department of Energy Sciences
Faculty of Engineering LTH | Lund University

2026

Master Thesis

ISRN: LUTMDN/TMHP-26/5699-SE
ISSN: 0282-1990
Published by
Department of Energy in collaboration with BorgWarner Sweden AB
Faculty of Engineering LTH, Lund University
P.O Box 118, SE-221 00 Lund

Subject: Project in Energy Sciences (MVKM01)
Division: Division of Sustainable Energy Systems
Supervisor: Martin Tuner and Hans Jacobsson from (BorgWarner Sweden AB)
Co-supervisor: Morgan Palm from BorgWarner Sweden AB
Examiner: Per Tunestål

Abstract

Limited-slip differentials (LSDs) are commonly used in high performance vehicles to improve handling by reducing differential speed and balancing torque between the driving wheels. BorgWarner develops electronically activated LSDs and Electric Cross Differentials (eXD), which dynamically control torque distribution to improve traction and vehicle performance. However, current electrically activated LSDs struggle to continuously eliminate differential speed over extended periods due to heat generation that can overload the actuator and the ECU.

To address this issue, BorgWarner proposed a dual-functional clutch pack with two clutch packs connected in series. Depending on the applied actuator force, either one clutch pack (Normal Mode) or both clutch packs (Overlock Mode) can be engaged. This allows the differential to operate as a traditional LSD in Normal Mode and as a fully locked differential in Overlock Mode.

This Master's thesis focuses on developing an activation solution for engaging the different modes depending on the applied force. A locking mechanism for maintaining clutch pressure with reduced energy consumption is also investigated.

A modified V-shaped development methodology was used throughout the project. Several concepts were generated and evaluated, after which the final concept was selected, further developed, and validated using finite element analysis (FEA). The final concept shows promising results, although further improvements are still required before all requirements can be fully satisfied.

Sammanfattning

Differentialbromsar används vanligtvis i högpresterande fordon och racingbilar för att förbättra väghållningen genom att minska skillnaden i rotationshastighet och balansera vridmomentet mellan drivhjulen. BorgWarner utvecklar elektroniskt aktiverade LSD:er och Electric Cross Differentials (eXD), vilka dynamiskt styr vridmomentsfördelningen för att förbättra grepp och fordonsprestanda. Nuvarande elektriskt aktiverade LSD-system har dock svårt att kontinuerligt eliminera differenshastighet under längre tidsperioder på grund av värmeutveckling som kan överbelasta aktuatorn och ECU:n.

För att hantera detta problem föreslog BorgWarner ett dubbelverkande lamellkopplingspaket med två kopplingspaket kopplade i serie. Beroende på den applicerade aktuatorkraften kan antingen ett kopplingspaket (Normal Mode) eller båda kopplingspaketen (Overlock Mode) aktiveras. Detta gör det möjligt för differentialen att fungera som en traditionell LSD i Normal Mode och som en helt låst differential i Overlock Mode.

Detta examensarbete fokuserar på att utveckla en aktiveringslösning för att koppla in de olika lägena beroende på den applicerade kraften. En låsmekanism för att bibehålla kopplingstrycket med minskad energiförbrukning undersöks också.

En modifierad V-formad utvecklingsmetodik användes genom hela projektet. Flera koncept genererades och utvärderades, därefter det slutliga konceptet valdes, vidareutvecklades och validerades med hjälp av finita elementanalyser (FEA). Det slutliga konceptet visar lovande resultat, även om ytterligare förbättringar fortfarande krävs innan alla krav kan uppfyllas fullt ut.

Acknowledgments

We would like to express our sincere gratitude to everyone who has supported us throughout this project.

First and foremost, we would like to thank our supervisors at BorgWarner, Hans Jacobsson and Morgan Palm, for giving us the opportunity to conduct our master's thesis at BorgWarner and for the guidance throughout the work. We would also like to thank Erik Kalen for providing guidance on specific topics, and Per Söderberg for helping us to get this opportunity.

We would like to thank our supervisor at Lund University Martin Tunér, for his guidance and constructive feedback.

Lastly we would like to thank our families for supporting us during tough times.

Lund,
January 2026

Contents

1 Introduction **9**
1.1 Introduction . . . 9
1.2 Background . . . 9
1.3 Purpose and Scope . . . 11
1.4 Delimitation . . . 12

2 Methodology **13**
2.1 Workflow Stages . . . 13
2.1.1 Decomposition and Specification . . . 13
2.1.2 Concept Synthesis and Selection . . . 14
2.1.3 Integration and Verification . . . 14

3 Theory **16**
3.1 Working Principles of an Open Differential . . . 16
3.2 Working Principle of a Limited Slip Differential . . . 19
3.3 Working Principle of BorgWarner electro-hydraulically actuated LSD . . . 20

4 Boundary Conditions **22**
4.1 Boundary Conditions . . . 22

5 Patent Research **25**
5.1 Patent Analysis and Prior Art Review . . . 25
5.2 Search Strategy . . . 25
5.3 Keywords and Search Strings . . . 25
5.4 Patent Search Results . . . 26
5.4.1 Hydraulic and Static Architectures . . . 26
5.4.2 Electro-hydraulic and Disconnect Systems . . . 26
5.4.3 Mechanical Flow Regulation . . . 27
5.5 Patent Discussion . . . 27

6 Customer requirements **28**

7 Concept Generation **29**
7.1 Belleville Friction Washer Mechanism (Concept 4) 29
7.2 Ball ramp with friction face(Concept 13) 30
7.3 Locking ring with ramps (Concept 15) 31
7.4 Push-lock mechanism (Concept 17) 33

8 Concept Evaluation **35**
8.1 Design Criteria 35
8.2 Evaluation Methodology 38
8.2.1 Concept screening 38
8.2.2 Concept Scoring 38
8.2.3 The result of the first evaluation 39
8.2.4 The result of the second evaluation 39

9 Concept Development **41**
9.1 Ball ramp with friction face(Concept 13) 41
9.1.1 Self locking of Ball Ramp 47
9.1.2 Discussion of Ball Ramp 48
9.2 Belleville Friction Washers (Concept 4) 49
9.2.1 Discussion Friction Washers 55
9.3 Locking ring with ramps (Concept 15) 55
9.3.1 Self locking of concept 15 60
9.3.2 Discussion of concept 15 61
9.4 Push lock mechanism (Concept 17) 61
9.4.1 calculation 63
9.4.2 Geometric Relations 63
9.4.3 Force Equilibrium and Friction 64
9.4.4 Final Actuation Calculation 65
9.4.5 Final Actuation Without friction 65
9.4.6 Variable Definitions 65
9.4.7 Push lock mechanism Discussion 66

10 Final Development and Design **67**
10.1 Final Development 67
10.2 Final Design 70
10.3 Result 73
10.3.1 Actuator Force 73
10.3.2 Mechanism Size 73
10.3.3 Torque Transfer 73
10.4 Discussion 74

11 FEA Simulation **77**
11.1 FEA Simulation Setup . . . 77
11.1.1 Materials and Connections . . . 77
11.1.2 Meshing . . . 78
11.1.3 Boundary Conditions and Loading . . . 79
11.2 Final Simulation Results . . . 80
11.2.1 Result Analysis: scenario 1 . . . 80
11.2.2 Result Analysis: scenario 2 . . . 82
11.3 FEA Discussion . . . 85

12 Future Development **86**
12.1 Geometry Analysis . . . 86
12.2 Functionality Simulation . . . 86
12.3 Selection of Friction Discs . . . 87
12.4 Locking Mechanism . . . 87

13 Conclusion **88**

14 Appendix **91**
14.1 Appendix A - Concepts . . . 91
14.1.1 Spring-Loaded Shaft Mechanism(Concept 1) . . . 91
14.1.2 Shaft with Conical Head Mechanism (Concept 2) . . . 92
14.1.3 Belleville Spring Washer Mechanism (Concept 3) . . . 93
14.1.4 Split Hub with springs (Concept 5) . . . 95
14.1.5 Extended Piston Architecture (Concept 6) . . . 96
14.1.6 Dual-Piston Independent Actuation (Concept 7) . . . 98
14.1.7 Separate Hubs with Compression Bushing (Concept 8) . . . 99
14.1.8 Nested Concentric Piston with Transmission Shafts (Concept 9) . . . 101
14.1.9 Dual Hydraulic Cavity and Secondary Piston (Concept 10) . . . 102
14.1.10 Hydrostatic Bearing Interface (Concept 11) . . . 103
14.1.11 Flexible Bushing Mechanism (Concept 12) . . . 105
14.1.12 Concept 14: Separation ring with spiral groove . . . 106
14.1.13 Stair Plate Activation Mechanism (Concept 16) . . . 107
14.2 Appendix B - Result of the Screening and Scoring . . . 109
14.2.1 The Result of the Screening . . . 109
14.2.2 The Result of the Scoring . . . 110
14.3 Appendix C - Project time plan . . . 111
14.3.1 Project plan Preliminary vs Actual . . . 111

List of Abbreviations

ECU Electronic Control Unit

EMA Electro-Mechanic Actuation

FEA Finite Element Analysis

HFCP High Friction Clutch Pack

NFCP Normal Friction Clutch Pack

LSD Limited Slip Differential

Chapter 1

Introduction

1.1 Introduction

Modern vehicle dynamics rest on a fundamental contradiction. For a car to accelerate effectively, its driven wheels must grip the road and transfer torque to the surface, ideally both wheels pushing equally. Yet the moment that same car enters a corner, the two driven wheels must rotate at different speeds, as the outer wheel travels a longer arc than the inner one. A rigid connection between the wheels satisfies the first demand but violates the second; a completely free differential satisfies cornering geometry but surrenders traction the instant one wheel loses grip.

This tension between traction and handling is not a new problem, engineers have grappled with it since the earliest days of the automobile. What has changed is the stakes. As vehicle performance increases and consumer expectations for both safety and driving dynamics rise, the margin for compromise narrows. The limited slip differential emerged as the engineering answer to this dilemma: a device that allows torque to be distributed intelligently between wheels, adapting to conditions rather than surrendering to them.

It is in this context that BorgWarner, one of the world's foremost suppliers of drivetrain technology, develops and refines LSD solutions that must meet the competing demands of performance, efficiency, and reliability in modern vehicles.

1.2 Background

Electronic limited slip differentials in the automotive industry are primarily used in off-road vehicles and race cars. These systems are either electrically or electro-hydraulically actuated and consist of two main rotating components: an axle shaft connected to the wheel, and a hollow shaft connected to the case of an open differential. Torque is transmitted from the hollow shaft to the axle shaft through a clutch pack, which is activated by the actuator.

By controlling the torque distribution between the driven wheels, the LSD provides the vehicle with a range of dynamic benefits, including improved traction during cornering, greater vehicle stability, enhanced cornering performance, and more effective use of engine power.

However, the current design is limited in terms of operating time. Activating the clutch pack requires a significant and continuous force from the actuator throughout the entire engagement period. This sustained load risks thermally overloading the ECU of the actuator, which restricts the duration for which both wheel sides can remain continuously locked.

To address this limitation, BorgWarner is developing a new LSD concept that introduces two clutch packs arranged in series. The first is the conventional Normal Friction Clutch Pack (NFCP), using standard friction-on-steel disc pairs as in the current design. The second is a High Friction Clutch Pack (HFCP), which uses friction disc pairs with significantly higher friction characteristics, which enable greater torque transfer for the same applied force. This dual-pack arrangement introduces two distinct operating modes: a **Normal Mode**, where only the NFCP is engaged, and an **Overlock Mode**, in which both the NFCP and HFCP are engaged simultaneously. In the overlock mode the differential effects are almost completely eliminated. The new concept aims to improve overlock performance while preserving normal LSD functionality during standard driving conditions. A schematic figure of the dual clutch pack is shown in figure 1.1.

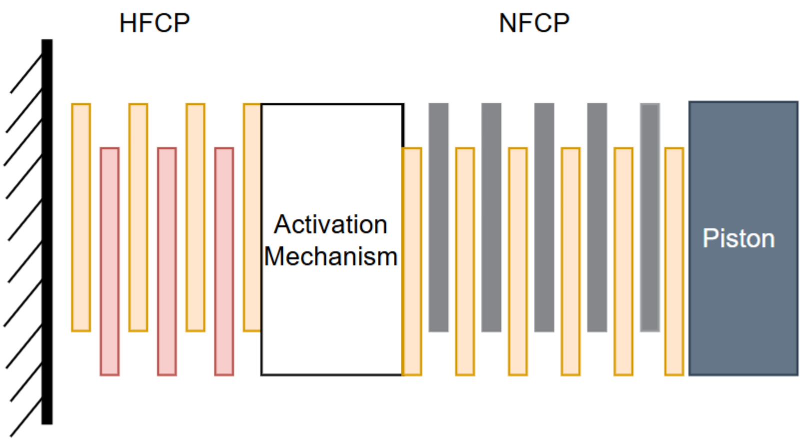

Figure 1.1: Illustrative figure for the dual functional clutch pack.

For this concept to be realized, a suitable activation mechanism must be identified and investigated. The mechanism should be positioned between the two clutch packs and capable of independently activating either the normal or overlock mode. Furthermore, since minimizing power consumption is a key requirement in modern vehicles, particularly electric and hybrid platforms, the preferred solution should incorporate a self-locking capability. This would allow the clutch packs to remain engaged without continuous actuator operation. This will minimize the power consumption as the actuator will be used during engagement and disengagement of the clutch pack only, thereby significantly reducing overall energy consumption.

1.3 Purpose and Scope

The aim of this thesis is to propose a concept for an activation mechanism for a dual-functional clutch pack system, capable of engaging either one or both clutch packs independently. In addition, the thesis investigates the feasibility of incorporating a self-locking mechanism into the proposed concept. To fulfill this purpose, the following objectives have been established:

- Generate concepts that can serve as viable activation solutions for the dual-functional clutch pack system.
- Evaluate the generated concepts and further develop the most promising candidates.
- Re-evaluate the developed concepts based on refined criteria and engineering judgment.
- Create a detailed design for the most promising concept.
- Validate the final design through FEM analysis and evaluate the overall performance of the LSD system.

1.4 Delimitation

This thesis focused exclusively on product development of a working activation solution for the LSD. Furthermore, an insight of a self-locking solution will be considered. Since the time of the thesis is limited to 20 weeks, some delimitations have been made.

- Physical wear, heat generation, and vibrations will not be included
- Cost analysis is excluded.
- The activation of the clutch pack is done by an electro-hydraulic actuator.
- Design of manufacturing is excluded.
- The system analyses will assume a steady state.

Chapter 2

Methodology

The original V-model is a software development framework. The horizontal axis represents the progression of time or project completion from left to right, while the vertical axis reflects the level of abstraction, with more abstract concepts at the top. The left side of the V-model consists of top-down verification phases, where the system is gradually refined into more detailed components. The right side consists of bottom-up validation phases, where these components are tested and integrated. Each verification phase on the left has a corresponding validation (testing) phase on the right [1].

In this master thesis, a modified V-shaped model will be used. This will mainly enable rapid product development, ensure structured verification and validation, and break down the complexity of the work into manageable components. In this work, the left branch of the V-shaped model is Decomposition and Specification, while the right branch is Integration and Verification. Unlike the traditional V-model, this project incorporates an iterative "interim loop" at the base, allowing for the analytical screening and refinement of mechanical concepts before moving toward detailed verification. Figure 2.1 gives an illustration of the method, and the next section gives an explanation of the method.

2.1 Workflow Stages

2.1.1 Decomposition and Specification

The downward slope of the V-model focuses on decomposing high-level project goals into specific, measurable technical constraints. The phases in the left branch are:
Discovery phase: The project commenced with an extensive literature review of open and Limited Slip Differentials (LSD). This stage established a foundational understanding of the mechanical working principles and the underlying physical and mathematical frameworks. Internal BorgWarner documentation was analyzed to extract boundary conditions and operational constraints specifically for the activation mechanism.

Define Phase: Insights from the Discovery phase were translated into quantifiable Key Design Criteria (KDC). These criteria serve as the benchmarks for design success. A concurrent patent study was conducted to identify the current state-of-the-art and ensure the novelty of the design.

2.1.2 Concept Synthesis and Selection

At the vertex of the V-model, the project transitions from theoretical requirements to physical architectural solutions.

Concept Generation: Multiple concepts that can possibly solve the problem and work as an activation mechanism were generated.

Initial Screening: Concepts were filtered using Screening and Scoring Matrices (e.g., Pugh Matrix) based on the established specifications and customer requirements. This ensured that only the most viable candidates, according to the predefined specification phase, proceeded to technical development.

2.1.3 Integration and Verification

The upward slope of the V-model focuses on the Integration and Verification of the chosen concept and its verification against the initial requirements.

Detailed Development: To mitigate the risk of selecting a non-functional architecture, an iterative development stage was implemented. Promising concepts underwent design optimization and analytical calculations to illustrate the working principle clearly. A second, more rigorous scoring matrix was then applied to select the final concept for delivery.

Delivery Phase: In the final phase, the chosen concept was further developed and evaluated against the original requirements and boundary conditions. This confirms that the proposed activation mechanism is functionally suitable for the BorgWarner generic-LSD.

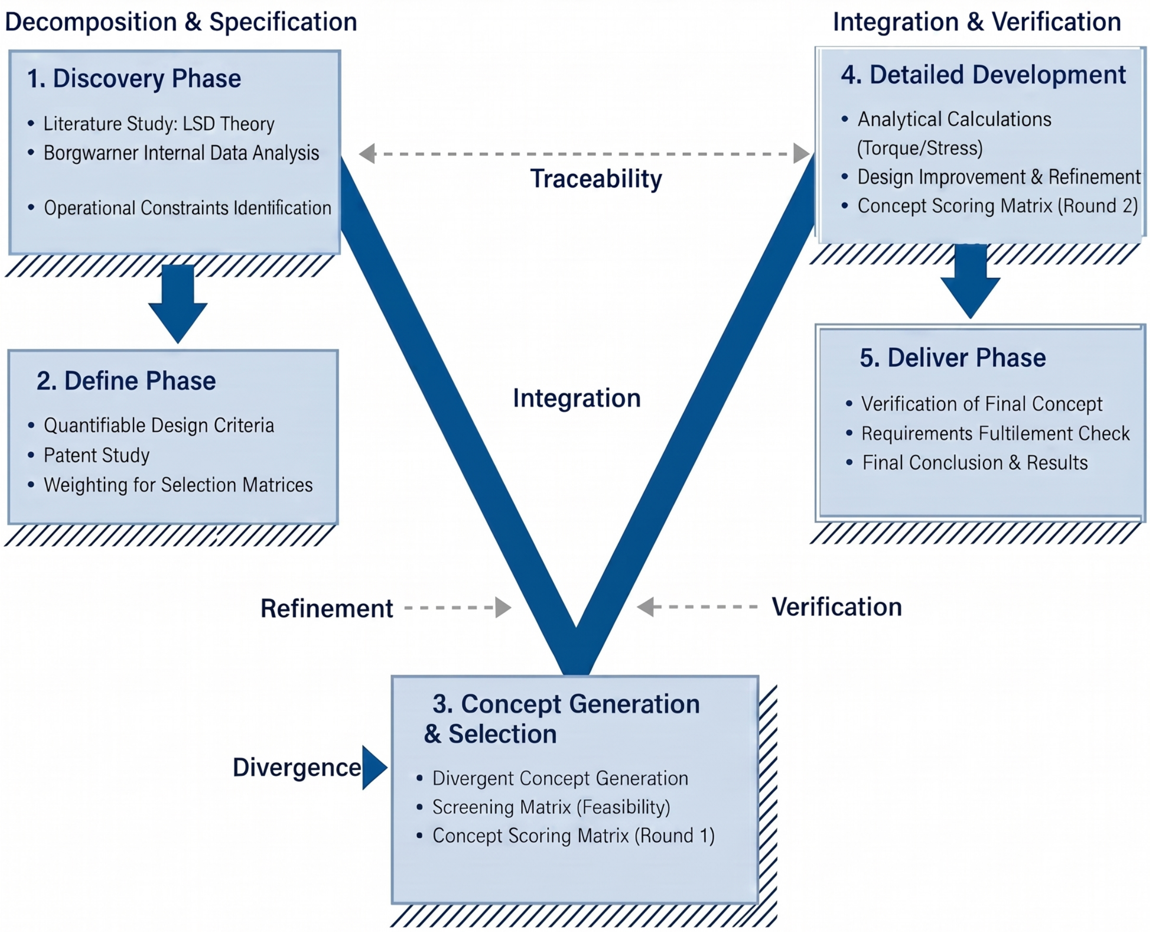

Figure 2.1: A schematic figure of the V-shape method used in this project

Chapter 3

Theory

The differential is one of the central components in the vehicles. Its main function is to allow the different angular velocity of the wheel while maintaining the driving torques. This function is crucial for vehicles, especially in turns where the outer wheels in a corner travel a longer distance than the inner wheels. Thus the outer wheel has to rotate faster than the inner wheel, while they have to maintain the tractive torque. Even during straight-line driving, variations in tire dimensions, inflation pressure, wear, and road irregularities lead to differences in wheel rotational speeds. Under these conditions, the driving torques at both output shafts must remain equal. Any torque imbalance would produce unequal tractive forces, thereby compromising driving stability 2. In this chapter, a brief explanation of the working principle of Open Differential, Limited Slip Differential, and BorgWarner's generic LSD that will be considered in this thesis.

3.1 Working Principles of an Open Differential

The two wheels on a driven axle must be connected so that one engine and transmission can drive both of them. The mechanism that connects the two wheels on the same axle is called a differential[5]. As previously mentioned the main function of open differential is to allow the different angular velocity of the wheel. The main components of the open differential are the ring bevel gear, side bevel gears, spider bevel gears and the casing. A schematic view of the open differential in figure 3.1.

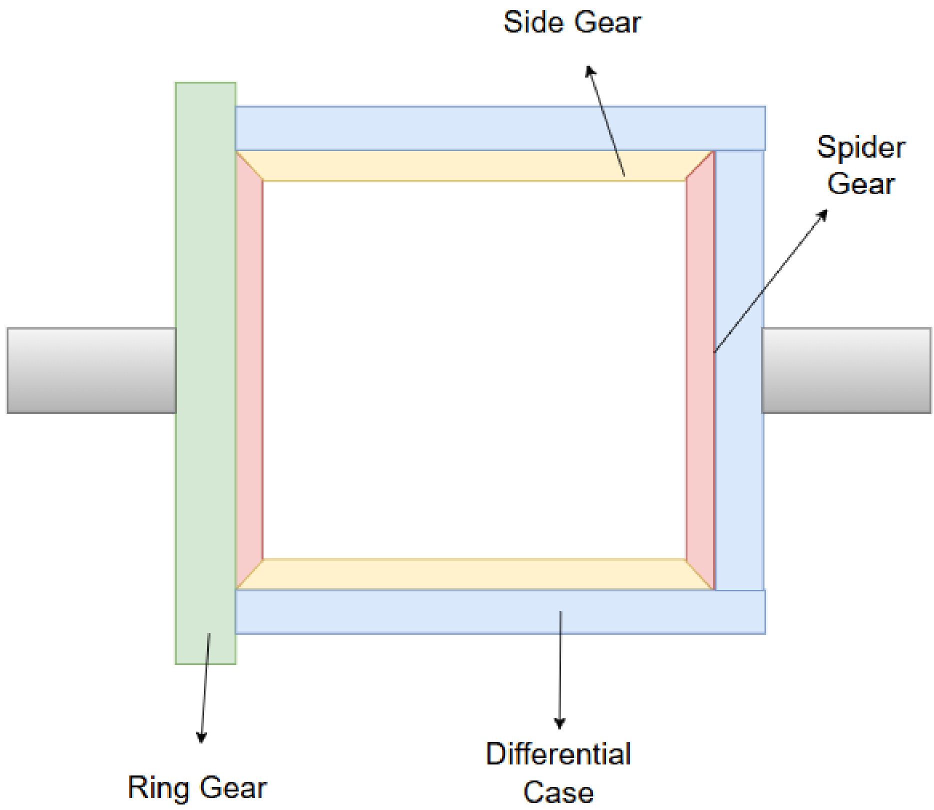

Figure 3.1: A schematic figure of the open differentials bevel gears.

In open differential, the ring gear is bolted to the differential case. When the driveshaft rotates, it turns the ring gear and therefore the whole case. Inside the case, the spider gears sit on a pinion shaft. They are carried around by the cage and mesh with the two side gears, which are splined to the left and right axle shafts. When both wheels have the same resistance (straight line driving), the spider gears do not spin on their own axis, they just orbit with the case, so both side gears are forced to rotate at the same speed. When one wheel needs to rotate faster (in turns), the speed difference appears between the two side gears. The spider gears then begin to spin on their own axis while they orbit with the case, so one side gear speeds up and the other slows down, but the torque is still split equally [3][4].

A free body diagram of the open differential is shown in figure 3.2. For the open differential to allow angular speed difference, the differential must fulfill a specific kinematic relation called Willis formula[5], and it is given by:

$$\frac{\omega_3 - \omega_h}{\omega_4 - \omega_h} = -1 \tag{3.1}$$

where ω_h gives the angular velocity of the housing of the differential. The Willis formula can be rewritten to

$$\omega_h = \frac{\omega_3 + \omega_4}{2} \tag{3.2}$$

The force and torque equilibrium applied on the spider gear, and a torque equation applied to the side gear give the following equation:

$$M_3 = M_4 = \frac{M_{FD}}{2} \tag{3.3}$$

Where M_3 and M_4 are the torques on each side, and M_{FD} are the driving torque on the ring gear[4]. This basic equation shows that the input torque arriving at the drive wheel is always distributed symmetrically to both axle and drive shafts.

Equation 3.3 and 3.2 are the governing equations of the open differentials, and this shows that the torque is equally distributed between the wheels and that the speed of the differential cage is just equal to the average speed of the two axle shafts [4][5].

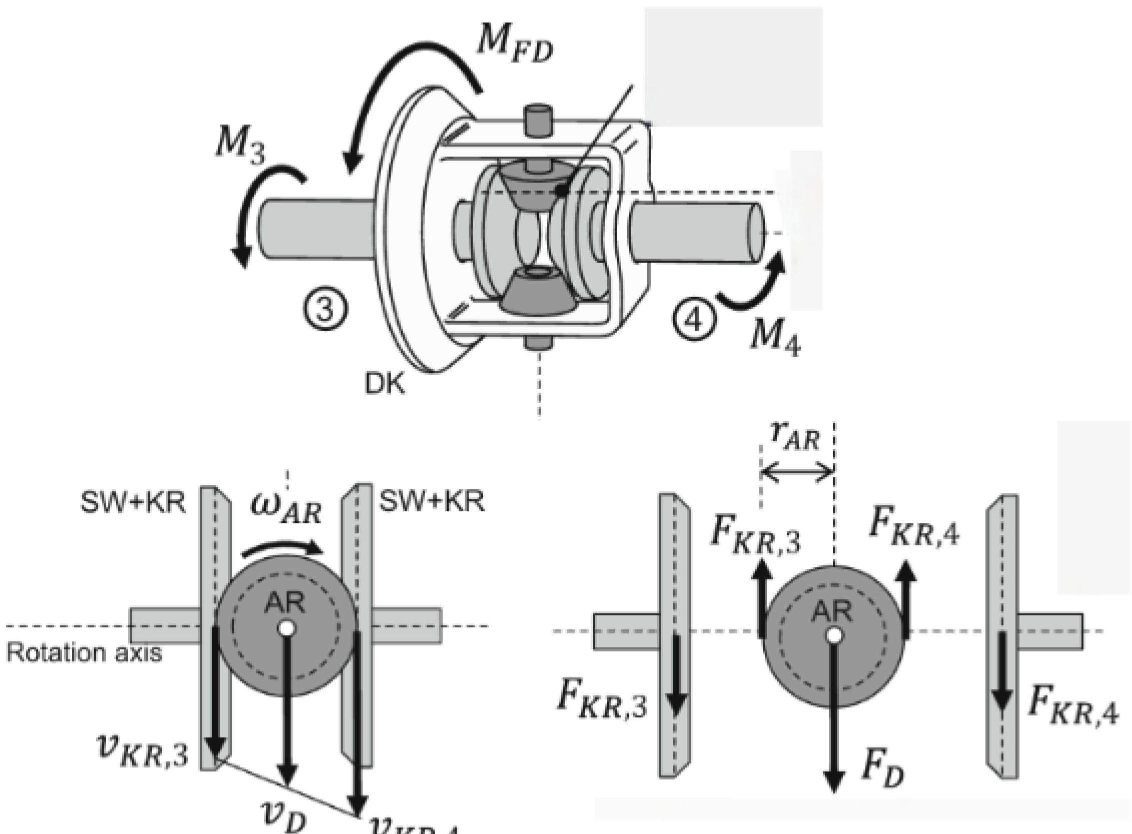

Figure 3.2: Free body diagram of open differential, DK: Differential cage/ SW: drive shaft, 3 left, 4 right / KR: Side gear / AR: spider gear[4].

When one wheel is on a slippery surface and the other is on dry asphalt, the open differential's equal torque split becomes a problem. Both wheels receive the same torque, but the wheel on the slippery surface reaches its traction limit first and starts spinning. Because the torque is equal, the wheel on the high-grip surface is limited to the same low torque. As a result, the vehicle cannot take full advantage of the wheel with good traction, struggles to accelerate. To overcome this problem, the Limited Slip Differential was introduced [4][5].

3.2 Working Principle of a Limited Slip Differential

A limited-slip differential (LSD) based on a clutch system combined with an open differential offers the ability to cover the full spectrum between a standard open differential and a solid spool. This type of passive LSD can be highly effective in high-performance applications, such as sports and racing cars, by improving traction, enhancing vehicle balance, and increasing stability during dynamic driving conditions. One of the fundamental features of the LSDs is that they do not obey equation 3.3 [5] [6].

The most common LSD type in road vehicles, sports cars and racing vehicles is the Torque sensitive devices clutch pack based, a schematic figure for this type of differential and for its internal parts is shown in figure 3.3. In this system, the differential case (2) transmits torque to the satellite gear pins (6) through side rings (11). Each pin interacts with a pair of inclined surfaces, known as ramps (3). The ramp geometry generates a wedging force that pushes the side rings apart, creating a contact force proportional to the input torque and the cotangent of the ramp angle σ. This force presses the rings against one or, usually, two wet clutch packs situated between each ring and the differential carrier (8 and 9), which produce the friction torque given by

$$M_f = \frac{\mu n (R_y + R_i) F}{2} \tag{3.4}$$

where μ is the friction coefficient, n is the friction faces, F is the applied force, R_y and R_i is the outer and inner radius respectively[6][7].

The frictional torque brakes the faster-rotating side and accelerates the slower rotating side, reducing the differential action. For torque equilibrium to be maintained, a greater portion of the torque is transmitted to the wheel with better traction [4][5].

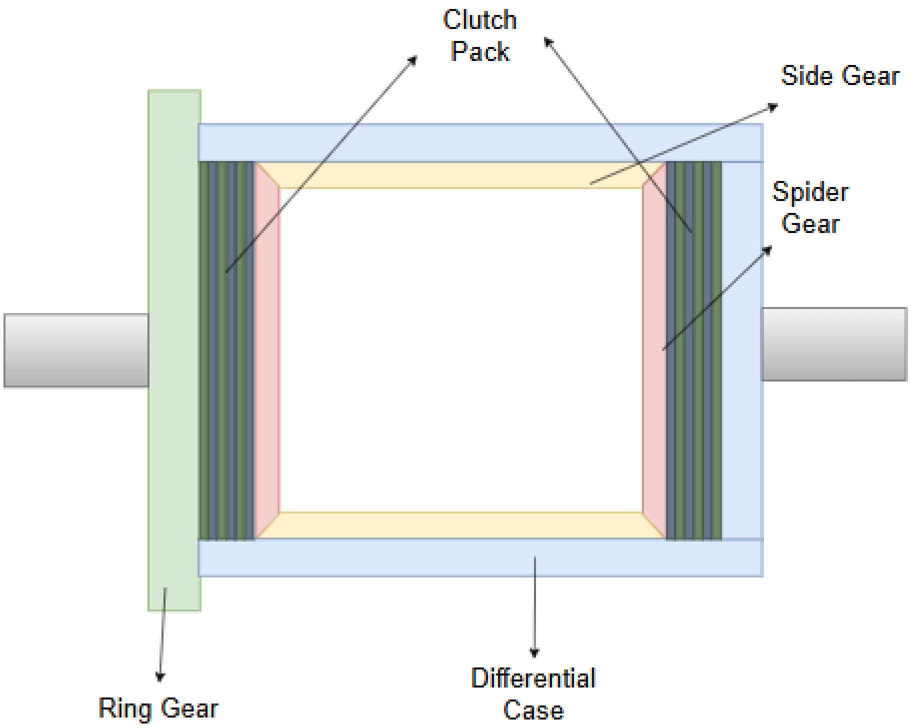

Figure 3.3: Schematic figure of the Limited Slip Differential.

3.3 Working Principle of BorgWarner electro-hydraulically actuated LSD

The differential that was discussed in the previous section is the passive differential. One of the most advanced differentials is electronically controlled limited slip differentials, especially active systems. In active LSDs, the locking torque is generated using external energy sources such as electrohydraulic, electromechanical, or electromagnetic actuators. This means the system does not rely on driving conditions to create locking, it can apply any desired amount of locking torque at any time, regardless of wheel slip, speed differences, or engine torque. Because of this full controllability, active systems can continuously adapt to changing driving conditions using sensor data and control units. This allows for highly optimized vehicle behavior in terms of traction, stability, and driving dynamics.[4].

As previously mentioned, a limited slip differential operates by generating frictional torque between its rotating components. In the hydraulically actuated design shown in Figure 3.4, this effect is produced by a disc pack located between the differential housing and the right side gear or the right axle shaft.

To allow the limited slip differential to be mounted outside the gearbox, the differential cage is extended by a hollow shaft that is connected to the cage through a spline. The discs are splined so that they can move axially while remaining fixed in rotation relative to their associated components. The steel discs engage with the hollow shaft, whereas the friction discs connect to the axle shaft, which can be recognized from the opposite orientation of their teeth.

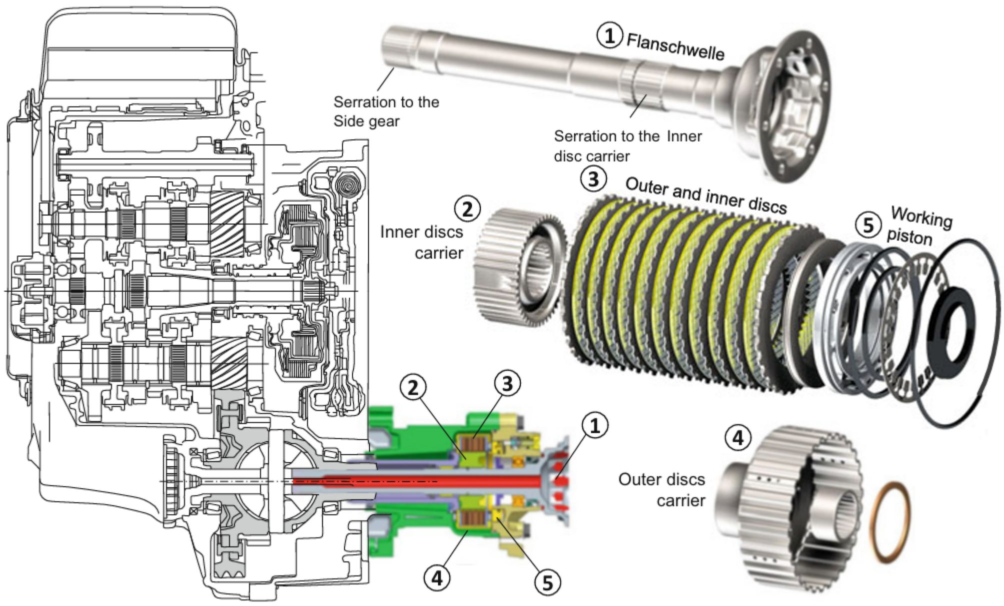

Figure 3.4: Design of a hydraulically actuated limited slip differential for a front-wheel-drive trans verse engine vehicle. [4].

A working piston compresses the disc pack and applies pressure through an axial needle bearing. The hydraulic pressure required for this action is supplied by a pump and controlled by a valve when necessary. The resulting frictional torque is proportional to the applied hydraulic pressure as shown in equation 3.4. This torque breaks the faster rotating component while accelerating the slower one, thereby reducing the speed difference and partially or completely limiting the differential action between the wheels, and thereby transferring torque from the faster rotating wheel to the slower rotating wheel [4].

It should be noted that the system is not symmetrical, and the torque transfer takes different paths depending on which wheel has higher angular speed. This is described in detail in pages 356-362 in [4].

Chapter 4

Boundary Conditions

In this chapter, an analysis of the LSD will be conducted with the objective of determining the operational boundary conditions of the system. Since the main limitation lies in the ECU, which heats up when the actuator operates at high capacity, a safe operating limit for the actuator will be calculated and considered during the development stage.

4.1 Boundary Conditions

The LSD discussed above consist of several minor subsystems, which are the actuator that consist of an electric motor and pump, a piston and a clutch pack, as a schematic figure for the system is shown in figure 4.1. An energy loss between the input and output of each subsystem due to friction, temperature, and deformation is assumed. To compensate for that loss, each subsystem assumed to have an efficiency η.

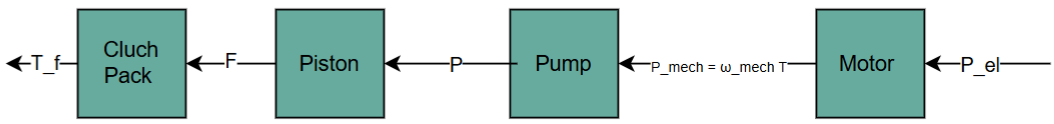

Figure 4.1: A flow diagram for the subsystems in the LSD

To facilitate a clear understanding of the subsequent derivations, Table 4.1 defines the physical quantities and their respective units used throughout this section. The relation between the electrical power to motor, and the output mechanical power is given by the following power balance

$$P_{el} * \eta_m = P_{mech} \tag{4.1}$$

Name	Symbol	Unit
Electrical Power	P_{el}	Watt (W)
Motor Efficiency	η_m	Dimensionless
Mechanical Power	P_{mech}	Watt (W)
Angular Velocity	ω	rad/s
Torque	T	Nm
Hydraulic Power	P_{hyd}	Watt (W)
Pump Efficiency	η_p	Dimensionless
Pressure Difference	Δp	Pascal (Pa)
Volume Flow Rate	Q	m^3/s
Pump Displacement	D	m^3/rad
Piston Area	A	m^2
Force	F	Newton (N)

Table 4.1: System Variables and Units

Where η_m is the efficiency of the motor. This relation can be written as

$$P_{el} * \eta_m = \omega T \tag{4.2}$$

Where T is the output torque and ω is the angular velocity of the output shaft.The power balance between the pump and the pump output gives

$$P_{hyd} = \eta_p P_{mech} = \eta_p * P_{el} * \eta_m \tag{4.3}$$

Where P_{hyd} is the hydraulic power and it is given by

$$P_{hyd} = \Delta p Q \tag{4.4}$$

Δp is pressure difference and Q is the volume flow rate given by

$$Q = D\omega \tag{4.5}$$

D is displacement of the pump (m^3/rad) and it is design parameter of the pump.
By substituting equations 4.2, 4.4 and 4.5 in 4.3, and by utilizing the fact that the pump and the motor sits on the same axle, the following equation yields

$$\Delta p = \frac{\eta_p T}{D} \tag{4.6}$$

Thus, the force that pressurize the clutch pack is given by

$$F = \frac{\eta_p T A}{D} \tag{4.7}$$

Where A is the area of the piston. Consider now that the motor has a maximum torque T_{max} and safe torque limit T_{safe} where T_{safe} can be used without thermally overloading the actuator. That yields that the portion of the force that can be used without thermally overloading the actuator over time is given by

$$\frac{F_{safe}}{F_{max}} = \frac{T_{safe}}{T_{max}} \tag{4.8}$$

The data needed to calculate the fraction 4.8 has been estimated by BorgWarner based on **ONE** experimental test at a specific ambient temperature is

$$\frac{F_{safe}}{F_{max}} = 0.70 \tag{4.9}$$

A more conservative ratio will be used so that

$$\frac{F_{safe}}{F_{max}} = 0.5 \tag{4.10}$$

Chapter 5

Patent Research

5.1 Patent Analysis and Prior Art Review

The patent search constitutes a critical phase of this thesis, serving two purposes. First, it ensures that the proposed designs do not infringe upon existing intellectual property (IP). Second, it provides technical inspiration for the Concept Generation phase by identifying established and emerging mechanical architectures.

To manage the volume of search results and maintain technical relevance, the following criteria were established:

- **Inclusion Criteria:** Patents filed within the last 20 years; mechanisms specifically addressing compact "dry" or "wet" clutch packs; and solutions involving electromechanical or hydraulic-to-mechanical power conversion.
- **Exclusion Criteria:** Heavy-duty industrial machinery clutches and purely software-based control logic patents lacking specific mechanical claims.

5.2 Search Strategy

The primary search was conducted using Google Patents due to its robust indexing and the accessibility of high-resolution technical diagrams. While the search focused on a 20-year window (2006–2026) to capture modern dual-clutch technologies, foundational patents exceeding this age were selectively reviewed to understand the mechanical evolution of ball-ramp and hydraulic pressure-ring mechanisms.

5.3 Keywords and Search Strings

The search utilized a combination of specific technical keywords and Boolean operators to refine the results. Key terms included:

- "Dual-clutch activation mechanism"
- "LSD clutch pack"
- "Electromagnetic clutch actuator"
- "Hydraulic piston differential"
- "Ball-ramp activation mechanism"

5.4 Patent Search Results

While no single patent was identified that directly restricts the specific embodiments discussed in this thesis, several documents provided critical architectural inspiration for the Concept Generation phase.

5.4.1 Hydraulic and Static Architectures

Patent US8596436B2: "Idle-able auxiliary drive system"
This patent describes a power transfer unit (PTU) utilizing a hydraulically actuated piston assembly to provide axial force on a clutch pack. Upon receiving actuation force, the torque-transferring clutch causes the inner housing to rotate, facilitating power engagement. 10

Patent US3390593: "Traction Equalizer"
Originally introduced as a foundational architecture in limited-slip differential (LSD) design, this system utilizes a pair of spring-loaded clutches to maintain a normally locked state between the side gears and the differential casing. Unlike modern torque-sensing mechanisms, the clamping force is static and functions independently of engine torque. Integrated retainers are employed to secure the clutch discs, preventing axial misalignment during high-speed rotation. 11

5.4.2 Electro-hydraulic and Disconnect Systems

Patent US10378633B2: "Electronic limited-slip differential with separation of clutch and actuator"
This patent outlines a classic electro-hydraulic LSD architecture where a standard open-gear set is enhanced by an integrated friction-control system. A pair of pinion gears is mounted on a cross-shaft to distribute torque between two side gears. To manage wheel-speed differentiation, an actuator assembly containing a piston is positioned to compress a clutch pack of interleaved annular plates. When activated, the axial force "locks" the side gear to the differential casing, transferring torque to the wheel with higher traction.12

Patent US11231098B2: "Differential disconnect assembly"
This design addresses parasitic drag by using a spline ring to act as a mechanical bridge between the ring gear and the internal gear nest. When all-wheel drive is not required, the actuator moves the spline ring to physically disconnect the ring gear. This allows the internal components to come to a complete stop while the wheels spin, significantly improving fuel economy. This provides a reference for potential disengagement strategies for dual-clutch packs.13

5.4.3 Mechanical Flow Regulation

Patent CN108374846B: "Clutch assembly for a drive train"
This patent demonstrates the integration of a mechanical flow regulator into an electromechanical ball-ramp actuator. To reduce the drag losses typical of wet clutches, this solution uses the axial travel of the pressure plate to physically throttle the oil supply via a Z-shaped setting member. This ensures maximum cooling only during slip conditions and minimizes parasitic drag during open states.14

5.5 Patent Discussion

A comprehensive search was conducted to identify any existing IP that might interfere with the proposed activation mechanism. The review concluded that no patents currently pose a technical or legal limitation to the study. Conversely, established benchmarks from industry leaders like BorgWarner regarding friction material interfaces and LSD architectures provide a validated technical foundation. These existing designs serve as a springboard for the unique mechanical integration proposed in the following chapters.

Chapter 6

Customer requirements

Several requirements were provided from Borgwarner in accordance to the OEM customer to be maintained within the scope of the thesis. Some of the requirements are presented in table 6.1. Due to confidentiality, numbers are not specified.

Requirement	**Symbol**	**Value**
Dynamic pack Torque	T_{HFCP}	Newton Meter (Nm)
Static Pack Torque	T_{NFCP}	Newton Meter (Nm)
Accumulated Torque	T_{Total}	Newton Meter (Nm)
Hydraulic Force Range	F_p	Newtons (N)
Max length of Activation Mechanism	a	Millimeters (mm)

Table 6.1: Customer requirements values

The main specifications were the amount of torque that is required from each clutch pack. The Normal friction pack under normal conditions, and the over locked mode where the torque required is the sum of torque from the HFCP and NFCP combined (Accumulated Torque).

Chapter 7

Concept Generation

7.1 Belleville Friction Washer Mechanism (Concept 4)

Working principles: This innovative concept replaces conventional friction plates within the High-Pressure Friction Clutch Pack (HFCP) with specialized Belleville friction washers. These conical discs utilize a hybrid surface geometry: the outer edges are curved and treated with a low-friction coating, while the central annular section features a flat profile lined with high-friction material. Under low axial loads, the curved edges facilitate a "slip" state with minimal parasitic resistance. Upon reaching a calibrated force threshold, the washers undergo elastic deformation toward a flattened state, bringing the high-friction central zones into full contact to lock the pack and enable torque transfer. A schematic figure for the concept and the assembly of the discs is shown in figure 7.1.

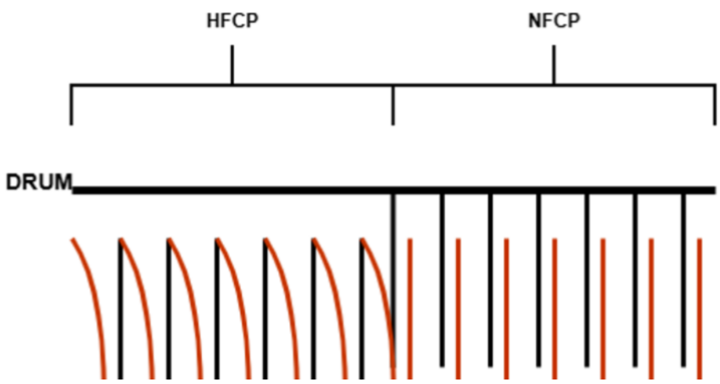

Figure 7.1: Hybrid Belleville washer assembly.

Advantages:

- **Integrated Functionality:** By consolidating the spring biasing element and the friction interface into a single component, the necessity for independent actuation linkages is eliminated.

- **Spatial Efficiency:** This design is exceptionally compact, significantly reducing the axial footprint of the clutch assembly by removing the need for dedicated spring seats.
- **Simplified Architecture:** The multifunctional nature of the component reduces the total part count, potentially streamlining the assembly process and reducing the bill of materials (BOM).

Disadvantages:

- **Manufacturing Complexity:** Applying high-friction linings to a flat center and low-friction coatings to a curved edge on a single disc presents a significant production challenge, likely requiring advanced additive manufacturing or specialized bonding techniques.
- **Extensive R&D Requirements:** This approach necessitates a comprehensive study into differential material wear rates, heat dissipation characteristics, and the tribological transition phase between the "slip" and "grip" states.

Technical Summary: The design proposes a dual-material Belleville washer that acts as both the spring and the friction interface. By utilizing low-friction curved edges for the 'open' state and a high-friction central band for the 'compressed' state, the mechanism achieves passive engagement based on axial load. While this saves considerable space, the primary hurdles remain the specialized manufacturing of the friction gradients and the need for a dedicated housing to manage the unconventional plate geometry.

7.2 Ball ramp with friction face(Concept 13)

Working principles: This concept consists of four main parts: a movable plate, a fixed plate, a friction face (clutch pack), and a ball ramp. All of these parts are fitted between the clutch packs. A schematic drawing of the concept is shown in Figure 7.2. The movable plate is used to transfer axial force and torque. The fixed plate is used to lock the NFCP and enable the activation of the normal mode. The friction interface acts as a torque-limiting element that transmits torque to the ball ramp mechanism. The ball ramp opens when it receives a specific magnitude of torque, which is dependent on the input force. When the ball ramp opens, its axial position increases, which causes the NFCP, the HFCP, and all the parts between them to be pressed against each other. As a result, the HFCP receives the same pressure as the NFCP.

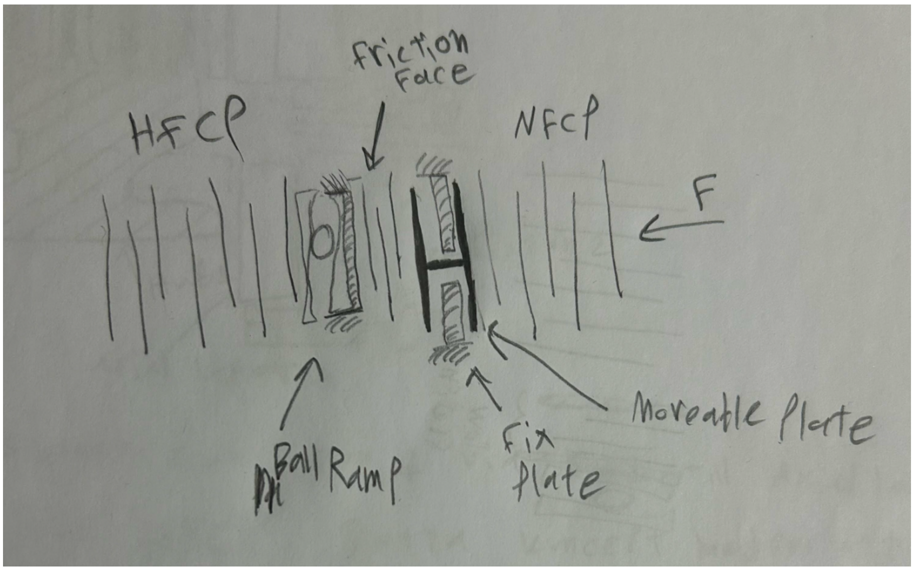

Figure 7.2: Schematic drawing of the ball ramp with minor clutch concept.

Advantages: This concept has instantaneous response, because the system utilizes a rigid mechanical ramp the force transmission is instantaneous once the force threshold is met. It has also high performance as it can be controlled easily by the applied force of the actuator.

Disadvantages: This concept may occupy a large axial length, since it consists of several components arranged in series. Another disadvantage is in the clutch pack between the movable plate and the ball ramp, this clutch pack should transfer a specific magnitude of torque depending on the input force according to 3.4. the torque that is needed for the activation of the ball ramp is relatively small compared to the torque used in NFCP and HFCP, therefore it may be hard to dimension and design that clutch pack reliably.

7.3 Locking ring with ramps (Concept 15)

Working principles: This concept consists of a ring that is positioned axially between the NFCP and HFCP, and radially out of the drum. In the drum there will be some grooves that will enable a parallelogram shaped plates to enter the drum. When these plates enter the drum they will prevent the NFCP to transfer the pressure to the HFCP, because it will prevent the axial movement of the NFCP. Thus the normal mode will be activated. To activate the overlock mode, the plates need to exit the drum and reenter the ring, and then any pressure put in the NFCP will be directly transferred to the HFCP. Figure 7.3 shows four plates that are inside the drum, and one plate inside the ring.

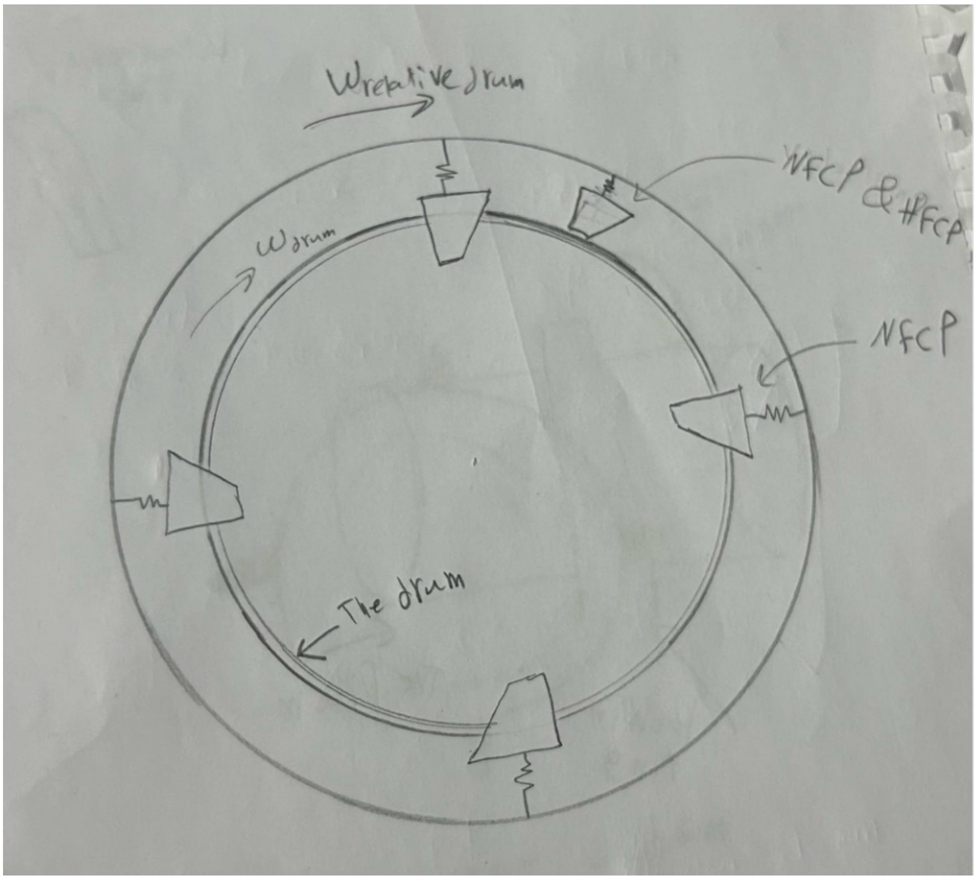

Figure 7.3: Schematic drawing of the Separation ring with ramps concept(From axial direction).

The activation of this concept is based on the difference in the rotational speed. The ring will rotate at the same angular speed as the drum. If the rotational speed of the ring is reduced, the resulted difference in the rotational speed will force the plates to enter/exit the drum. The reduction of the rotational speed of the ring may be achieved in several ways. The suggested way is to place a small hydraulic piston outside the housing, that piston will create a braking effect on the ring when it activated, which will create the difference in the rotational speed. For better illustration, figure 7.4 show a section of the concept from radial direction.

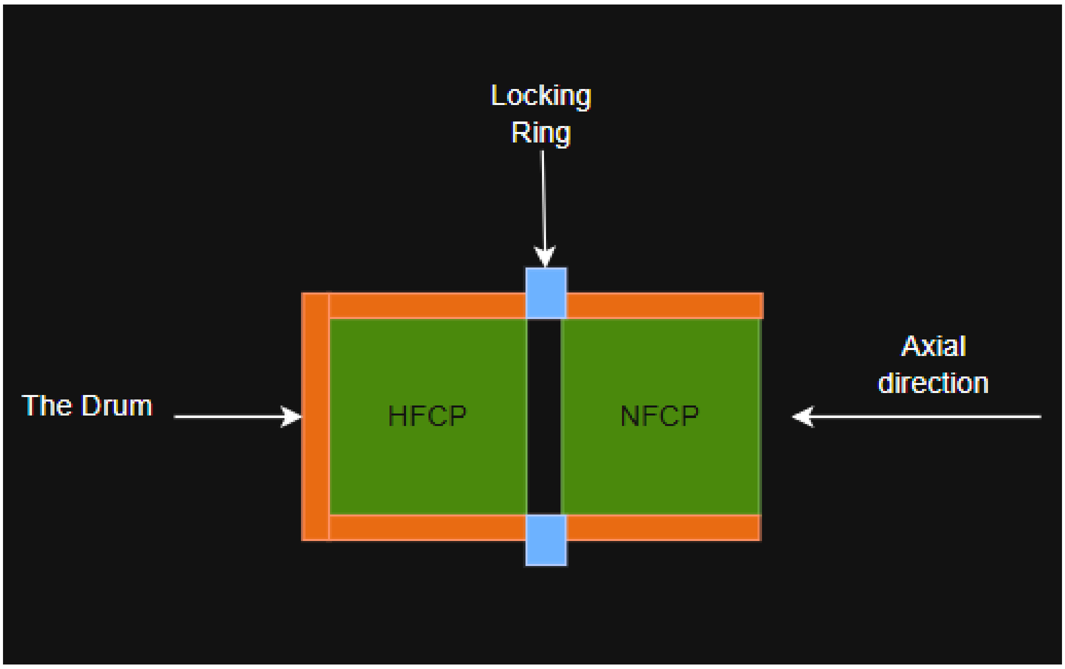

Figure 7.4: Schematic view of the Separation ring with ramps concept (From radial direction).

Advantages: This concept has small axial distance, the only distance needed between the NFCP and the HFCP is for the plates, The working principle of this concept is quite simple and effective. This concept is also good from performance and control perspective, since it can seamless activate and deactivate the HFCP.

Disadvantages: The main disadvantage of this concept is that it requires several modifications. Changes are needed in the housing and the drum, and an oil channel must be added from the pump to the small piston. Additionally, the control logic may need to be updated, since activating and deactivating of the normal/overlock mode needs the activation of both the primary piston and the added small piston on the housing.

7.4 Push-lock mechanism (Concept 17)

Working principles This concept consists mainly of three parts, two exocentric plates to lock and unlock and one plate with spring-ramps objects that will hold the locking plate. A schematic figure of the concept is shown in figure 7.5. The NFCP presses on the red plate, which open the locking ramps and enable the red plate to reach the HFCP and presses further on it. When the head of the red plate enter the HFCP section the locking plate lock it in that position. To revoke the locking, the black plate needs to pressed so it reach the ramps, that will open the ramps and the spring between the red plate and the

HFCP will take the red plate out of the HFCP.

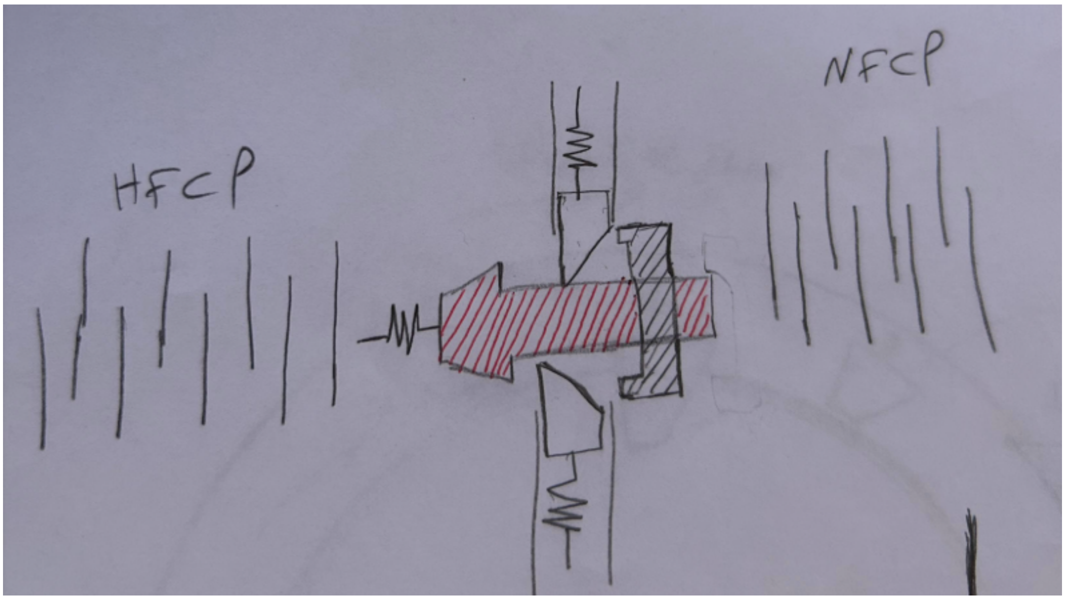

Figure 7.5: Schematic figure of concept 17, with the lock plate in red, and the unlocked plate in black.

Advantages: The biggest advantage with this concept is the possibility of locking. In this concept it is possible to press the HFCP and lock it to maintain the pressure without the need constant use of the actuator. This feature minimises the energy needed to operate the LSD, and allow the usage of full capacity of the actuator. This is because there is no need for constant usage of the actuator, and thus no temperature limitation needs to be considered.

Disadvantages: As presented in figure 7.5 the mechanism may occupy huge axial distance. In addition, it may be complicated to fix the spring-ramps object in the drum. That is because the assembly of the friction and steel discs is automated in the manufacturing line, thus the spring-ramps objects needs to be integrated and fixed to the drum in an efficient way which may be hard to realize.

Chapter 8

Concept Evaluation

In this chapter the criteria that will be used to evaluate the concepts will be explained. Further the methodology that will be used for the evaluation will also be explained. Eventually the result of the evaluation will be mentioned.

8.1 Design Criteria

There are several factors that are important for BorgWarner regarding design of new or for modifying existing products. Some of these factors were given by BorgWarner and were verbally explained by the supervisors in BorgWarner. The factors are simplicity, performance, safety, size, rigidity, repeatability, and manufacturability, and they are described below. To ensure an objective evaluation, key parameters that can be measured, calculated, or can be reasoned about have been established for each factor.

Simplicity: refers to the minimization of design complexity across multiple dimensions. It necessitates a streamlined construction using standardized components to ensure cost-efficiency. Furthermore, it dictates that the solution's functionality must require minimal modifications to the core LSD architecture. This ensures high modularity, allowing the unit to be configured with or without the HFCP to meet diverse customer specifications without significant re-engineering.

Key parameters:

- **Number of parts:** Total number of components required.
- **Modification:** If the concept requires modification of other components.
- **Cost:** Approximations of the cost required.

Performance: this criterion refers to the fundamental working principle and operational efficiency of the proposed concept. It means evaluating the transition dynamics during the activation and deactivation phases of both the "Normal" and "Overlock" modes. Furthermore, it assesses the system's ability to maintain torque stability and minimize parasitic losses during sustained operation in either mode.

Key parameters:

- **Torque loss:** Torque loss of NFCP when the HFCP is engaged.
- **Activation/Deactivation Time:** The time required for activation or deactivation of HFCP.
- **Hold Time:** The maximum duration for which the LSD can remain in overlock mode.

Safety: This criterion refers to the operational integrity of the proposed solution. It means the system must engage and disengage the HFCP seamlessly, ensuring no mechanical damage to the activation mechanism or to the surrounding components. It should also not affect the vehicle's dynamic stability. Furthermore, any modifications required by the new concept must not invalidate existing safety standards or degrade the baseline performance of the LSD.

Key parameters:

- **Cycle Life:** Number of successful engagement/disengagement cycles without fatigue failure.
- **Safety Margin:** Factor of safety for all components under peak torque or load.

Size: Refers to the size occupied by the solution. The distance between the NFCP and HFCP is limited, thus the solution has to follow specific axial and radial dimensions given by BorgWarner. A smaller size of the solution is preferred, because it means that a larger clutch pack can be used and torque transfer is enhanced.

Key Parameters:

- **Axial Length:** Maximum allowed length of the solution.
- **Radial Length:** Maximum allowed radial size.

Rigidity: This criterion refers to the mechanical stiffness of the solution under the operational loads. It refers to the solution's ability to withstand high loads while still enabling seamless activation and deactivation of the HFCPs.
Key Parameters:

- **Moveable parts:** Number of movable parts in the solution.
- **Structural instability:** Number of parts with small size compared to the applied load.
- **Deflection:** Max allowable displacement under maximum operating load.

Repeatability: The solution should be able to engage and disengage the HFCP repeatedly, thus the functionality of the solution should be possible to be repeated. It must also be repeated without the need for service or replacement after a certain number of operating cycles.

Key parameters:

- **Hysteresis:** The variance between the torque engagement and disengagement curve.
- **Fatigue of parts:** Parts susceptible to fatigue failure due to cyclic loading.

Manufacturability: To ensure commercial viability, the proposed solution must be compatible with high-volume mass production. Cost-efficiency is a primary driver; therefore, any modifications to existing LSD components must be evaluated against their impact on manufacturing processes. This is critical because any modification to a production line involves significant costs and consequences for other products.

Key parameters:

- **Tooling change:** Number of components requiring custom production method.
- **Modification of critical parts:** Whether a modification is made to a part that is manufactured with mass production.
- **Realization:** Possible to manufacture the product with existing production method.

8.2 Evaluation Methodology

To evaluate the concepts that are generated, the methodology that is proposed by Ulrich, K.T. & Eppinger will be followed. In U& E the concepts will initially be evaluated by a screening matrix, and then some of the concepts will move forward for further development. Eventually, the concepts will be evaluated using a scoring matrix and the final concept will move forward for final development stage.

8.2.1 Concept screening

The concept screening stage aims to quickly narrow down the number of potential concepts and identify those with the highest potential for further development. This process helps improve the quality of selected concepts while maintaining efficiency in evaluation.

During the concept screening stage, the key design parameters discussed in Section 8.1 are used as evaluation criteria, each assigned equal weight. A reference concept, or benchmark, is then chosen for comparison. This benchmark may represent an industry standard, an existing product, a previous generation of the design, or one of the proposed concepts.

Each alternative concept is evaluated against the reference using a simple rating system:

- ”+” indicates the concept performs better than the reference.
- ”0” indicates it performs the same as the reference.
- ”–” indicates it performs worse than the reference.

After completing the evaluation, the total number of “better than,” “same as,” and “worse than” ratings is summed. These results help identify the most promising concepts, allowing the focus to be placed on the strongest options for further refinement and development in subsequent stages.

8.2.2 Concept Scoring

Following the initial screening phase, Concept Scoring provides a higher resolution analysis to differentiate between the remaining top-tier design options. In this stage, a selection matrix where each criterion can be assigned a relative importance weight, typically expressed as a percentage, to reflect its impact on product success. Each concept is then rated on a fine scale from 1 to 10 against the predetermined reference concept. The final performance of each design is determined by calculating a weighted score, defined as $S_j = \sum r_{ij} w_i$, where the rating for each criterion is multiplied by its specific weight. This mathematical rigor allows a sensitivity analysis to be conducted, exploring how shifts in priorities might change the ranking, ultimately ensuring that the final selection is based on objective data rather than subjective preference.

8.2.3 The result of the first evaluation

The first evaluation refers to the process of selecting concepts that will continue to the development phase. First, a screening matrix was established to minimize the number of concepts. Concept 3 was chosen as a reference concept as it has good score relative to the established design criteria. A similar solution has also been thoroughly discussed in another master's thesis on a similar problem, conducted by Eric Winterfield [8].

Subsequent to the screening, a scoring has been conducted because the number of concepts that had passed the screening was relatively large. The scoring in this stage has been done without weighting of the design criteria factors, since the aim of this scoring was to reduce the number of concepts that will continue to the development in an objective manner. The evaluation matrices are shown in 14.2.1.

8.2.4 The result of the second evaluation

The detailed development of the concepts is presented below in chapter 9. After the detailed development, the chosen concept that will move on to the final development is the ball ramp concept. The result of the second evaluation is presented in figure 8.1.

Selection Criteria	Key Parameters	Weight	4		13		15		17	
			Rating	Weighted	Rating	Weighted	Rating	Weighted	Rating	Weighted
Simplicity	Number of parts	1	6		4		5		4	
	Modification	1	6		7		4		5	
	Cost	1	5		6		3		6	
Performance	Torque loss:	1	3		6		9		5	
	Activation/Deactivation Time	1	7		7		8		9	
	Hold Time	1	5		6		8		5	
Safety	Cycle Life	1	5		8		7		7	
	Safety Margin	1	5		8		4		6	
Size	Axial Length	1	8		3		8		3	
	Radial Length	1	8		8		4		6	
Rigidity	Moveable parts	1	7		5		4		4	
	Structural stability	1	7		9		6		5	
	Deflection	1	7		8		5		5	
Repeatability	Hysteresis	1	3		9		8		8	
	Fatigue of parts	1	5		8		8		7	
Manufacturability	Tooling change	1	5		7		7		7	
	Modification of critical parts	1	4		7		6		6	
	Realization	1	6		8		7		7	
NET			102		124		111		105	
RANK			4		1		2		3	
CONTINUE			No		yes		No		No	

Figure 8.1: The result of the second evaluation.

Chapter 9

Concept Development

In this chapter the concepts will be explained in detail in terms of the working principles and in terms of the design. Possible refinements or changes will also be mentioned and motivated. Some calculations will be performed to determine the torque-transfer capability of the concept and compare it with customer requirements. In order to compare it with the customer needs later. Eventually, each concept will be discussed, and critical issues will be pointed out.

9.1 Ball ramp with friction face(Concept 13)

One of the major components in this concept is the ball ramp. The working principles of the ball ramp is shown in figure, 9.1. The balls are fitted between the curved grooves on the two plates and always maintain point contact with both ramps. When plate A rotates, the balls will roll and rise with the ramp, that will increase the axial distance between the two plates[9].

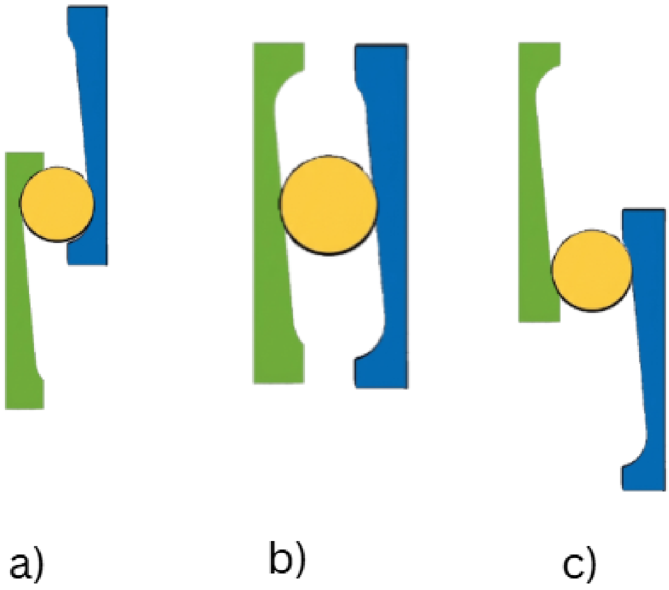

Figure 9.1: Schematic figure of the ball ramp mechanism, a) closed ball ramp, b)half-open ball ramp, c) open ball ramp.

To follow the calculation that is presented in this section, the used symbols are presented in table 9.1. If the NFCP is pressed by a piston force F_a, the activation clutch and the ball ramp are also pressed by the same force is the friction in the spline is neglected. If plate A in the ball ramp is affected by a torque T_c from the clutch pack, it is convenient to construct the free-body diagram as in figure 9.2.

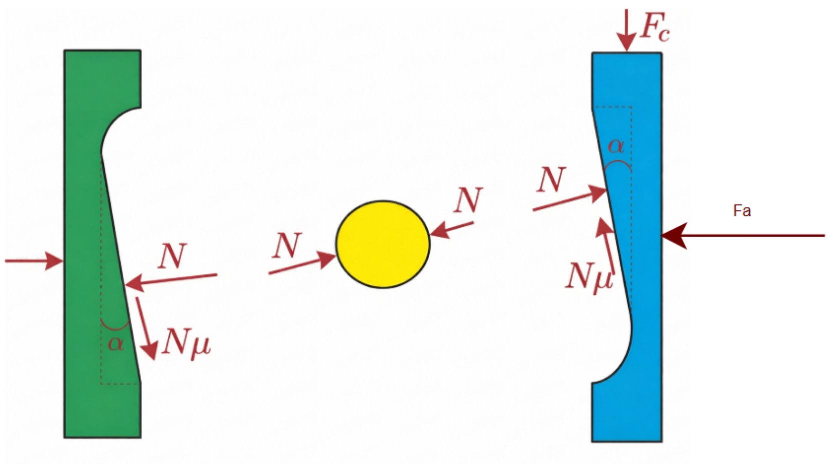

Figure 9.2: The free body diagram of ball ramp mechanism.

Table 9.1: List of symbols used in the ball ramp calculations

Symbol	Description	Symbol	Description
T	Applied torque [Nm]	T_c	Activation clutch torque [Nm]
$T_{c\max}$	Max clutch torque capacity [Nm]	F_c	Force from clutch torque [N]
F_a	Piston force [N]	F_b	Force through NFCP [N]
F_d	Force through HFCP [N]	N	Normal force [N]
μ	Coefficient of friction of the ball ramp [-]	α	Ramp angle [rad]
R_e	Effective radius of the ball ramp [m]	n	Number of friction faces [-]
R_y	Outer radius of the friction disc [m]	R_i	Inner radius of the friction disc [m]
η_{NFCP}	Efficiency of NFCP [-]	η_c	Clutch efficiency [-]
η_{HFCP}	Efficiency of HFCP [-]		

where the force F_c is caused by the clutch torque Tc and it is given by

$$F_c = \frac{T_c}{R_e} \tag{9.1}$$

The equilibrium force equations of plate A in vertical and horizontal direction give

$$N\mu\cos\alpha + N\sin\alpha - F_c = 0 \tag{9.2}$$

$$N\cos\alpha - N\mu\sin\alpha - F_a = 0 \tag{9.3}$$

Combining equations 9.1, 9.2 and 9.3 give

$$T_c = R_e F_a \frac{\mu\cos\alpha + \sin\alpha}{\cos\alpha - \mu\sin\alpha} \tag{9.4}$$

Which is the minimum torque required to keep the plate in equilibrium, thus the torque T that are needed for the activation of the ball ramp should satisfy

$$T > T_C \tag{9.5}$$

However the torque T that can be applied to the ball ramp is limited by the maximum clutch torque capacity T_{cmax}, which can be calculated by equation 3.4, therefore the inequality 9.5 becomes

$$T_{cmax} > T > T_C \tag{9.6}$$

In other words, the activation torque T is a function of α, n, R_y, R_i, μ and F_a. However, in reality the applied torque is always equal to the clutch maximum capacity torque given by equation 3.4, thus only the inequality 9.5 need to be verified. The minimum torque needed for the activation of the ball ramp T_c, at a specified force F_a that satisfy 4.10 and 4.9 is shown in figure 9.3 and 9.4 respectively as function of mu, R_e and α.

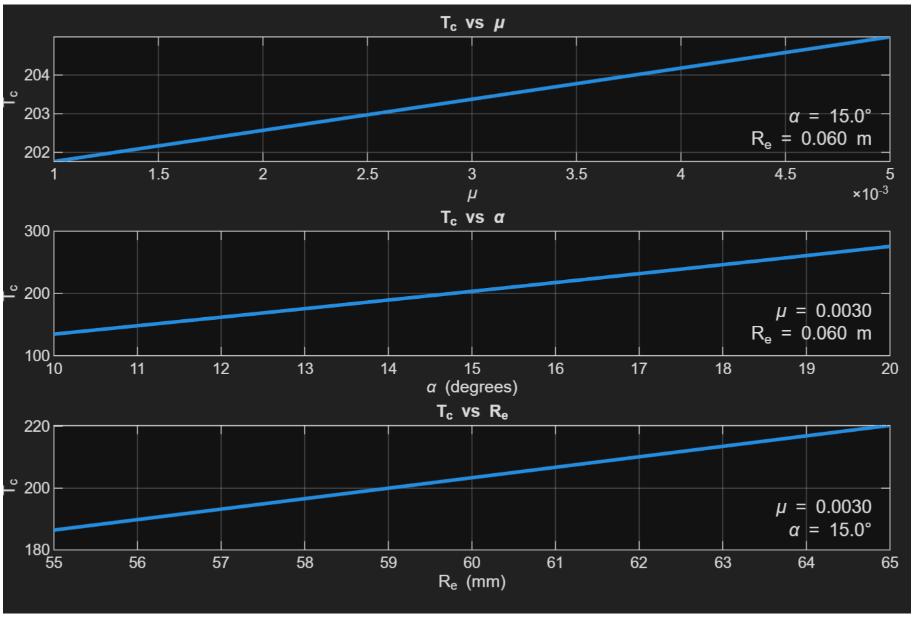

Figure 9.3: T_C as a function of mu, R_e and α for actuator force that satisfy 4.10

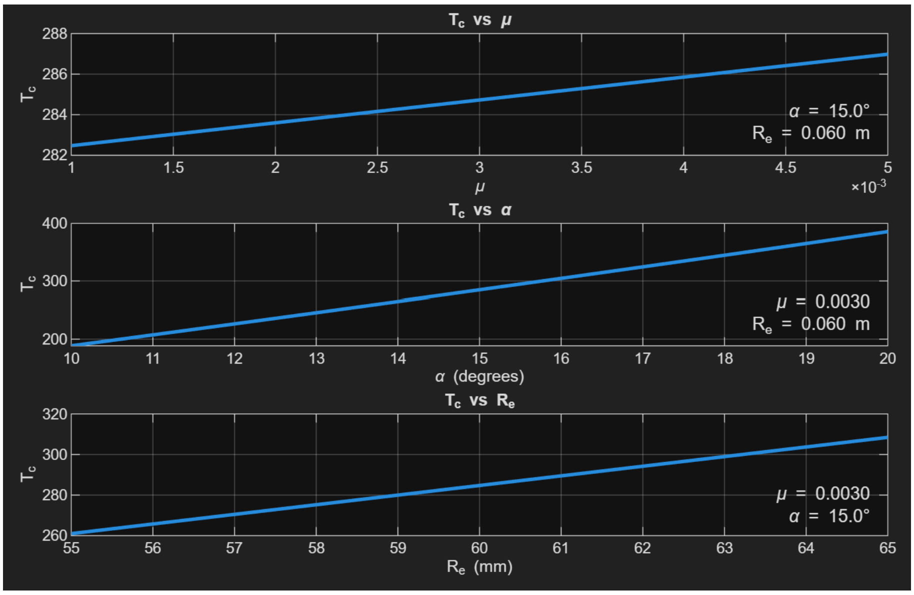

Figure 9.4: T_C as a function of mu, R_e and α for actuator force that satisfy 4.9

The maximum torque capacity for actuator forces that satisfy 4.10 and 4.9 is shown in figure 9.5 and 9.6 respectively.

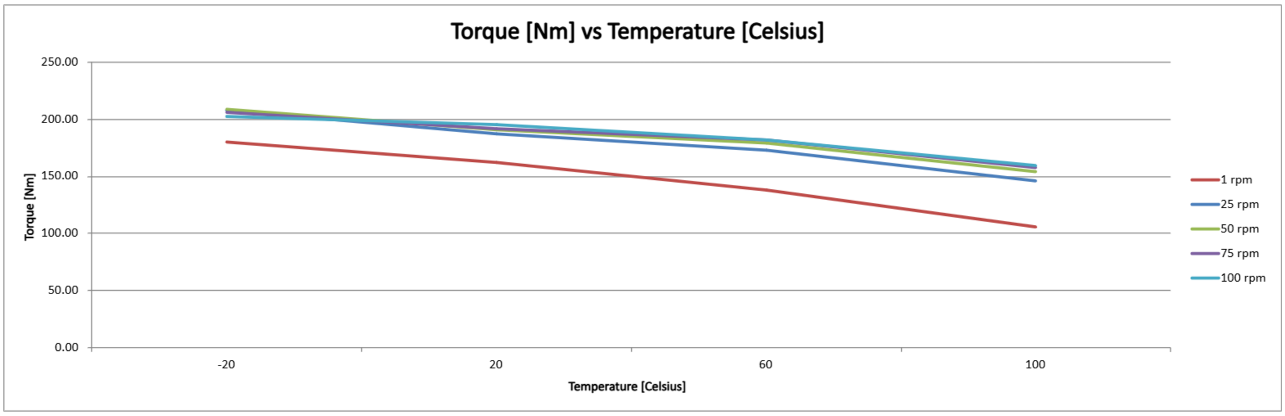

Figure 9.5: The torque from the clutch pack at the pressure given by 4.10

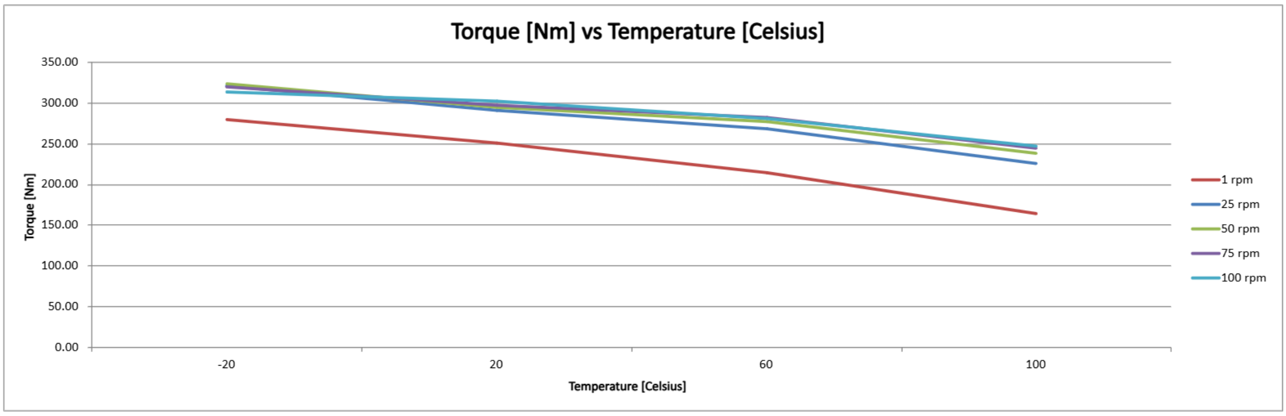

Figure 9.6: The torque from the clutch pack at the pressure given by 4.9

Comparing the minimum torque in 9.3 to the applied torque in 9.5 and minimum torque in 9.4 to the applied torque in 9.6 show that it is possible to design the ball ramp in such a way that if the actuating force is according to 4.8, the normal mode will be active and the ball ramp will not be activated since the activation clutch is not providing enough torque. When the actuating force is increased to 4.9, the ball ramp will open, because the activation clutch is transferring more torque than what the ball ramp can sustain under equilibrium. Note that the activation force of the ball ramp does not need to be equal to 4.9, but it is dependent on the design of the ball ramp, but it should be larger than 4.10. However it is advantageous to choose larger activation value because it allows operating the NFCP at normal mode with higher force.

One of the major refinements in this concept is to remove the fix plate and embed it within the ball ramp instead. This will reduce the axial distance of the concept, because the moving plate no longer needs to be as big and complex as the one shown in figure

7.2. This refinement is also necessary as the ball ramp in this concept need to be axially fixed to prevent the activation of HFCP in normal mode, but it needs also to give axial displacement to connect the HFCP and the NFCP in overlock mode. The resulting ball ramp consists of three plates, right plate, fix plate and left plate. A 3D model is shown in figure 9.7. In this ball ramp the fix plate have no axial movement, and it will prevent the axial force from reaching the HFCP. In overlock mode however, the right plate will rotate the balls, and that will enable the axial force to be transmitted from the right plate through the balls and further to the left plate and eventually to the HFCP.

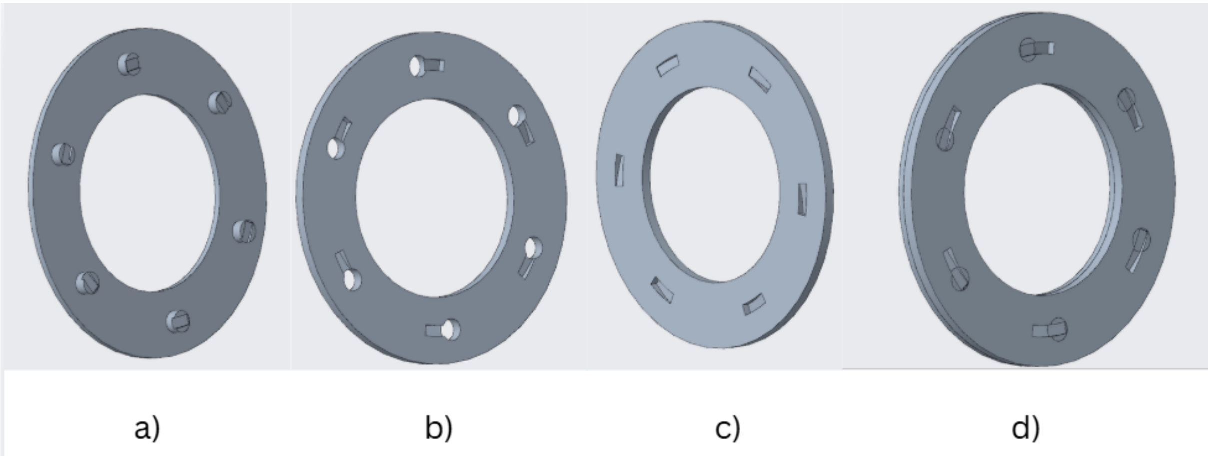

Figure 9.7: Schematic 3D model of the ball ramp plates, a) the left plate, b) the fix plate, c) the right plate and d) the assembly of left plate and fix plate.

Assuming that there is no losses in the LSD except losses in the clutch packs mainly due to spline friction, the free body diagram of the NFCP and HFCP in normal and overlock mode is shown in figure 9.8 and 9.9 respectively. Consider that F_b, F_c and F_d are given by

$$F_b = \eta_{NFCP} F_a \tag{9.7}$$

$$F_c = \eta_c F_b \tag{9.8}$$

$$F_d = \eta_{HFCP} F_c \tag{9.9}$$

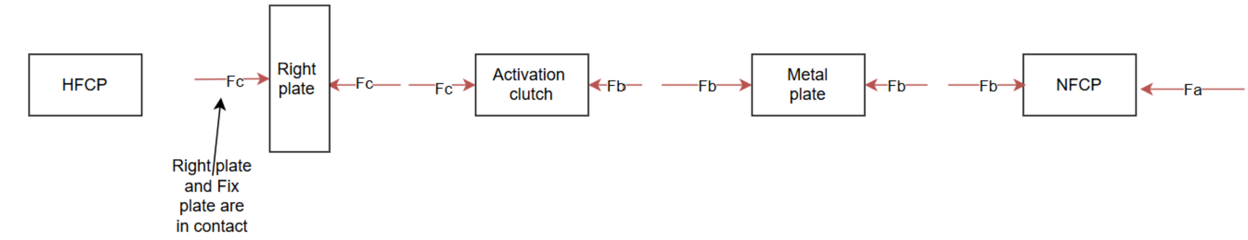

Figure 9.8: Free body diagram of the clutch pack and the ball ramp mechanism in normal mode.

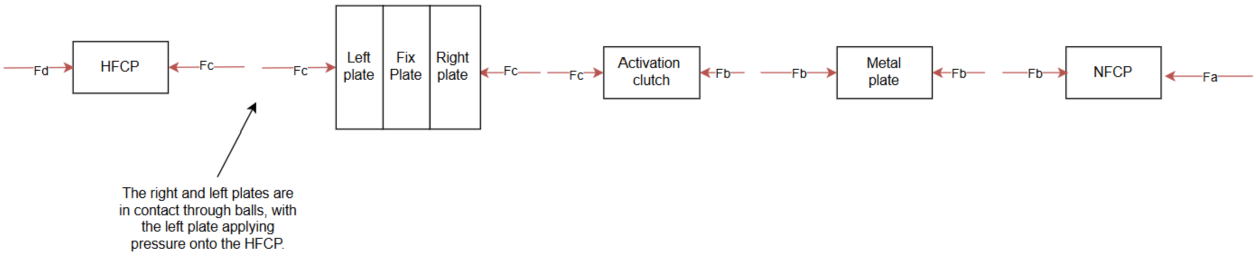

Figure 9.9: Free body diagram of the clutch pack and the ball ramp mechanism in overlock mode.

Force equilibrium yields the forces that act on each clutch pack in respective mode. In normal mode only the NFCP is active and the force F_b is given by equation 9.7. In overlock mode both NFCP and HFCP are active and the force on NFCP is again given by equation 9.7, while on HFCP the force is F_d and it is given by 9.9.

9.1.1 Self locking of Ball Ramp

When investigating the locking of the ball ramp, several changes needs to be made for the ball ramp. The first one is to make it symmetric, which means it can be activated irrespective of the rotational direction. And the second one to hold it self activated. The changes has been made for the fixed and left plate as shown in figure 9.10. The ramps in fix and left plate are made inclined against each other, this allow to lock the ball between the inclination of the left plate. To deactivate the mechanism a similar torque should be applied, which will move the ball to the inclination of the fix plate and the mechanism is then deactivated.

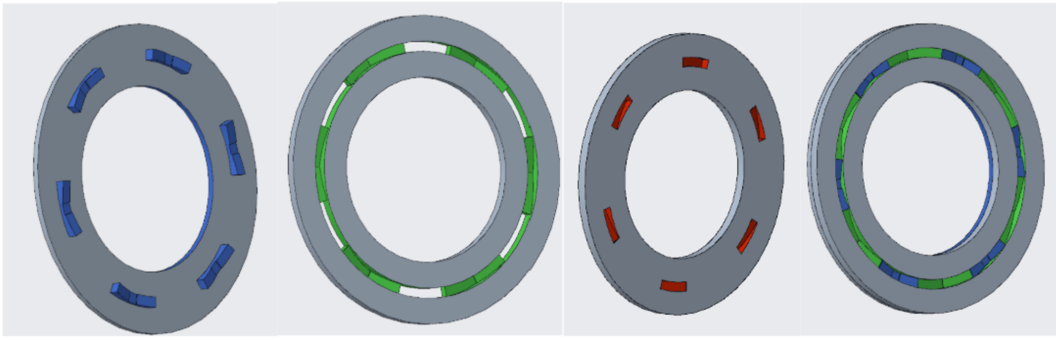

a) b) c) d)

Figure 9.10: Schematic 3D model for the adjusted ball ramp that can be self locked. a) the left plate, b) the fix plate, c) the right plate and d) the assembly of left plate and fix plate.

This locking solution is limited because the actuator still needs to be used. When this locking solution is activated, the pressure that is put on the NFCP is also directly transferred to the HFCP. Thus to take full advantage of this solution and be able to lock the pressure in the clutch packs while the actuator is shut down, the NFCP needs to be locked. This thesis is limited to proposing an activation solution and discuss how the locking of the HFCP can be achieved, so the locking of NFCP will not be discussed in detail. However some of the solutions presented for locking of HFCP can also be applicable to locking of the NFCP.

9.1.2 Discussion of Ball Ramp

This concept is quite simple and has good potential as it can effectively activate both modes depending on the applied force. However, there are several drawback with this concept. The axial occupation of this concept needs to be investigated further. Since there are several plates and an activation clutch, the axial occupation may be larger than the available place.

The largest drawback of this concept lies in the activation clutch, the friction disc will be slipping almost all the time. This may cause wear particles in the oil, unwanted thermal loading that can affect the disc and the surrounding components. This can also affect the disc's ability to transfer torque over the time, since the disc may wear out.

There are also several aspects that need further investigation for this concept. One important aspect is the need for a method to lock the ball ramp axially to the drum. This is necessary because the drum assembly is automated, whereas welding the ball ramp must currently be done manually, which requires time and effort. Therefore, a locking solution that can be integrated into the automated assembly line would be beneficial. Since the ball ramp must be fitted into the drum, it must be splined to engage with the drum geometry.

Another challenge with this concept is to ensure enough angular velocity between the drum and the hub at the activation pressure, i.e., the pressure that will be used for opening the ball ramp. If the drum and the hub have no difference in angular velocity at that pressure, the friction disc and the steel drum will then has also the same angular velocity. Thus, the ball ramp will not be activated because the right plate and the fix-plate is rotating at the same angular velocity. However, the relative slip behavior of the steel and friction disc at that pressure is unknown, and it cannot be analytically calculated since it depends on the torque in the drum and in the hub. This issue can be further investigated via a multi-physical simulation.

9.2 Belleville Friction Washers (Concept 4)

The main idea of this concept is to replace the friction plates themselves with spring washers. This saves space in comparison to having a whole mechanism placed between the two friction packs. The plate consists of two design regions, where the upper and lower portions of the disc are constructed as spline curves that act as the spring mechanism. The middle part of the disc is a flat surface where friction material is added.

When the HFCP is not engaged, the flat surfaces are not in contact, as the springs hold the forces transferred from the NFCP. The spring compression has a nonlinear relationship with the force transferred to the HFCP. The higher the deformation, the less the spring resists the force transferred from the NFCP. The uncompressed spring is illustrated in figure 9.11.

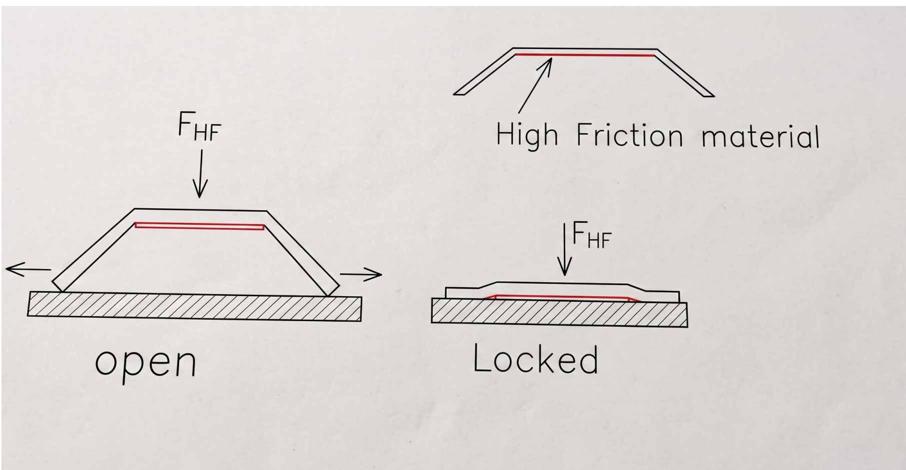

Figure 9.11: The friction disc functionality.

The curved surface is a low-friction zone where the friction plates slide against the steel plates as they are always in contact, thus transferring negligible torque. When the HFCP is to be engaged, the springs are totally compressed, allowing the high-friction flat surface to reach the steel discs and create friction, thus transferring torque.

To illustrate how the force flow is directed, a chart was made to clarify how force is transferred from the piston to the HFCP where the friction springs are located. According to the chart 9.12, the main route of the force is from the piston to the NFCP and finally to the HFCP. The HFCP is supported by the end surface of the drum.

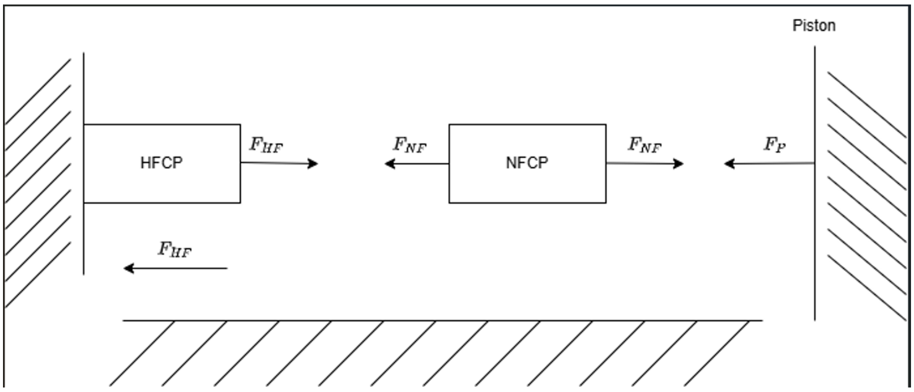

Figure 9.12: Force flow illustrated

Table 9.2: List of symbols used in the friction washers calculations

Symbol	Description	Symbol	Description
F_p	Force from the hydraulic piston [N]	F_{NF}	NFCP force [N]
F_{HF}	Force on HFCP [N]	F_{HFCP}	Force on Friction material [N]
F_{HFs}	Spring force [N]	F	Force [N]
E	Elasticity modulus [N/m^2]	δ	Axial deformation [m]
ν	Poisson's ratio [-]	R	Outer radius [m]
r	Inner radius [m]	h	Disc spring height [m]
t	Spring Thickness [m]	C_i	Geometry constant [-]
β	Angle [rad]	α	Angle [rad]
ϕ	Angle [rad]	n	Number of disc springs [-]

The operation of the LSD is divided into three modes, the clutch disengaged mode, which is shown in 9.13, where none of the friction packs are engaged. The normal mode where only the NFCP is engaged as shown in figure 9.14, thus transferring a specific amount of torque. Finally, the over-locked mode, where both the NFCP and HFCP are engaged as illustrated in figure 9.15 to clarify the difference of each mode.

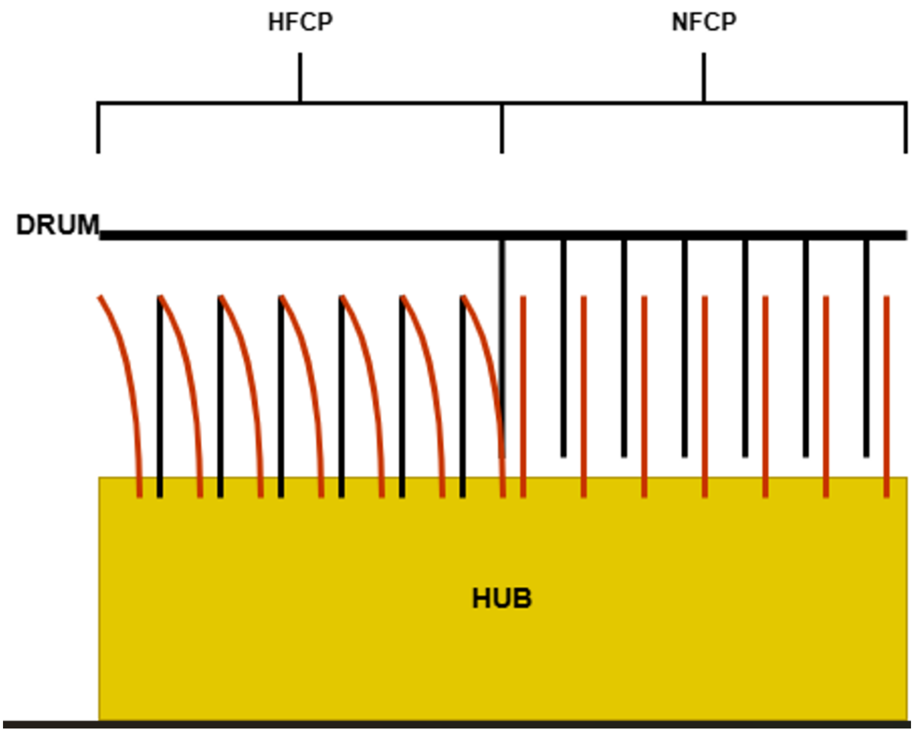

Figure 9.13: Clutch Disengaged Mode

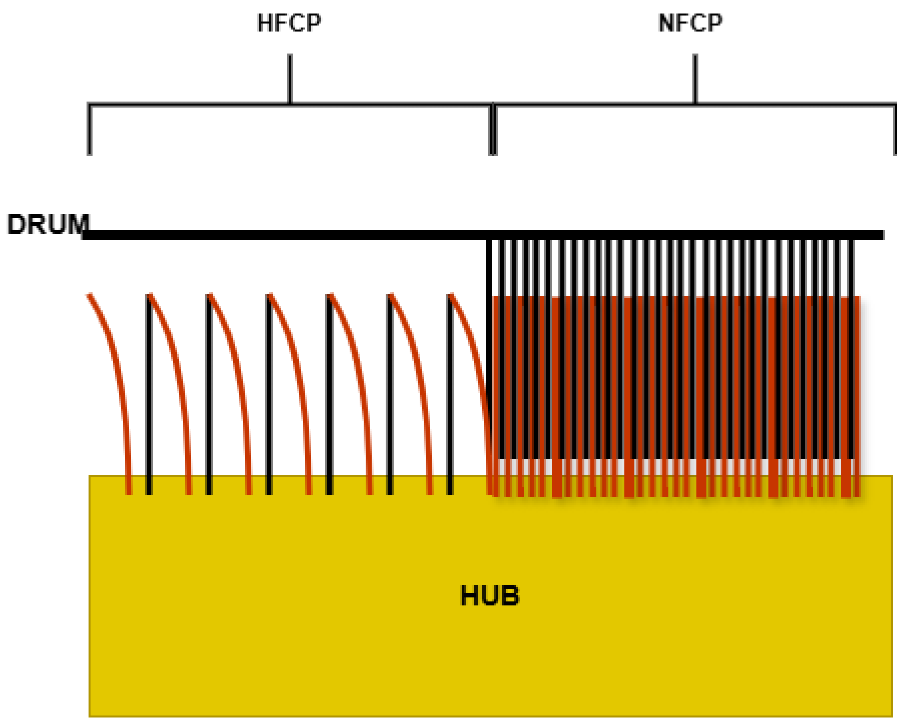

Figure 9.14: Normal mode

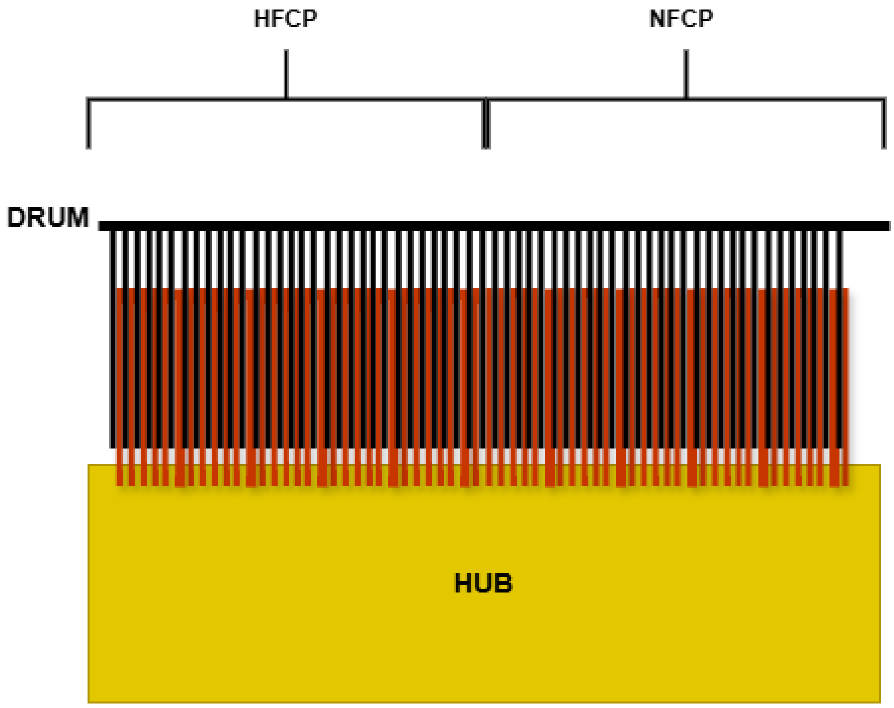

Figure 9.15: Over-Locked Mode

A study was carried out on Belleville friction washers to increase knowledge of them and to be able to decide the curvature of the spring part of the disc. One of the main advantages of this concept is that we have several clutch plates that are to be made into springs. All discs in the HFCP can be made into springs, but to optimize and lower the consumption of the main clutch force provided by the piston, the number of spring discs is to be decided accordingly.

Force reaching the clutch packages occurs under 2 scenarios. Normal friction mode and high friction mode.

Clutch Pack Force Scenarios

The force F_p reaching the clutch packages occurs under two scenarios.

Scenario 1: Normal Friction Mode

In this state, the pressure force is equivalent to the normal and static high friction forces.

$$F_p = F_{NF} = F_{HFs} \tag{9.10}$$

Scenario 2: High Friction Mode

In this state, the total force is partitioned between the static threshold and the force applied to the clutch pack (F_{HFCP}). Use the `align` environment here to keep the equals signs stacked and centered.

$$
\begin{align}
F_p &= F_{NF} = F_{HF} \tag{9.11} \\
F_{HFCP} &= F_{HF} - F_{HFs} \tag{9.12} \\
F_p &= F_{HFCP} + F_{HFs} \tag{9.13}
\end{align}
$$

Spring calculation

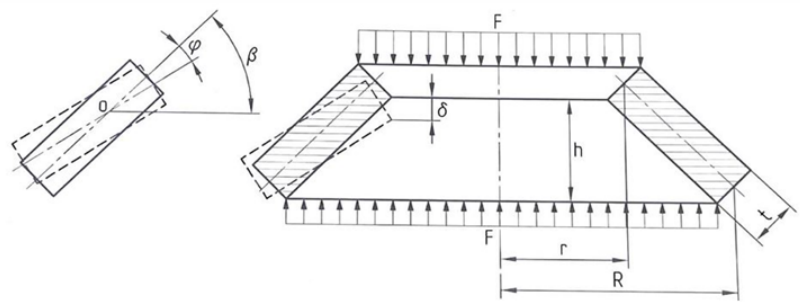

Figure 9.16: Disc spring

The effective force reaching the friction material in the HFCP is F_{HFCP} . Which is the force provided by the hydraulic system with the springs force deducted. The spring force is studied to estimate the amount of spring force assuming that all friction plates are washers inside the HFCP. This study is based on the literature provided in 7.

Figure 9.16 shows the relation of the spring force in relation to δ Which is the deformation of the spring . the Almen-Laszlo equations gives us a good understanding of the reaction of the spring. The Ratio of h/t is the Key.

$$F = \frac{E\delta}{(1-\nu^2)R^2}\left[C_1(h-\delta)\left(h-\frac{\delta}{2}\right)t + C_2t^3\right] \tag{9.14}$$

$$\beta = \frac{h}{R-r} \tag{9.15}$$

$$\alpha = \frac{R}{r} \tag{9.16}$$

$$\phi = \frac{\delta}{R-r} \tag{9.17}$$

$$C_1 = \left(\frac{\alpha+1}{\alpha-1} - \frac{2}{\ln(\alpha)}\right)\frac{\pi\alpha^2}{(\alpha-1)^2} \tag{9.18}$$

$$C_2 = \frac{\pi\alpha^2\ln(\alpha)}{6(\alpha-1)^2} \tag{9.19}$$

The behavior of a Belleville spring is almost entirely determined by the ratio of the initial dish height (h) to the material thickness (t). Depending on the ratio, the spring has several behaviors. Progressive, regressive and bistable. In the progressive regime, the force increases continuously with compression. In the regressive regime, the spring stiffness decreases significantly during the middle portion of the stroke. The spring becomes bistable (snap-action). It will actually "pop" into a second position and stay there until you pull it back. The behavior that is in focus is the regressive behavior. Where the activation point is when the spring is flat. The force required to flatten the springs drops significantly after reaching its peak. We can take advantage of that to maintain a certain amount of force provided to the NFCP without the HFCP engaging. Figure 9.17 Shows the regressive behavior with a ratio of 2.5 for h/t.

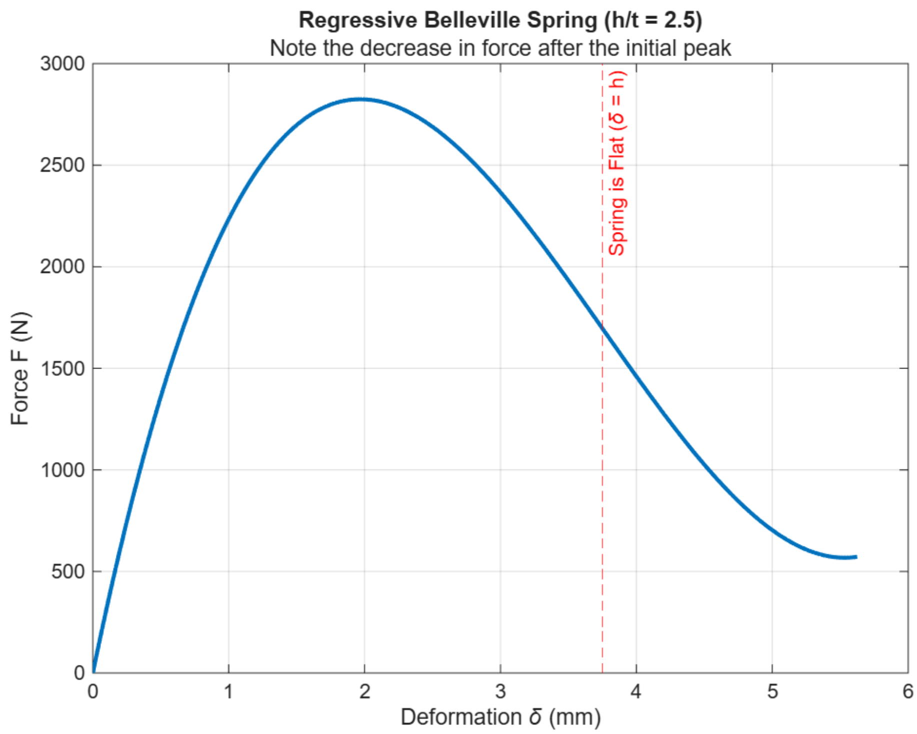

Figure 9.17: Disc spring

9.2.1 Discussion Friction Washers

The same principle can be applied on the steel plates instead of the friction plates. With other words, the spring mechanism can be delivered by the steel plates instead of the friction plates. Thus easier to manufacture as no friction material needs to be applied on the plates.

9.3 Locking ring with ramps (Concept 15)

One of the critical components in this concept is the plates, which are shown in figure 7.3. One of the limitations of this design is that it is dependent on the rotation direction. To make it independent of rotation direction, the design of the plate is changed and the new shape of the plates is shown in figure 9.18. This new design allows the activation of this concept regardless of the rotation direction of the drum, since the new plates have two ramps instead of one.

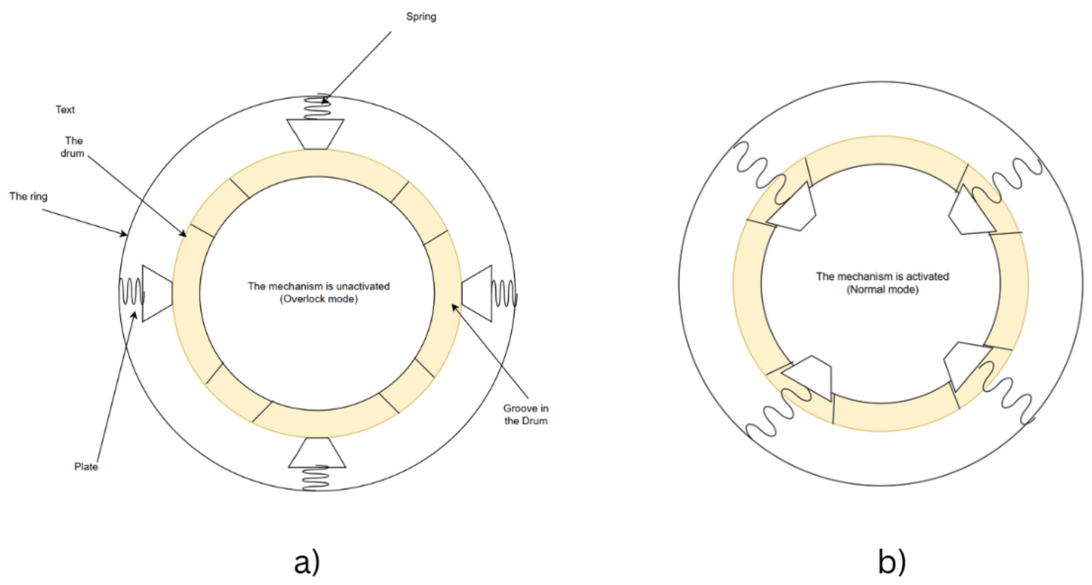

Figure 9.18: Detail view of concept 15 with the new shape of the plates, a) when the mechanism is not activated, b) when the mechanism is activated.

For improved clarity in the calculations presented later in this section, Table 9.3 provides an overview of the parameters used.

Table 9.3: Parameters used in Concept 15: Locking ring with ramps

Symbol	Description	Symbol	Description
T_f	Friction torque rotating the ring [Nm]	T_{dr}	Drum friction resisting torque [Nm]
f	Friction force between plate and drum [N]	f_{dr}	Friction force between ring and drum [N]
f_p	Friction force on plate surface caused by the auxiliary piston [N]	F_p	Force from auxiliary piston [N]
F_s	Spring force [N]	k	Spring stiffness [N/m]
x_a	Spring displacement when the mechanism is not activated (spring compression) [m]	N	Normal force on ramp [N]
m	Mass of plate [kg]	M	Mass of the ring [kg]
g	Gravitational acceleration [m/s^2]	R	Effective radius [m]
μ	Friction coefficient (plate–ramp) [-]	μ_p	Friction coefficient (ring - auxiliary piston) [-]
μ_{dr}	Friction coefficient (ring–drum) [-]	α	Ramp angle [rad]
ω	angular velocity.	F_c	The normal force due to circular movement

One of the fundamental features in this concept is that the ring will rotate at the same angular velocity as the drum when it is not activated (Overlock mode). A free body diagram of one of the plates and for the ring when the concept is not activated is shown in figure 9.19. The springs in this concept have a crucial role, it is used to increase the friction force when the mechanism is not engaged. When the mechanism will be activated, the springs will push the plates inside the drum when the plates are aligned with the grooves. A force equilibrium between the drum and the plate and assuming fully developed friction yields the friction force f between the plates and the drum

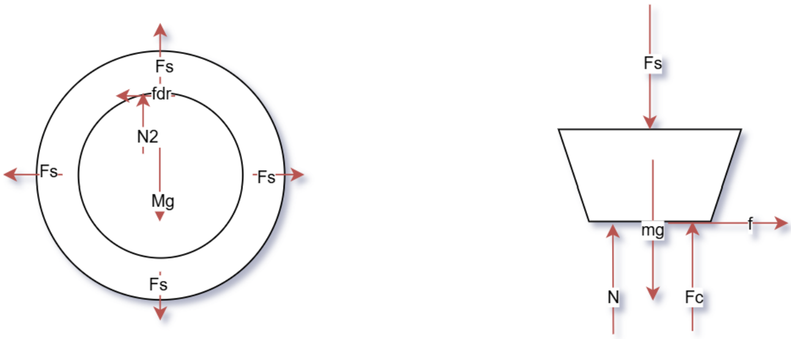

Figure 9.19: Free body diagram for one of the plates and for the ring when the mechanism is not activated.

$$f = \mu(mg + kx_a - mR\omega^2) \tag{9.20}$$

Thus, the torque that will rotate the ring at the same angular velocity as the drum is given by

$$T_f = 4\mu(mg + kx_a - mR\omega^2)R \tag{9.21}$$

This torque T_f must satisfy the following equation in order for the ring to rotate with the drum

$$T_f > T_{dr} \tag{9.22}$$

Where T_{dr} is given by

$$T_{dr} = f_{dr}R = \mu_{dr}MgR \tag{9.23}$$

And f_{dr} is given by a force equilibrium and assuming fully developed friction between the ring and the drum

$$f_{dr} = \mu_{dr}Mg \tag{9.24}$$

The free body diagrams of the ring and plate under two operating conditions are presented in figures 9.20 and 9.21, respectively. Figure 9.20 corresponds to the activated state of the mechanism, whereas figure 9.21 represents the state in which the auxiliary small piston is engaged to deactivate the mechanism and withdraw the plate from the drum.

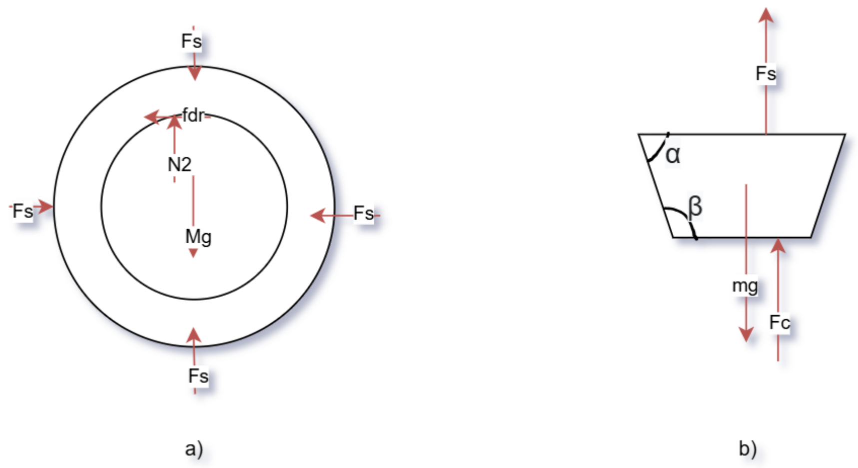

Figure 9.20: Free body diagram for one of the plates and for the ring when the mechanism and auxiliary small piston is not activated.

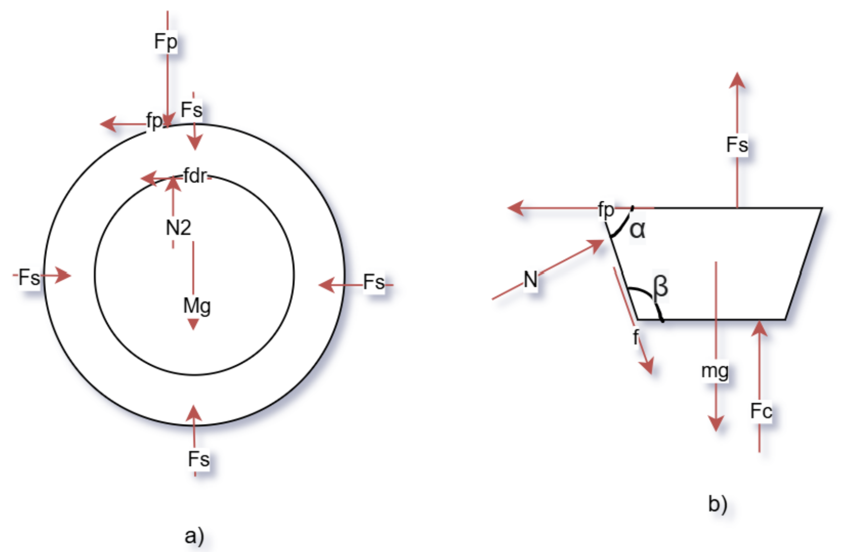

Figure 9.21: Free body diagram for one of the plates and for the ring when the mechanism is not activated.

In figure 9.21 a) the only force that contribute the torque is the friction force f_p, which is given by

$$f_p = \mu_p F_p \tag{9.25}$$

The force equilibrium in the horizontal and vertical directions of the plate in figure 9.21 b) gives

$$N \sin\alpha + f \cos\alpha - f_p = 0 \tag{9.26}$$

$$F_s - mg + N \cos\alpha - f \sin\alpha + mR\omega^2 = 0 \tag{9.27}$$

The relation between the friction force in the inclined surface and the normal force is given by the slip condition

$$f = \mu N \tag{9.28}$$

Combining equations 9.25, 9.26, 9.27 and 9.28 and solving for F_p give

$$F_p = \frac{(mg - F_s - mR\omega^2)(\sin\alpha + \mu\cos\alpha)}{\mu_p(\cos\alpha - \mu\sin\alpha)} \tag{9.29}$$

Which is the minimum force that should be provided by the auxiliary small piston to activate the mechanism and force the plates to exit the drum. Since this force depends on many unknown parameters, any further analysis requires many assumptions and estimations, thus the estimation of F_p will not be conducted.

9.3.1 Self locking of concept 15

This concept has promising results regarding the self locking. There are two methods for maintaining pressure through self-locking without the actuator. The first depends on the elasticity of the HFCP. A locking sequence is shown in Figure 9.22. The force is applied as shown in 9.22 b), that will elastically deform the HFCP, then the plates will enter the drum (9.22 c) and prevent the HFCP from expanding back. Thus, the pressure is maintained without requiring continuous actuator force (9.22 d).

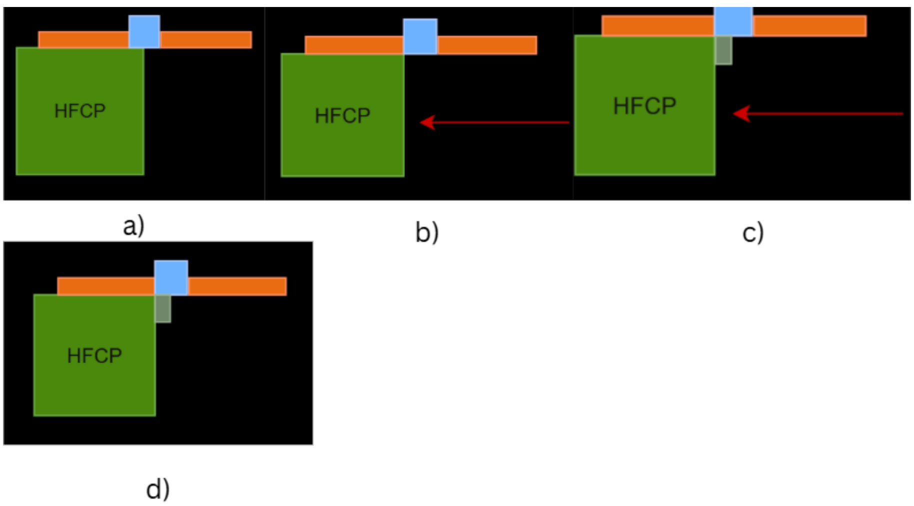

Figure 9.22: Method 1 to self lock concept 15.

The elastic deformation of the HFCP may be insufficient for practical implementation, and the method presented above may be hard to implement. Another method is to use a spring, a locking sequence is shown in Figure 9.23. A large spring is placed at the back of the HFCP to the left 9.23 a), the actuator force will press on the HFCP and thus the spring will be pressed 9.23 b), the plate enter the drum and the actuator force is removed. The spring is now pressed and will press further on the HFCP.

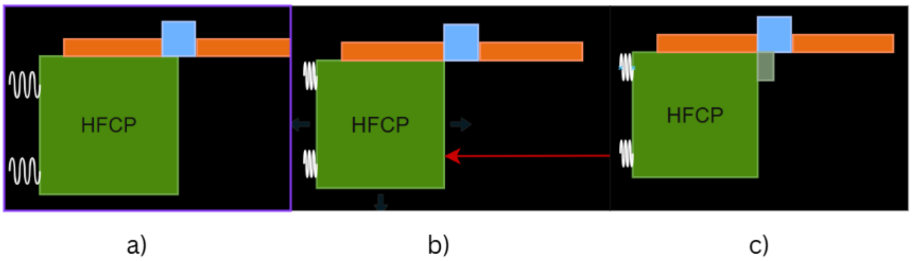

Figure 9.23: Method 2 to self lock concept 15.

9.3.2 Discussion of concept 15

This concept shows promising results, especially regarding the locking mechanism. However, several aspects still need to be investigated in greater detail. Since the proposed solution involves major modifications to the existing design, a detailed proposal for these modifications must be developed. The addition of an extra piston also requires modifications to the electronics and control software. Furthermore, the method for safely braking the drum must be investigated further. These aspects are beyond the scope of this master's thesis.

9.4 Push lock mechanism (Concept 17)

The main challenge in this concept is ensuring that the black plate is only actuated during HFCP deactivation. To solve this problem, an approach similar to the one used in concept 15 is used. In this approach the black plate is connected to a ring located outside of the drum. The ring is connected to the drum but can move axially relative to the drum. The connection is achieved through a link arm via a groove in the drum. A schematic figure for this concept in both activated and non-activated phase is shown in figure 9.24. To deactivate the lock, an auxiliary small piston needs to provide an axial force (figure 9.24 b)) that moves the ring in the axial direction. When the ring is moved, the black plate will raise the spring-ramps objects, and the red plate will be ejected from the HFCP engagement region via the spring between the plate and the HFCP.

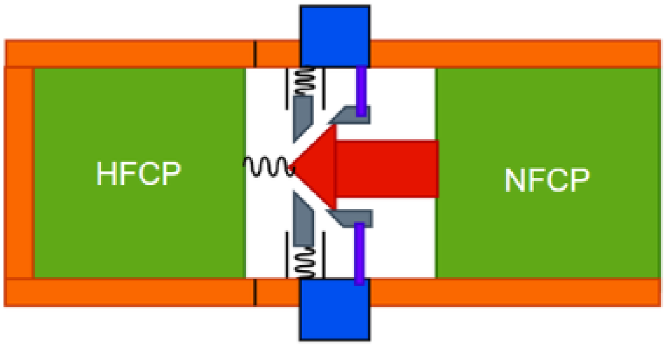

a)

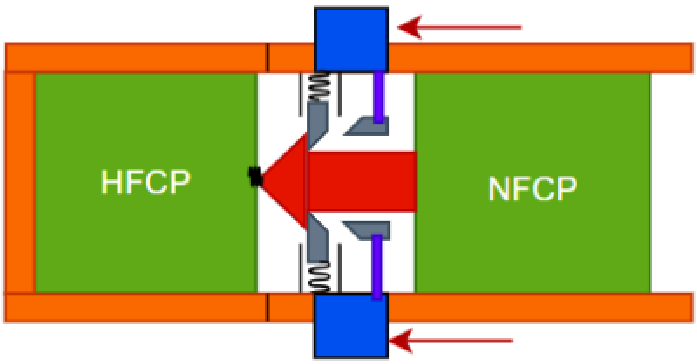

b)

Figure 9.24: A section of concept 17, a) the mechanism is not activated. b) the mechanism is activated.

The free body diagrams for each clutch pack in normal and overlock modes, respectively, are shown in figure 9.25

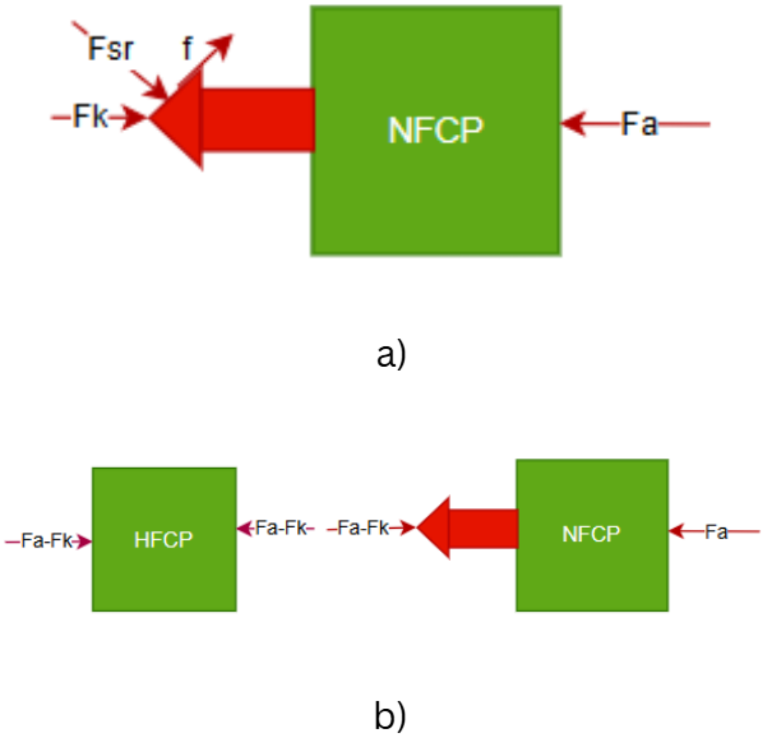

Figure 9.25: Free body diagram for each mode, a) Normal mode. b) Overlock mode.

9.4.1 calculation

To evaluate the feasibility of the conical head mechanism, a static force analysis is performed. The core principle of this concept is the conversion of axial input force into radial displacement through a wedge interface.

9.4.2 Geometric Relations

The geometry of the conical section is defined by its axial length (L_c) and the radial displacement (h) it provides to the pistons. The cone half-angle, α, is the critical design parameter governing the mechanical advantage:

$$\tan(\alpha) = \frac{h}{L_c} \tag{9.30}$$

Given that the conical section length L_c, the angle α can be adjusted by varying the radial lift h required to fully engage the HFCP.

9.4.3 Force Equilibrium and Friction

The mechanism consists of a shaft with a conical head interacting with two radial pistons. The system is governed by two distinct spring forces:

- F_k: The axial return spring force acting directly on the shaft (as per the design schematic).
- F_{rad}: Two radial spring forces acting perpendicular to the shaft's travel direction via the pistons.

The main equation is given by:

$$F_{Total} = (F_K + 2 \cdot F_{Wed}) \tag{9.31}$$

Where F_{Wed} is given by:

$$F_{Wed} = (F_{sr} \sin\alpha + f \cos\alpha) \tag{9.32}$$

Where:

- F_{sr} is the normal reaction force acting perpendicular to the conical surface.
- f is the friction force acting along the surface, defined as $f = \mu F_{sr}$.
- μ is the coefficient of friction between the shaft and the piston.

The normal force (F_{sr}) acting on the contact interface is a function of the radial spring resistance (F_{rad}) and the cone geometry. By resolving the forces in the radial direction, the following relationship is expressed as:

$$F_{sr} = \frac{F_{rad}}{\cos\alpha - \mu \sin\alpha} \tag{9.33}$$

By substituting the expression for the normal force (F_{sr}) into the axial equilibrium equation for the wedge, we obtain the following relationship for F_{wedge}:

$$F_{wed} = \left(\frac{F_{rad}}{\cos\alpha - \mu \sin\alpha} \right) \cdot (\sin\alpha + \mu \cos\alpha) \tag{9.34}$$

By rearranging the terms to consolidate the geometric and frictional components, the expression is simplified to:

$$F_{wed} = F_{rad} \left(\frac{\sin\alpha + \mu \cos\alpha}{\cos\alpha - \mu \sin\alpha} \right) \tag{9.35}$$

Dividing both the numerator and the denominator by $\cos\alpha$ yields the final practical form:

$$F_{wed} = F_{rad} \left(\frac{\tan \alpha + \mu}{1 - \mu \tan \alpha} \right) \tag{9.36}$$

9.4.4 Final Actuation Calculation

To initiate movement, the total hydraulic force (F_{total}) must overcome both the axial spring and the transformed resistance of the radial pistons. By analyzing the equilibrium at the contact interface, where F_{sr} is the normal reaction force and μ is the friction coefficient, the following is derived:

$$F_a = F_k + 2 \cdot F_{rad} \left(\frac{\tan \alpha + \mu}{1 - \mu \tan \alpha} \right) \tag{9.37}$$

The term in the parentheses represents the mechanical advantage of the wedge, accounting for frictional losses across the two contact surfaces.

9.4.5 Final Actuation Without friction

In a high-performance LSD environment with optimal oil lubrication, the friction coefficient μ can be approximated as zero ($\mu \approx 0$). This simplifies the model to a purely geometric relationship, where all energy is assumed to be utilized for spring compression:

$$F_a = F_k + 2 \cdot F_{rad} \tan \alpha \tag{9.38}$$

To avoid transfer of pressure to the HFCP while only the NFCP is required to be engaged, a gap is to be placed before the spring rests on the conical shape. Thus, F_k is negligible in the calculation of the activation force. Thus, the force required to activate the HFCP is given by:

$$F_a = 2 \cdot F_{rad} \tan \alpha \tag{9.39}$$

9.4.6 Variable Definitions

The following table summarizes the physical parameters and variables used in the analytical derivation of the actuation force:

Table 9.4: Parameters for the Conical Actuation Mechanism

Symbol	**Description**	**Unit**
F_{total}	Total axial force required for actuation	[N]
F_k	Axial return spring force (Shaft spring)	[N]
F_{rad}	Radial threshold spring force (Piston spring)	[N]
α	Cone half-angle	[rad]
μ	Coefficient of friction at the contact interface	[-]
L_c	Axial length of the conical section	[m]
h	Radial displacement (lift) of the piston	[m]

9.4.7 Push lock mechanism Discussion

The mechanism is theoretically capable of meeting the project requirements. However, after evaluating the equations using realistic numerical values and adhering to customer specifications, it is evident that challenges remain. Even with an optimized cone angle, the axial hydraulic force is substantial, and the springs situated on the wedges are too space-constrained to counteract such high forces. Consequently, the HFCP engages at significantly lower than the pressure required for reliable HFCP engagement. Therefore, the mechanism is considered most effective if utilized as a locking mechanism rather than activation mechanism.

Chapter 10

Final Development and Design

In this chapter, the further development of the ball ramp concept (Concept 13) will be presented. The working principles will be further investigated through calculation and the challenges that have been pointed previously will be discussed further. Eventually, a detailed CAD design of the concept will be presented.

10.1 Final Development

For a properly working mechanism the following configuration is chosen: the fix plate will be radially and axially fixed to the drum, thus it will have angular velocity and torque that is equal to that of the drum and steel discs. The left plate is connected to the fix plate, and the right plate is mounted on the hub by a bearing. The balls are fitted between the fix plate and the right plate. Since the right plate is mounted on a bearing, when the LSD is not used it will rotate with the same angular velocity as the fix plate, because the rotation from the fix plate is moved to the right plate through the balls.

To the right of the right plate, there will be the activation clutch placed. The axial length of the activation clutch does not need to be included in the axial length of the mechanism, because the activation clutch can also contribute to the NFCP. This point will be discussed further in the discussion 11.3. The activation clutch is separated from the NFCP via a bearing, this is needed to prevent high pressure from building up in the activation clutch for low force, which can activate the mechanism easily. A schematic picture of the arrangement is shown in figure 10.1.

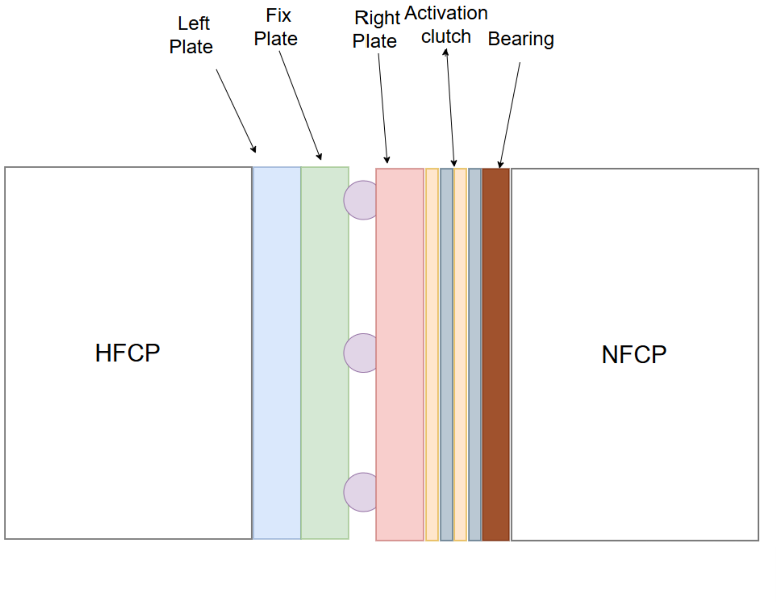

Figure 10.1: Schematic figure for the arrangement of the plates and activation clutch.

The activation of this mechanism is carried out in the following way: the pressure applied to the NFCP is forwarded through the bearing, activation clutch, right plate, and balls to the fixed plate. The fixed plate prevents the pressure from being further transferred to the left plate and the HFCP. This condition is maintained until a specific threshold pressure is reached. When the pressure applied to the NFCP exceeds this threshold, the right plate rotates. This rotation allows the balls to move and come into contact with the left plate. This means that the pressure is now transmitted through the NFCP, bearing, activation clutch, right plate, balls, left plate, to the HFCP, and the LSD is now operating in overlock mode. This means that any pressure applied to the NFCP will also be applied on the HFCP, as long as this pressure is below the threshold, because pressure equal to or greater than the threshold will rotate the right plate again. In other words, to deactivate the mechanism and restore the LSD to its normal mode, the pressure on the NFCP must exceed the threshold pressure once again.

The threshold pressure described above is corresponding to maximum torque that the ball ramp can take and still remain in equilibrium (not rotate), this is given by equation 9.4. The design parameters in equation 9.4 has been chosen with respective to the geometrical constraints, and the friction coefficient is chosen as maximum value for steel on steel with lubrication according to tribological tests[15]. The parameters for equation 9.4 are presented in table 10.1.

Table 10.1: Chosen design parameters and approximate friction coefficient.

Parameter	**Value**
α	$13°$
μ	0.08
R_e	47 mm

Using parameters in table 10.1 and the 50% and 60% of the maximum actuator force according to F_{max} in equation 9.4 yields the following torques respectively

$$T_c = 185[Nm] \tag{10.1}$$

$$T_c = 234[Nm] \tag{10.2}$$

The torque from the activation clutch at 50% and 60% of the maximum actuator force is given in figure 10.2 and 10.3 respectively.

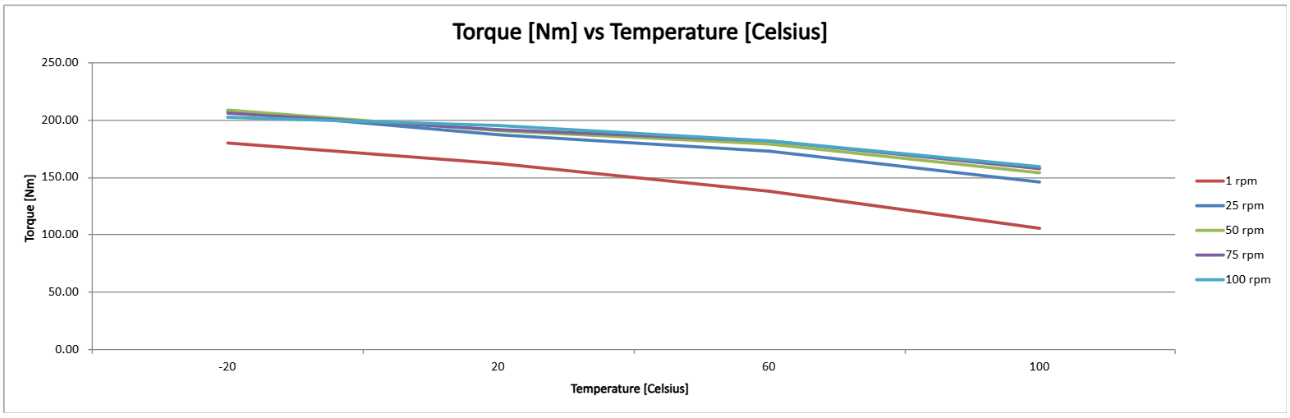

Figure 10.2: The torque capacity from the activation clutch for 50% of F_{max}.

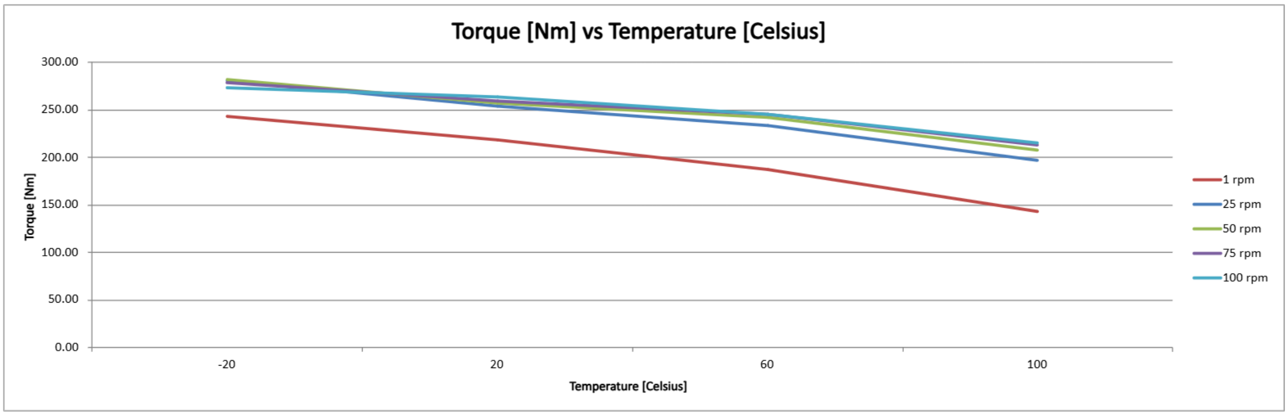

Figure 10.3: The torque capacity from the activation clutch for 60% of F_{max}.

Figure 10.2 shows that the provided torque from the activation clutch is less than the torque needed for activate the ball ramp (equation 10.1) at actuator force 50% of F_{max} (For temperature above 20 $C°$). When the actuator force is increased to 60% of F_{max}, the activation clutch provides enough torque for the activation of the ball ramp (more than the torque in 10.2). This result holds for temperature less than 60 $C°$ as figure 10.3 shows. Thus, 60% of F_{max} works as an activation force but only within specific temperature ranges as shown above.

10.2 Final Design

The final design of the fix plate, right plate and left plate is shown in Figures 10.4–10.6.

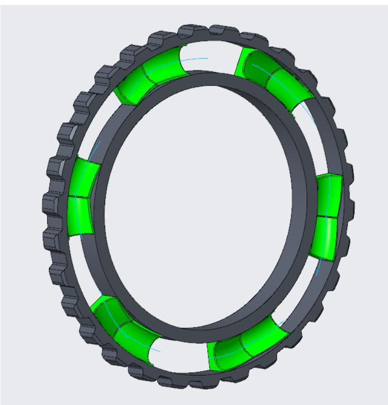

Figure 10.4: Final design of the fix plate.

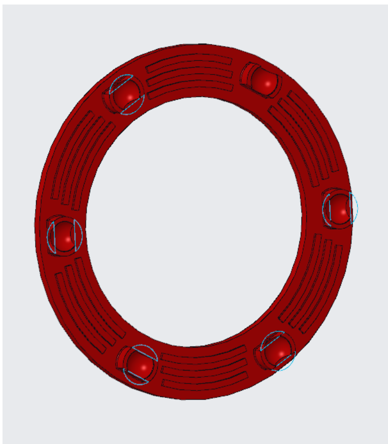

Figure 10.5: Final design of the right plate.

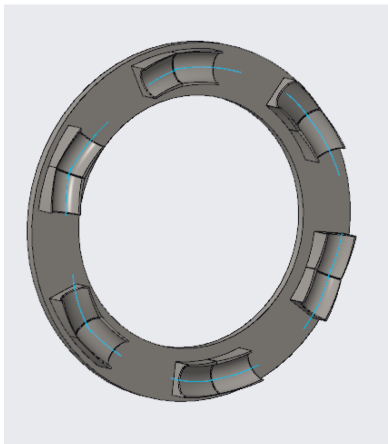

Figure 10.6: Final design of the left plate.

The fixed plate has the largest thickness, as it is designed to take most of the load, and it is also splined to fit into the drum and prevent relative rotation. The right plate contains ball-holder positions, where the balls are placed, and these positions will be used to push the balls along the ramp. Between these holders, a pattern of circular arcs has been introduced to increase strength and reduce deflection in those regions. The left plate is similar in shape to the fixed plate in terms of the grooves, but it has no splines and a smaller thickness.

The groove is rounded in both the radial and axial directions and is tilted, as illustrated in the section and detailed views in Figure 10.7. This design enables the ball to operate within the fixed plate, thereby reducing the overall axial space required by the mechanism. A further advantage of this groove geometry is that the contact between the ball and the groove forms a semicircular arc rather than a point contact, which leads to lower stress concentrations.

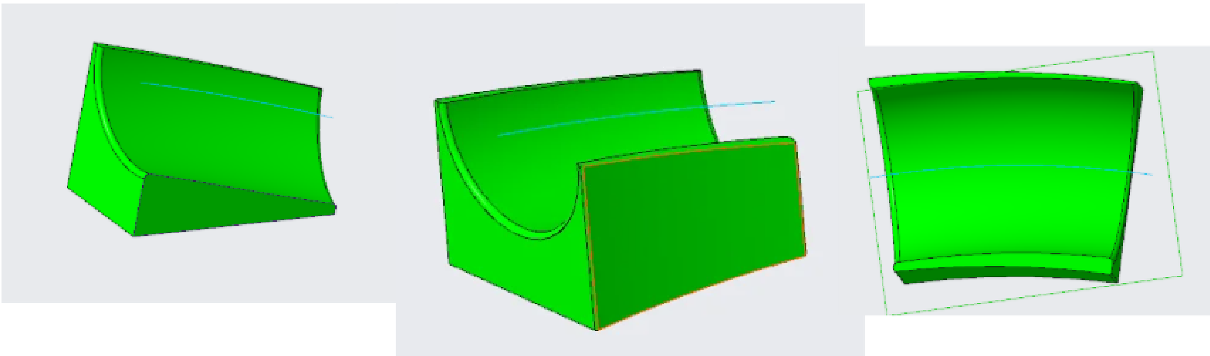

Figure 10.7: Section view of the groove and views from different angles.

The assembly of all plates is shown in Figures 10.8–10.11. The four sections provide a complete view of the assembled configuration.

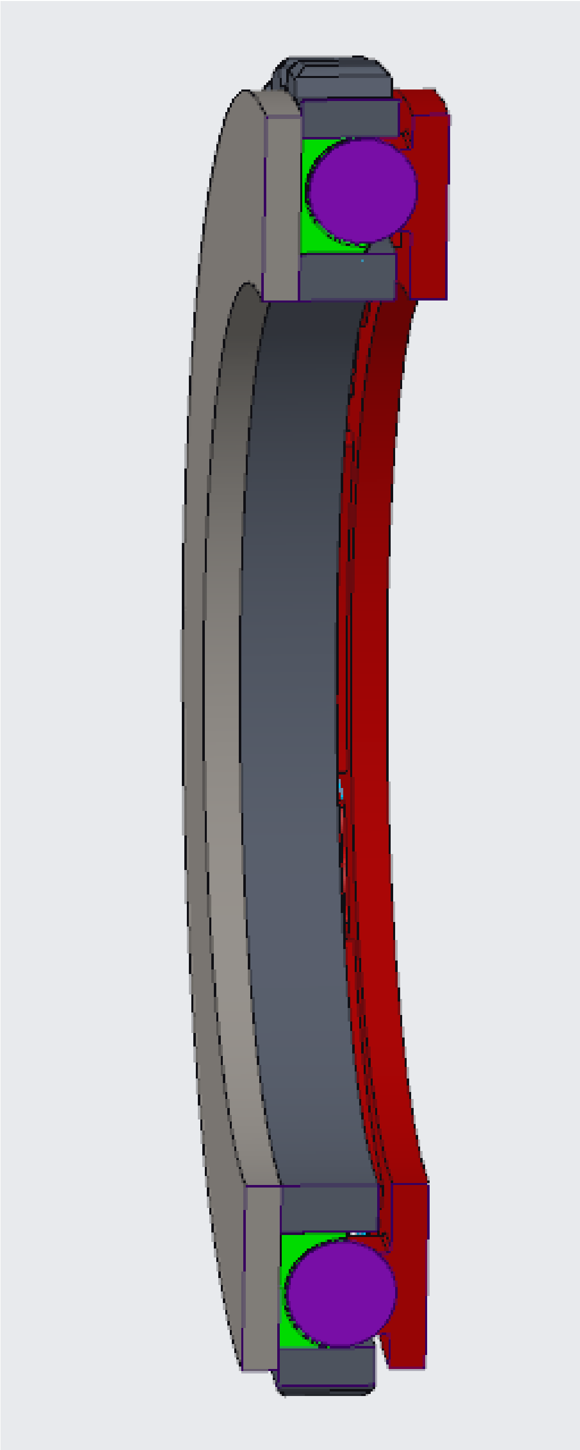

Figure 10.8: Section 1 of the assembly.

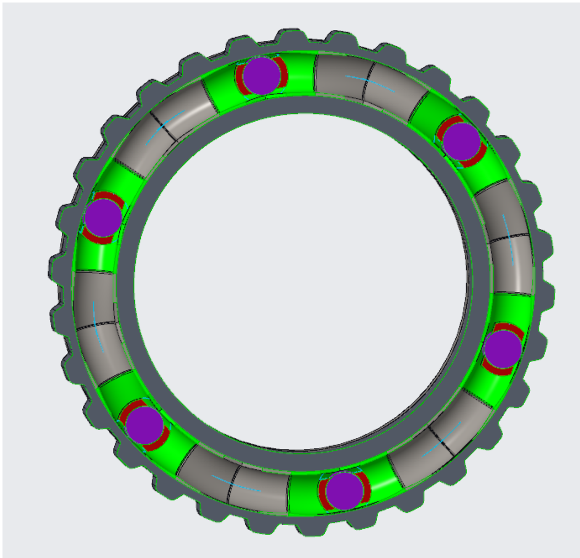

Figure 10.9: Section 2 of the assembly.

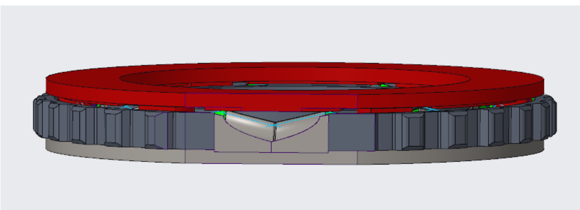

Figure 10.10: Section 3 of the assembly.

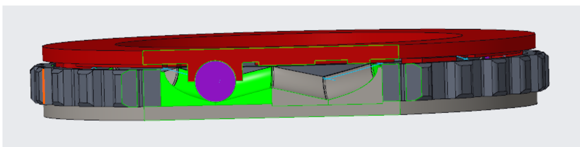

Figure 10.11: Section 4 of the assembly.

10.3 Result

As previously mentioned, BorgWarner had several requirements for the activation mechanism which are presented in section 6. These requirements are about the used actuator force, activation size and torque transfer during normal and overlock mode.

10.3.1 Actuator Force

The requirement of the actuator force is already fulfilled since the continuous force that will be used during the normal and overlock mode in the range of $50-60\%$ of the maximum actuator force F_{max}. In addition the used force range is within the force range discussed in Boundary Conditions (section 4.1), and the ECU of the actuator will not be overheated during the operation.

10.3.2 Mechanism Size

The axial size of the mechanism is given by a_1 and a_2, which correspond to the minimum and maximum axial size, respectively, i.e., when the ball ramp is closed and when the ball ramp is fully open. A relative comparison between a_1 and a_2 and the maximum allowed axial length of the mechanism a is presented below.

$$\frac{a_1}{a} = 0.775 \tag{10.3}$$

$$\frac{a_2}{a} = 0.9 \tag{10.4}$$

Thus the axial length requirements is also fulfilled, however more detail is provided in the discussion (section 11.3) about this requirement.

10.3.3 Torque Transfer

The friction coefficient is dependent on the angular velocity and the temperature, thus an average value will be used to estimate the clutch pack capacity. A relative comparison of the yielded and the required torque from each clutch which was presented earlier in section 6, is presented in table 10.2.

Table 10.2: Summaries torque capacity.

	NFCP torque	***HFCP torque***	***Total torque***
Torque capacity	45% (normal mode) 45% (overlock mode)	68% (overlock mode)	53% (overlock mod e)

10.4 Discussion

Although this concept shows potential, several challenges remain with this solution. As previously mentioned, the axial occupation may be a problem in this concept. The current design has a maximum axial occupation when the balls are at the highest point of the groove. The axial occupation at that point is around 90% of the maximum allowed length, which is still below the maximum length of the activation mechanism specified in the customer requirements.

However, the length of the activation clutch is not included here, because during normal mode, the activation clutch would typically contribute to NFCP. However, this is not entirely correct, because there are two possible routes for the torque, and it is currently unknown how the torque is transferred. This is illustrated in Figure 10.12. To verify the torque flow path and ensure that the ball ramp receives sufficient torque (route A) and that the activation clutch will contribute to the NFCP in normal mode, multiphysics simulations of the LSD and the activation clutch need to be performed. Eventually, the length of the bearing also needs to be investigated further. By adding a bearing, the maximum length of the activation mechanism may be exceeded.

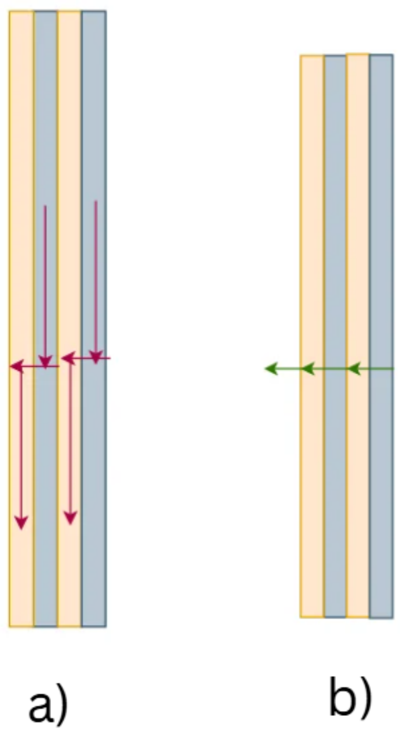

Figure 10.12: Possible routes for torque transfer.

The difference in angular velocity of the drum and the hub is critical for activating the mechanism. Further simulations are required to better understand how the drum and hub rotate relative to each other under different scenarios and to verify that the ball ramp mechanism is properly engaged. It is also important to analyze how the clutch behaves under different activation forces. Slip at the operating force is generally not a concern; rather, the critical case occurs when the force is high enough to fully lock the clutch and prevent sliding between the friction and steel discs. According to engineers at Borg-Warner, it is uncommon for the drum and hub to have identical angular velocities, but simulations would provide a clearer and more definitive understanding of this behavior. However, performing detailed simulations of the LSD is a substantial task and lies beyond the scope of this master's thesis.

Another challenge is during the deactivation of the overlock mode. As previously mentioned the left plate has the ability to move axially relative to the fix-plate. So when the overlock mode is engaged and the pressure is forwarded from the NFCP to the HFCP through the left plate, the left plate will have an axial displacement. Thus the fix-plate and left plate will not be aligned and that may make it hard for the ball to move from the left plate groove back to the fix-plate groove and deactivate the overlock mode. However, the misalignment is equal to the elastic deformation of the HFCP, when using 60% of F_{max} the elastic deformation of the HFCP is around 5 μm, which is too small compared to the size of the ball. Thus, the deactivation of the overlock mode will not be affected by the axial movement of the left plate.

A key consideration is that during activation of the overlock mode, the balls will move along the ramp of the fixed plate. This motion of the balls corresponds to an axial motion of the right plate in a direction opposite to the actuator force direction. This is only possible if the force from the right plate is larger than the actuator force, which means that the force balance in Equation 9.3 is not satisfied. The mechanical analysis performed in this thesis is insufficient to address this issue. This is because the right plate force depends on the normal force presented in the free-body diagram in Figure 9.2, and the normal force depends on T_c which represents the torque provided by the activation clutch to the ball ramp. Currently, it is unknown how the torque transfer behaves. For a better understanding of the magnitude of T_c, a multiphysics simulation needs to be conducted.

Chapter 11

FEA Simulation

In this section, FEM simulations will be conducted on the ball ramp concept. The purpose of these simulations is not to investigate the material behavior in detail, but rather to verify that the concept can withstand the operational loads without excessive deformations or stresses. The simulations will also help identify weak points in the design that may require further development. The components were analyzed using ANSYS Workbench 2025 R2. The simulations covered different scenarios:

- loads during Normal mode operations
- Loads during transitions from Normal mode to overlock mode

The simulation workflow followed an iterative approach, with multiple simulations conducted in parallel with the development of the final concept. This section presents the final simulations and their corresponding results.

11.1 FEA Simulation Setup

The simulation setup is a critical factor, because the result of the simulation will depend upon it. To get a result that is relevant and reflect real world deformation, the setup should be optimized to simulate real operational condition of the assembly. The setup includes boundary conditions, contact definitions, mesh refinement, and applied loads.

11.1.1 Materials and Connections

Structural steel was assigned to all components within the assembly even the balls. However, in real applications the balls have to be made from other material that have more strength and with some appropriate surface treatment. That is because all the pressure will go through the balls, and the contact regions are too small so the stress may be extreme on the balls. The data of the structural steel that has been used in the simulation is given in table 11.1

Table 11.1: The linear data of structural steel.

Property	Value
Young's modulus	210 GPa
Poisson's ratio	0.3
Yield stress	250 MPa
Density	7850 kg/m^3

The connection settings were configured to replicate the mechanical interactions of the physical product during a real-life activation scenario. The contacts between the balls and the other components of the mechanism were defined as frictional contacts, with friction coefficients according to 10.1.

In certain regions, contact occurs between the plates. Since these contact areas are small and the friction contribution is considered negligible, the interactions between these surfaces were instead defined as frictionless.

Furthermore, the fix-plate and the left-plate consist of several separate parts in the CAD model. In the final physical product, these components will be manufactured as single parts. However, due to the complex groove geometry, they were designed as separate bodies. The connections between the parts of the fix-plate/left-plate and the grooves were defined as bonded contacts.

11.1.2 Meshing

To achieve high numerical accuracy, a complex mesh was generated. While this increased the computational time, it ensured a more refined capture of stress concentrations. The global element size was set to 1.5 mm. The resulting mesh distribution is illustrated in Figure 11.1.

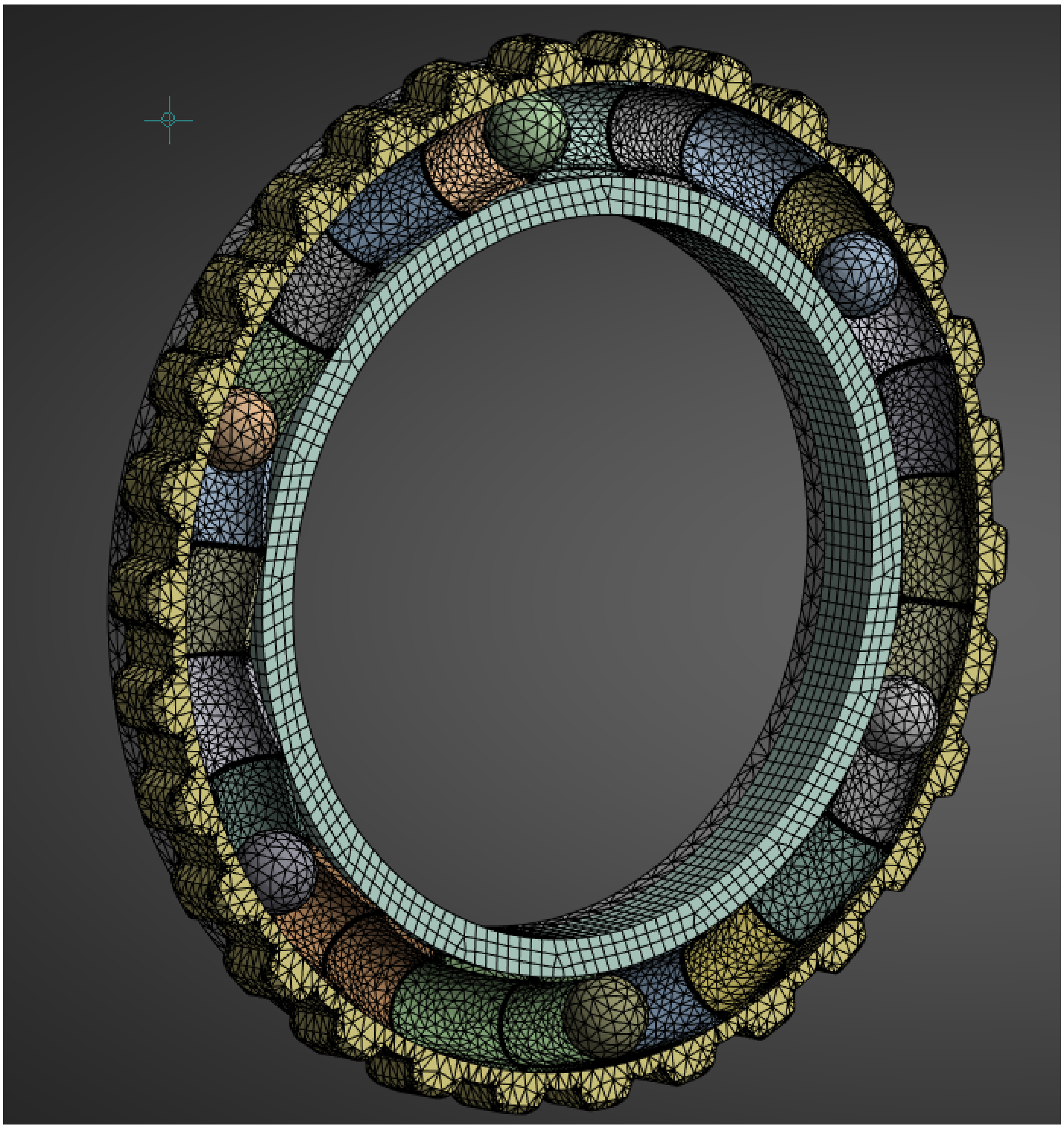

Figure 11.1: Mesh with 1.5mm sizing from the inside

11.1.3 Boundary Conditions and Loading

To simulate the resistance of the HFCP, a fixed support was applied to the left-plate to maintain equilibrium. The actuation force provided by the piston was simulated by applying a pressure load to the right-plate. Additionally, a clockwise torque representing the torque from the activation clutch. The values of the loads during the different scenarios is presented in table 11.2

Table 11.2: The values of loads during each simulation scenario.

Scenario	Pressure	Torque
1	2 MPa	185 Nm
2	2.7 MPa	234 Nm

11.2 Final Simulation Results

Two specific load cases were calculated. The first simulation focused on the Normal mode operation of the ball ramp, representing the loads described in scenario 1. In the second load case the loads under transition from normal mode to overlock mode and vice versa was focused on, which correspond to the loads described in Scenario 2. Two primary solutions were evaluated: **Total Deformation** and **Equivalent (von-Mises) Stress**.

11.2.1 Result Analysis: scenario 1

The results yielded reasonable values for both deformation and stress. Figure 11.2 illustrates the total deformation of the mechanism and its distribution across the right-plate.

Analysis of the ball ramp components, as shown in Figure 11.3, indicates that the highest points of deformation throughout the assembly are concentrated in the balls. This is expected due to the point-contact nature of the ball-ramp interface under high axial loads. The stress distribution is shown in figure 11.5.

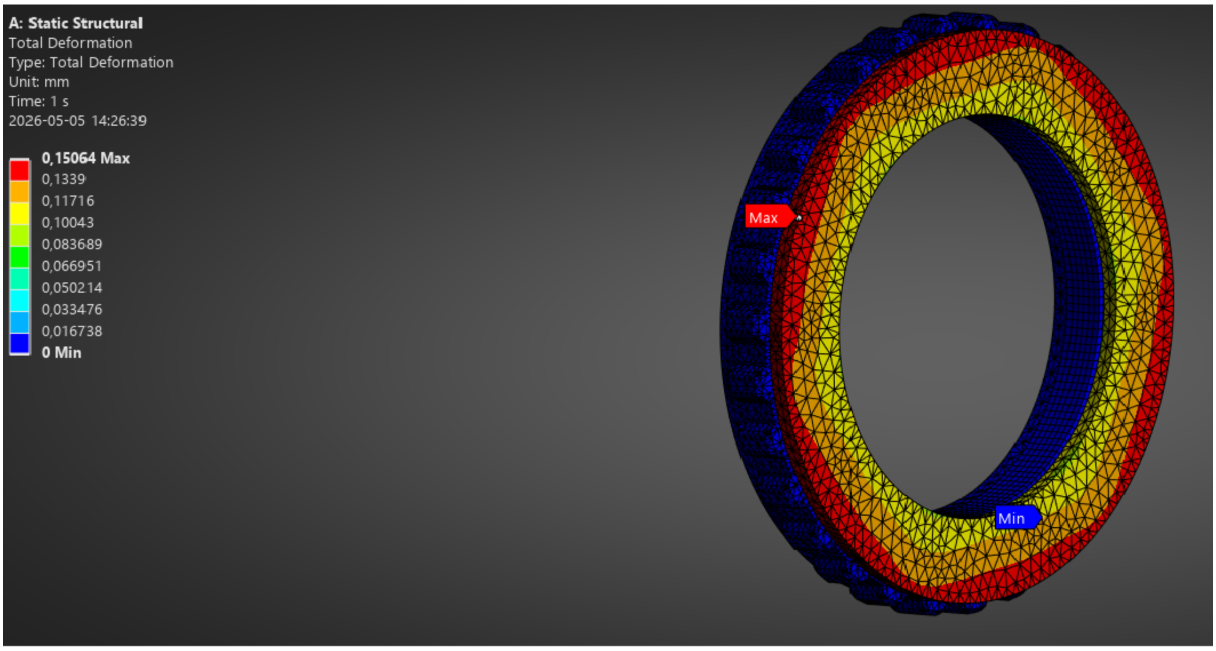

Figure 11.2: The deformation of the right-plate

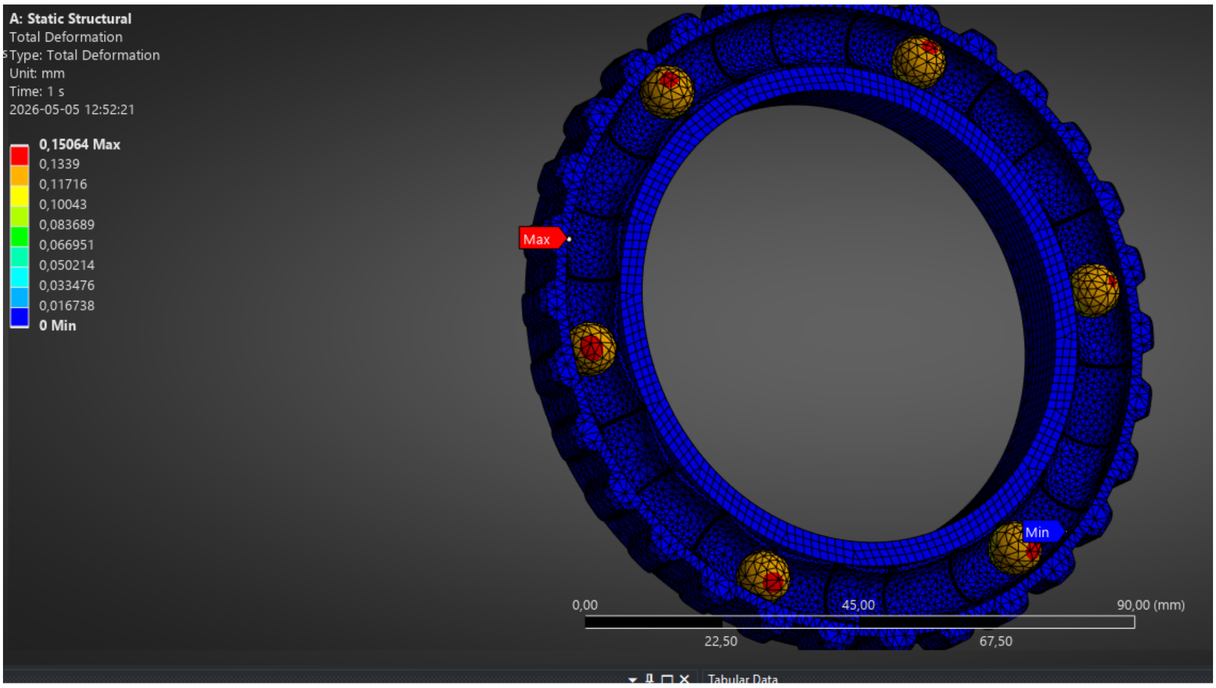

Figure 11.3: The deformation of balls

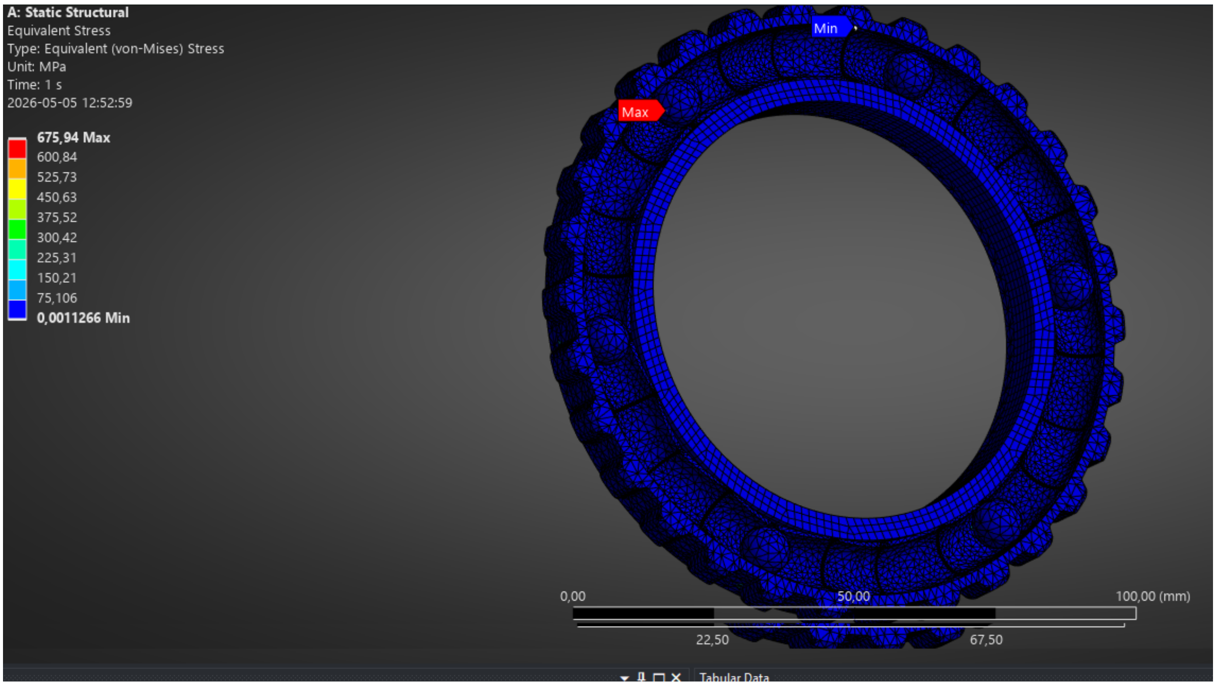

Figure 11.4: The stress of balls

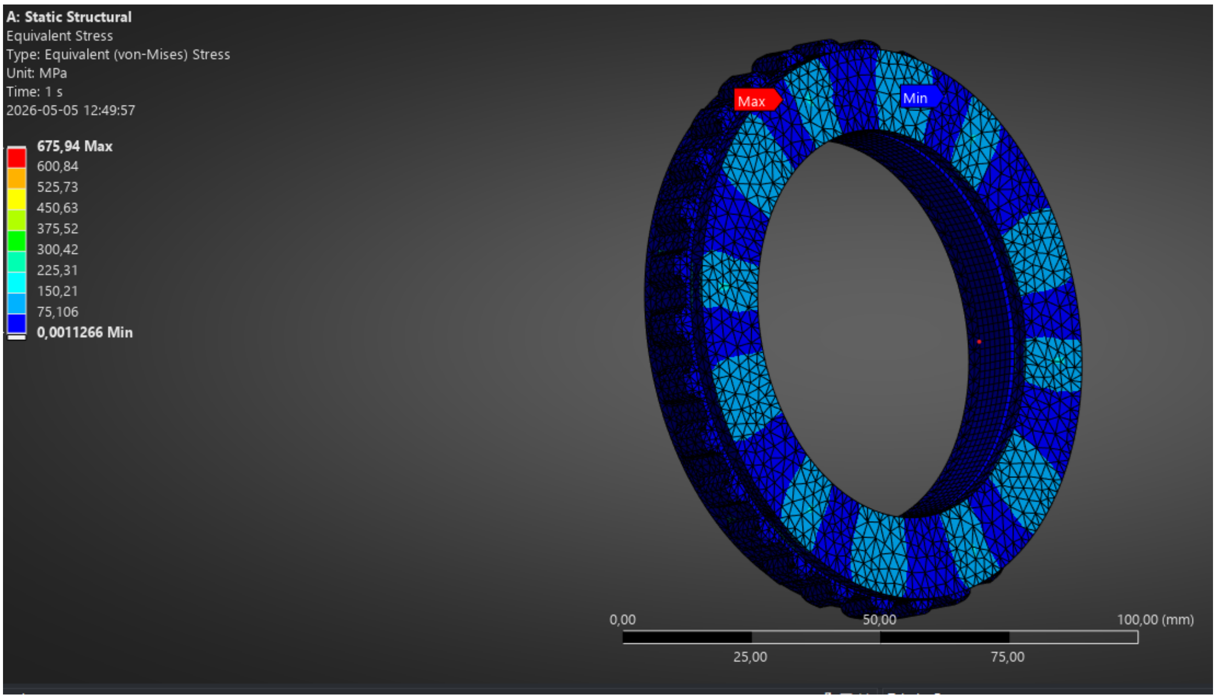

Figure 11.5: The stress distribution of the right-plate

11.2.2 Result Analysis: scenario 2

The second simulation was made on the mechanism with the ball ramp with the loads corresponding to Scenario 2. Stress and deformation results were higher as expected as the loads are higher, and they are shown in Figures 11.6-11.9.

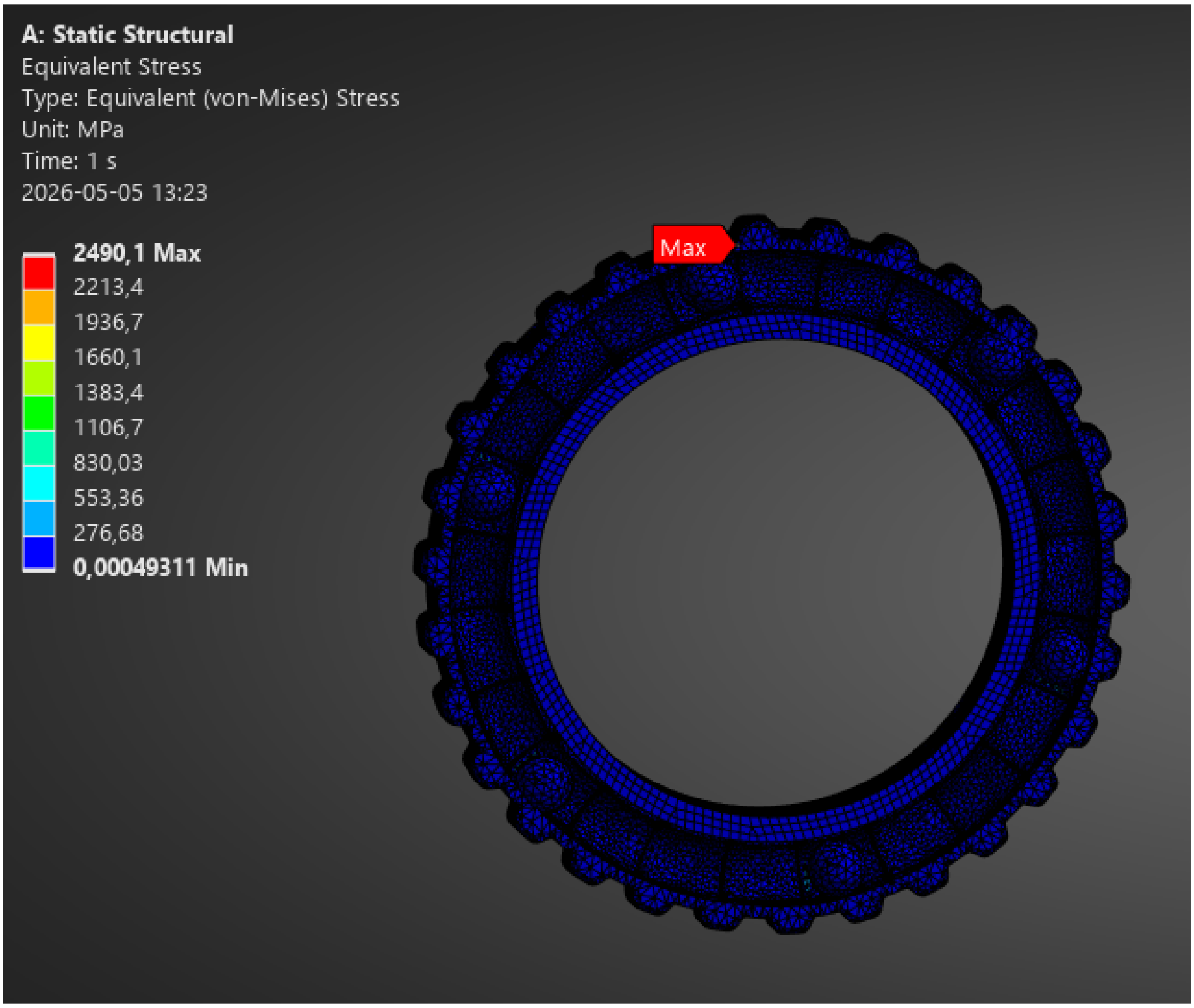

Figure 11.6: Stress distribution in the balls

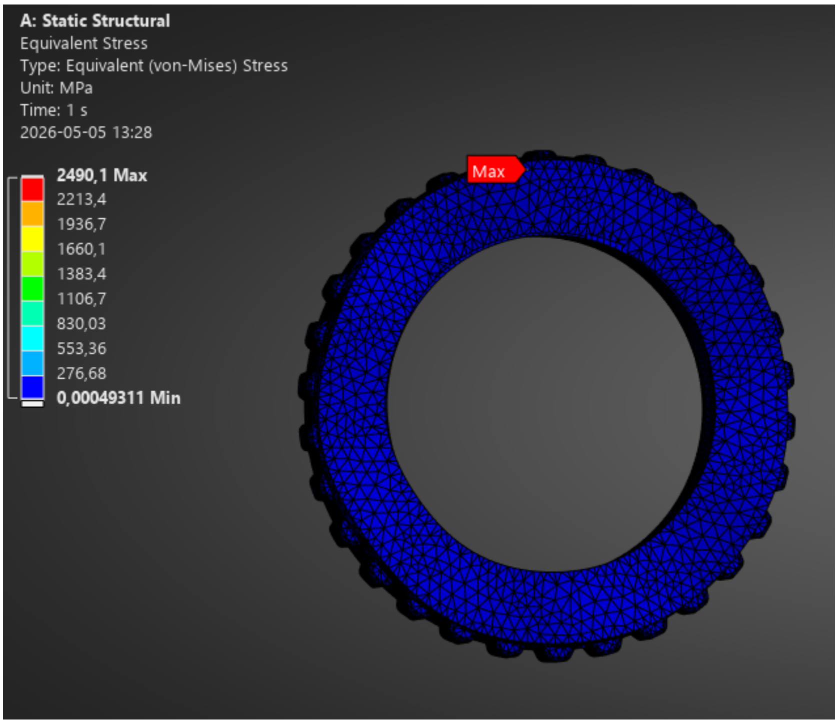

Figure 11.7: Stress distribution in the right-plate.

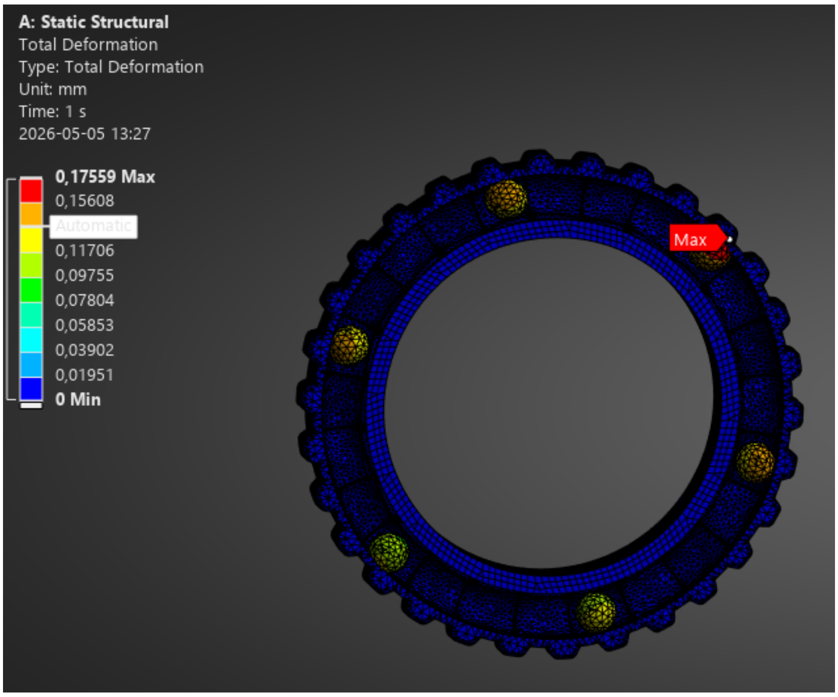

Figure 11.8: Deformation in the balls.

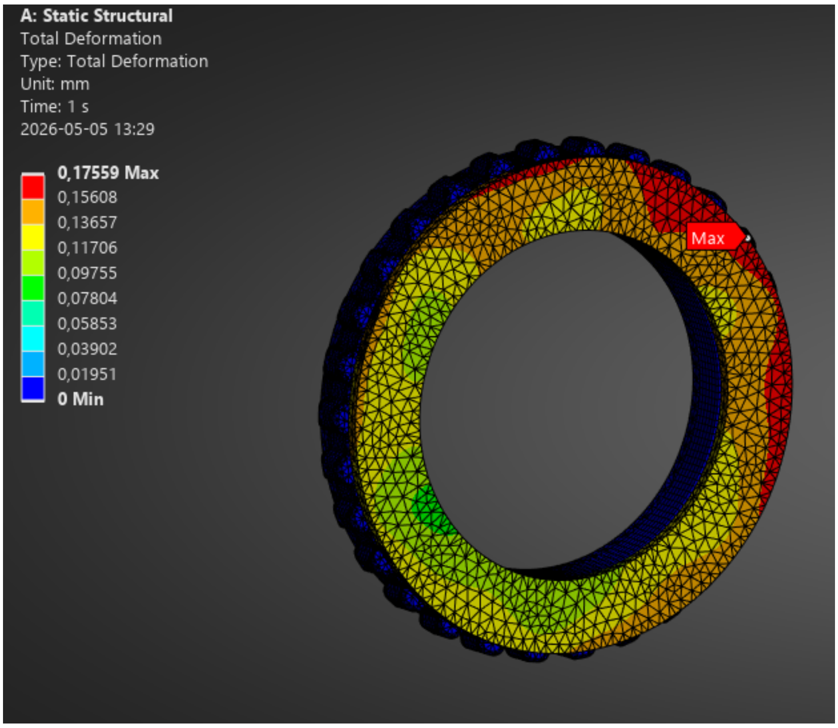

Figure 11.9: Deformation in the right-plate.

11.3 FEA Discussion

The results obtained from the simulations are considered reasonable, as both the deformation patterns and the regions of high stress are consistent with the loading conditions applied in the two scenarios. During Scenario 2, significantly higher stresses were observed. However, the regions with the highest stresses are very small and located in geometrically tight areas. Therefore, the elevated stress levels are likely caused by the presence of stress concentrations (stress risers) rather than representing critical stresses throughout the structure.

Another important aspect concerning the balls is the Hertzian stress, which refers to the localized contact stress that develops between two curved surfaces subjected to a load. According to a ball ramp specialist at BorgWarner, an appropriate Hertzian stress level for the balls is approximately 2600–2800 MPa. However, the calculated Hertzian stress between the balls and the grooves reached approximately 5000 MPa, which is significantly higher than the recommended values. Such high contact stresses may lead to severe damage to the balls and groove surfaces. Therefore, the FEM simulations performed in this work are not sufficient to draw definitive conclusions regarding the safety of the proposed ball and groove design under the applied loading conditions. Instead, a more detailed verification and contact stress analysis of the balls and grooves is required.

Chapter 12

Future Development

To ensure the functionality of the final concept, several critical aspects must be addressed before implementation. These primary considerations are discussed in the following sections.

12.1 Geometry Analysis

The shape and geometric configuration play a crucial role in the effective activation of the ball ramp mechanism. This includes the profile of the rounded grooves where the balls rest and the ball-retaining geometry of the right plate. While this thesis provides a detailed design that offers an understanding of the required shapes, further development is necessary to ensure smooth ball motion within the ramp mechanism. Refining the geometry through detailed functional simulations will be essential to optimize the mechanism's performance.

Material selection also plays a vital role in defining the geometry. Following internal discussions with BorgWarner, a sintered material was selected for the plate grooves to ensure more uniform pressure distribution across the contact surfaces. Furthermore, it was determined that the balls should be manufactured from hardened steel to withstand the operational loads.

12.2 Functionality Simulation

To verify the mechanism's performance, detailed simulations of the activation and deactivation cycles are required. While the Finite Element analysis (FEA) conducted in this thesis provided insights into deformation and stress distribution, it does not fully capture the dynamic functionality of the mechanism. Future work should focus on multibody dynamics or functional simulations to confirm that the system operates as intended under real-world conditions.

12.3 Selection of Friction Discs

As the activation torque is provided by a friction disc, the specific requirements for this component must be further evaluated. It may be necessary to move away from universal friction plates in favor of a specialized disc designed for this specific application. Since the disc will be subjected to high pressure and significant thermal load, selecting a disc that ensures system sustainability and durability is critical.

12.4 Locking Mechanism

Throughout this thesis, several locking mechanisms were discussed for various concepts; however, a final locking solution for the chosen concept has not yet been fully developed. Subsequent development must focus on designing and integrating a robust locking mechanism tailored to the final design to ensure operational stability.

Chapter 13

Conclusion

The primary objective of this thesis was to develop an activation mechanism integrated between a dual clutch pack within a Limited Slip Differential (LSD). This specific LSD utilizes a non-conventional approach compared to standard LSDs, which typically employ a single clutch pack. The mechanism was designed to meet customer requirements while adhering to a predefined set of performance criteria and constraints.

The research resulted in a technically sound and logical solution that fulfills the requirements without exceeding any design limitations. Throughout the project, an iterative design methodology was applied to address the problems that may arise.

The final concept, a ball ramp mechanism, demonstrated significant potential in meeting the specified performance targets with a high degree of accuracy. Both the simulation results and the mechanical design were thoroughly discussed and validated through consultations with industry experts at BorgWarner and academic supervisors at Lund University.

While the results are promising, the concept requires further development and dynamic simulation to fully verify the mechanism's functionality before moving toward production. The potential for future improvements, additional features, and continued optimization has been outlined to guide future development.

Bibliography

[1] P. S. Liu, J. F. Chin, H. Ab-Samat, Z. P. Xie, *Digital variant design V-model for rapid product development*, International Journal of Advanced Manufacturing Technology, 2025; 139:2103–2121. Available from: `https://doi.org/10.1007/s00170-025-15982-1`

[2] S. Verhelst, *Automotive Technology*, Faculty of Engineering and Architecture, Ghent University, Ghent, 2017.

[3] A. Khajepour, M. S. Fallah, A. Goodarzi, *Electric and Hybrid Vehicles: Technologies, Modeling and Control – A Mechatronic Approach*, John Wiley & Sons, Hoboken, NJ, 2014.

[4] Lars Frömmig, *Basic Course in Race Car Technology: Introduction to the Interaction of Tires, Chassis, Aerodynamics, Differential Locks and Frame*, Springer Vieweg; 2019, pp 343–391

[5] M. Guiggiani, *The Science of Vehicle Dynamics: Handling, Braking, and Ride of Road and Race Cars*,3rd ed , Springer, Cham, 2018, pp. 132–157.

[6] M. Gadola, D. Chindamo, B. Lenzo, *Revisiting the mechanical limited-slip differential for high-performance and race car applications*, Engineering Letters, 2021; 29(3):824–839. Available from: `https://shura.shu.ac.uk/30090/`

[7] M. Mägi, K. Melkersson, M. Evertsson, *Maskinelement*,Studentlitteratur, Lund, 2017, p.330, p.148.

[8] E. Winterfeldt, *Activation Solution for Dual Functional Clutch Pack for Limited Slip Differential*, Master's thesis, Division of Innovation, Department of Design Science, Faculty of Engineering LTH, Lund University, 2025.

[9] G. Dong, F. Wang, D. Meng, H. Chu, J. Hong, B. Gao, *Modeling and control of ball-ramp electromechanical clutch actuator for in-wheel AMT of electric vehicles*, Mechanism and Machine Theory, 2020; 151:103915. Available from: `https://www.sciencedirect.com/science/article/pii/S0094114X22003755`

[10] T. Suganuma, *Ball ramp clutch*, US Patent 8,596,436 B2, 2013. Available from: https://patents.google.com/patent/US8596436B2/en

[11] W. J. Shimanckas, *Ball ramp actuator*, US Patent 3,390,593, 1968. Available from: https://patents.google.com/patent/US3390593/en

[12] S. Yamazaki, K. Sato, *Ball ramp mechanism and power transmission device*, US Patent 10,378,633 B2, 2019. Available from: https://patents.google.com/patent/US10378633B2/en

[13] Y. Kamiya, S. Yamazaki, *Ball ramp mechanism and clutch device*, US Patent 11,231,098 B2, 2022. Available from: https://patents.google.com/patent/US11231098B2/en

[14] L. Shijie, X. Nan, *Ball ramp clutch for vehicle*, CN Patent 108,374,846 B, 2020. Available from: https://patents.google.com/patent/CN108374846B/en

[15] E. Oblak, M. Kalin, *Relationship Between the Nanoscale Topographical and Mechanical Properties of Tribochemical Films on DLC Coatings and Their Macroscopic Friction Behavior*, Tribology Letters, 2015; 59:14. Available from: https://doi.org/10.1007/s11249-015-0560-z

Chapter 14

Appendix

14.1 Appendix A - Concepts

14.1.1 Spring-Loaded Shaft Mechanism(Concept 1)

Working principles: This mechanism utilizes a shaft assembly positioned between the High-Pressure Friction Clutch Plate (HFCP) and the Normal-Pressure Friction Clutch Plate (NFCP). By arranging multiple springs in a predefined pattern, the system creates a resistance that must be overcome for the shaft to engage with the HFCP. Once the springs reach their solid height (full compression), the mechanical force is transferred directly to the HFCP. A schematic illustration is shown in figure 14.1.

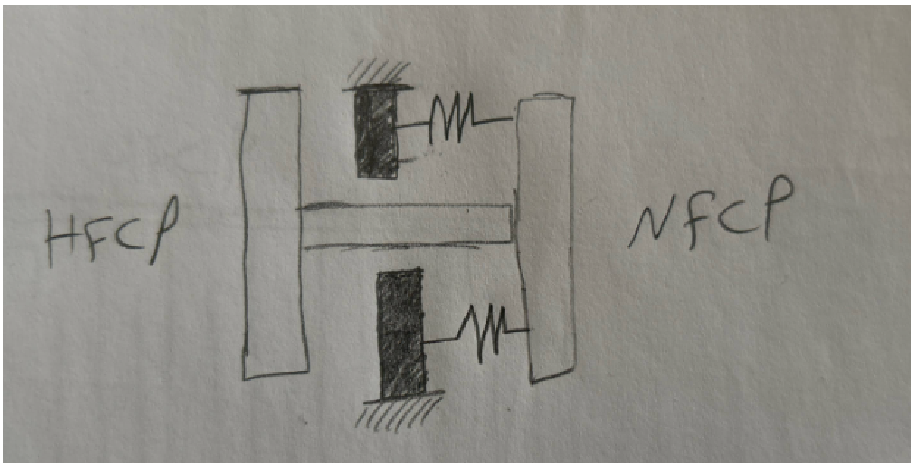

Figure 14.1: Schematic drawing of concept 1.

Advantages:

- **Mechanical Simplicity:** The straightforward design minimizes the number of moving parts, effectively reducing potential failure points and increasing long-term reliability.

- **Cost-Effectiveness:** Due to its uncomplicated architecture, the mechanism is inexpensive to manufacture and can be seamlessly integrated into existing systems with minimal modifications.

Disadvantages:

- **Material Stress Constraints:** Identifying spring materials capable of sustaining high cyclic loads and extreme compressive forces without deforming or failing is a significant engineering challenge.
- **Structural Rigidity:** The inherent reliance on spring deflection may compromise the overall axial rigidity of the assembly, potentially leading to alignment issues under heavy loads.

Technical Summary: The design features a spring-actuated shaft interface situated between the HFCP and NFCP. By configuring the spring constants and spatial patterns, the engagement threshold can be precisely tuned. While the design offers significant cost benefits and simplicity, its viability depends on overcoming material fatigue limits and ensuring the assembly remains rigid under peak operational pressures.

14.1.2 Shaft with Conical Head Mechanism (Concept 2)

Working principles: This design utilizes a translation to compression interface situated between the NFCP and HFCP. The mechanism features a shaft with a conical head that interfaces with vertically aligned springs. As axial force is applied, the angled surface of the cone acts as a mechanical ramp, converting axial motion into lateral/vertical displacement to compress the springs. Once the springs reach a specific load threshold, the axial force is transmitted directly to engage the HFCP. A schematic figure of this concept is shown in 14.2.

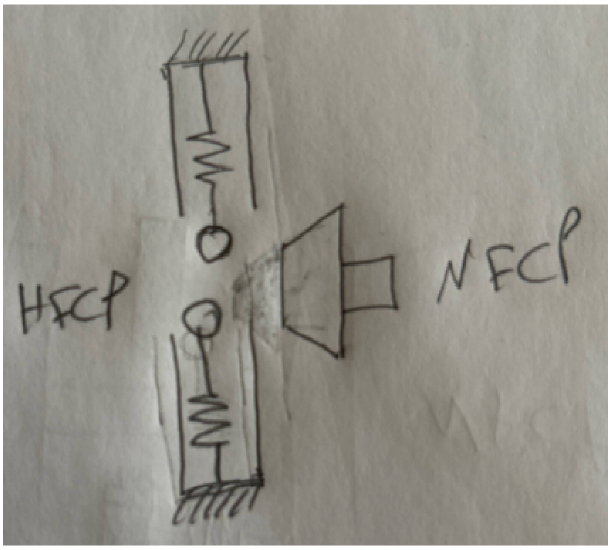

Figure 14.2: Schematic of the conical ramp-and-plunger actuation system.

Advantages:

- **Cost-Effective Implementation:** The mechanism relies on fundamental geometric principles and traditional machining, making it relatively inexpensive to manufacture compared to complex electronic actuators.
- **Versatility:** The design is highly adaptable and can be integrated into various Limited Slip Differential (LSD) models with minimal modifications to the core housing architecture.
- **Linear Tuning:** The engagement characteristics can be precisely tuned by altering the cone angle (mechanical advantage) or the spring rates of the vertical coils to meet specific vehicle performance profiles.

Disadvantages:

- **Packaging Constraints:** Fitting a vertical spring assembly within the tight radial tolerances of a standard differential housing presents a significant packaging challenge.
- **Structural Rigidity:** The requirement for multi-axis movement introduces additional degrees of freedom, which may decrease the overall axial rigidity of the assembly under high-torque conditions.
- **Component Modification:** Implementation requires structural redesign of the rotating drum or carrier to accommodate the vertical spring seats and shaft travel.
- **Inertial Lag:** The conversion of motion from axial to vertical introduces mechanical hysteresis, potentially resulting in a slower engagement response that requires compensation in the control calibration.

Technical Summary: The design employs a conical ramp and plunger system to manage the transition between clutch packs. By using a cone-headed shaft to actuate vertically oriented springs, the mechanism provides a tunable force threshold for HFCP engagement. While advantageous for its simplicity and LSD cross-compatibility, the design faces challenges regarding radial space claims and the inherent mechanical hysteresis caused by the multi-axis force transfer.

14.1.3 Belleville Spring Washer Mechanism (Concept 3)

Working principles: This design incorporates Belleville spring washers (conical disc springs) positioned concentrically between the High-Pressure Friction Clutch Plate (HFCP) and the Normal-Friction Clutch Plate (NFCP) as shown in figure 14.3. The washers function as a calibrated force-transmission element; once the axial load exceeds a specific threshold, the springs deflect toward a flattened state. This transition allows for the direct transfer of the resultant axial force to the HFCP, effectively engaging the secondary clutch stage.

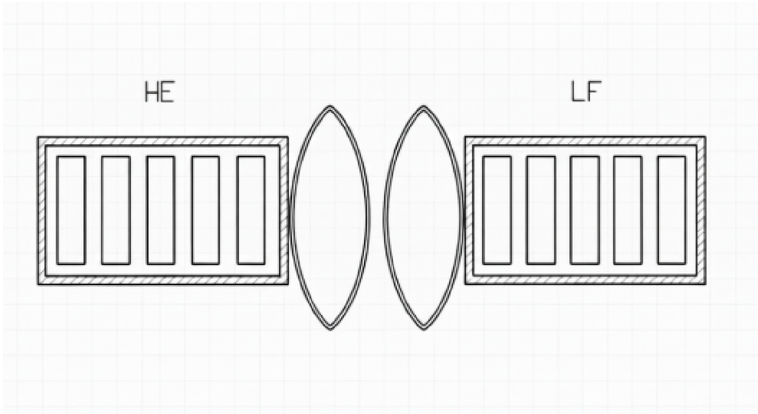

Figure 14.3: Clutch activation assembly utilizing a Belleville spring stack.

Advantages:

- **Design Modularity:** The compact, annular nature of disc springs allows for seamless integration into existing clutch baskets with minimal modifications to the housing or shaft assembly.
- **High Power Density:** Belleville washers provide an exceptionally high load-carrying capacity within a minimal axial envelope, significantly outperforming traditional helical springs in space-constrained applications.
- **Universal Application:** Due to the standardized sizing of disc springs, this mechanism is highly adaptable and can be retrofitted into various Limited Slip Differential (LSD) configurations with ease.

Disadvantages:

- **Non-Linear Response:** Precise tuning of engagement timing is challenging due to the characteristic non-linear load-deflection curve of conical springs, which may result in abrupt engagement or inconsistent response times.
- **Fatigue and Durability:** Sustaining the required clamping forces necessitates high spring rates. Operating in these high-stress environments increases the risk of material fatigue or hydrogen embrittlement, potentially leading to cracking over extended duty cycles.

Technical Summary: The design proposes a dual-material Belleville washer that acts as both the spring and the friction interface. By utilizing low-friction curved edges for the 'open' state and a high-friction central band for the 'compressed' state, the mechanism achieves passive engagement based on axial load. While this saves considerable space, the primary hurdles remain the specialized manufacturing of the friction gradients and the need for a dedicated housing to manage the unconventional plate geometry.

14.1.4 Split Hub with springs (Concept 5)

Working principles: In this concept the hub has been split and the NFCP and HFCP is placed on each side of the hub as shown in figure 14.4. In between the hub parts a spring is placed, and when the NFCP is pressed the spring will prevent the pressure from reaching the HFCP until a specific force threshold. When the force exceeds that threshold the pressure can reach the HFCP.

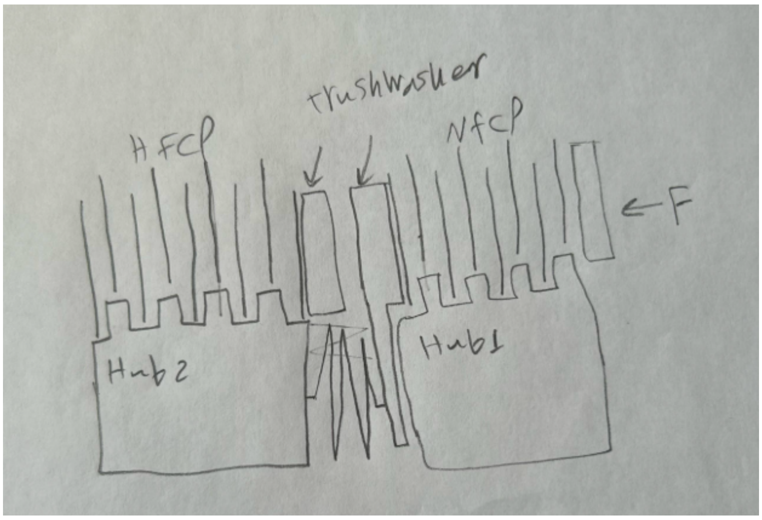

Figure 14.4: A schematic figure for the split hub with springs

Advantages:

- **Precision Activation Threshold:** This design offers superior control over the specific pressure point at which the HFCP engages, as there is larger distance to place the springs.
- **Rapid Engagement:** The direct mechanical linkage provided by the solid thrust washers ensures a near-instantaneous response time once the pressure threshold is breached, providing a crisp engagement feel.
- **System Rigidity:** The use of solid thrust washers provides high structural rigidity during the torque transfer phase. Unlike purely elastic interfaces, this rigidity ensures consistent pressure distribution across the clutch plates.

- **Versatile Design:** The fundamental mechanical principle is highly adaptable and can be integrated into several different Limited Slip Differential (LSD) Architecture with scalable force requirements.

Disadvantages:

- **Mechanical Complexity:** The requirement for a multi-piece split hub, precision-machined thrust washers, and calibrated spring seats results in a high part count and a complex internal assembly procedure.
- **High Manufacturing Cost:** Implementation is relatively capital-intensive, as it necessitates significant geometric modifications to multiple core components within the LSD housing and carrier.
- **Precision Tolerances:** Maintaining the axial alignment and synchronization of the split hub sections requires exceptionally tight machining tolerances to prevent binding and ensure long-term mechanical reliability.

Technical Summary: This concept utilizes a split hub design, with the NFCP and HFCP positioned on opposite sides of the hub and separated by a spring mechanism. The spring prevents pressure transfer to the HFCP until a predefined force threshold is exceeded, enabling controlled activation.

14.1.5 Extended Piston Architecture (Concept 6)

Working principles: This concept features a fundamental redesign of the primary hydraulic piston, incorporating a secondary extension or "tiered" profile. The assembly is engineered for a synchronized two-stage engagement: as hydraulic pressure increases, the primary face of the piston first overcomes a spring set acting on the Normal-Friction Clutch Pack (NFCP). Upon reaching a predetermined travel distance, the piston's secondary tiered extension makes physical contact with an intermediary mechanism situated between the packs. This direct contact bypasses the initial spring rate, transferring the full magnitude of the hydraulic force to engage the High-Friction Pack (HFCP). A schematic figure of this concept is shown in figure 14.5.

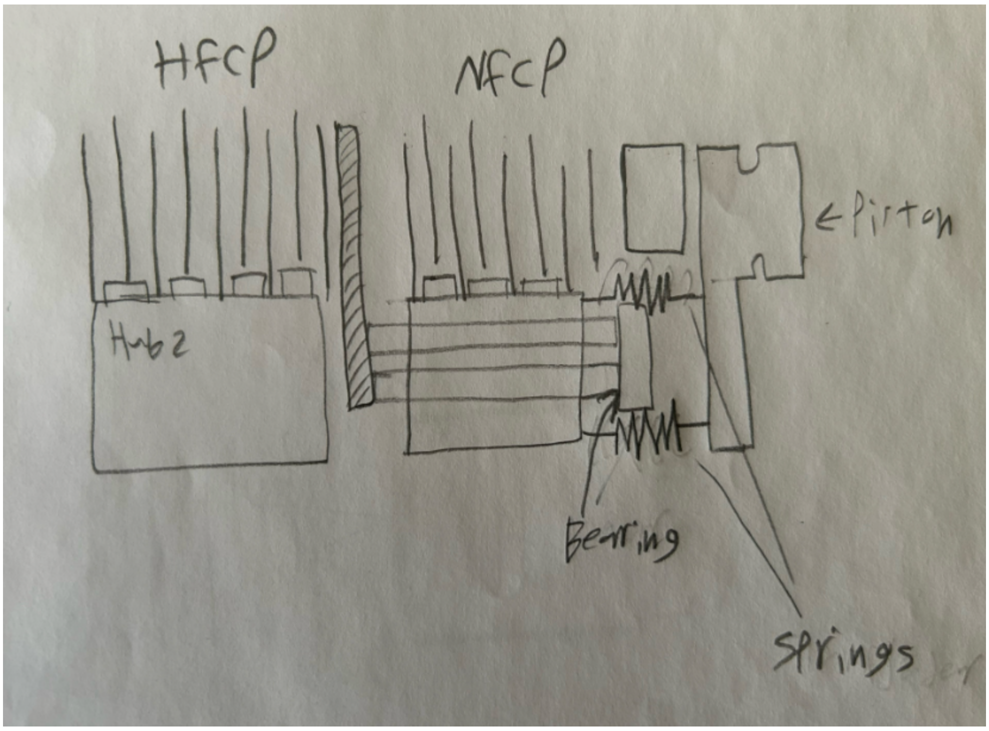

Figure 14.5: Schematic figure of Extended Piston Architecture

Advantages:

- **Dynamic Response:** By leveraging the primary hydraulic actuator directly, the system ensures rapid engagement with minimal mechanical hysteresis or lag between stages.
- **Structural Integrity:** The design is exceptionally rigid, capable of transmitting the maximum rated force of the hydraulic system without the structural deflection or alignment issues often associated with smaller auxiliary mechanisms.
- **System Stability:** It utilizes the existing hydraulic circuit and control logic, avoiding the requirement for complex fluid routing changes or additional proportional valves.

Disadvantages:

- **Extensive Redesign:** Implementation requires a significant overhaul of the differential's internal geometry and the integration of multiple precision-machined intermediary components.
- **High Manufacturing Cost:** The geometric complexity of a tiered piston, combined with the required intermediary hardware, results in a significantly higher unit cost compared to simpler spring-based concepts.

- **Limited Compatibility:** Due to its specific dimensional and stroke requirements, this design is difficult to standardize across different Limited Slip Differential (LSD) housing envelopes or varying brand architectures.

Technical Summary: The "Extended Piston" design introduces a dual-action hydraulic interface that sequences engagement through mechanical travel. By utilizing a tiered piston geometry, the system provides a modulated "soft-start" on the NFCP before locking the HFCP with the full force of the main actuator. While this offers superior rigidity and response times, the trade-off involves high architectural complexity and increased production costs, positioning it as a premium, application-specific solution.

14.1.6 Dual-Piston Independent Actuation (Concept 7)

Working principles: This architecture introduces a secondary, independent hydraulic piston positioned concentrically or adjacent to the main LSD shaft. Moving away from passive spring-based engagement, this design utilizes active control. By incorporating a dedicated hydraulic cavity and an auxiliary control valve, fluid can be diverted to actuate the secondary piston independently. This piston bypasses the NFCP entirely, acting directly upon the HFCP engagement mechanism to provide targeted locking torque.

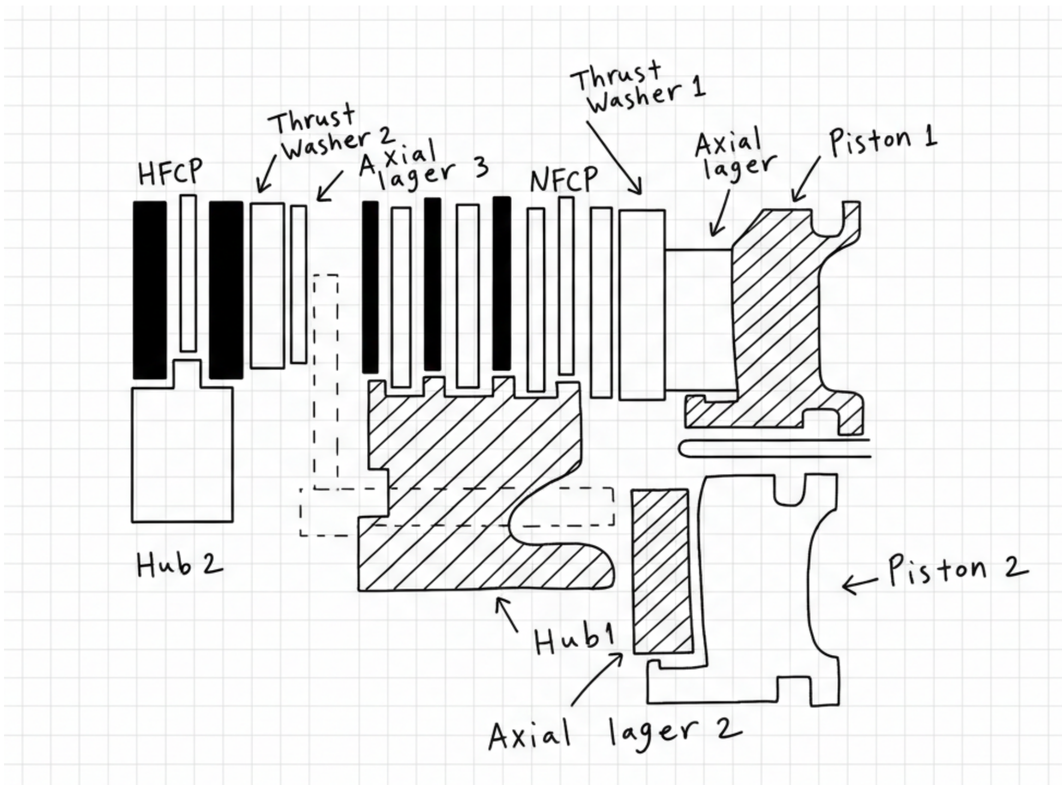

Figure 14.6: Image of a dual-piston hydraulic clutch actuator layout

Advantages:

- **Precision Control:** The ability to independently modulate the engagement of each clutch pack allows for fully customizable torque distribution profiles based on real-time sensor data.

- **Maximum Force Transmission:** High structural rigidity is maintained, as full system pressure can be directed to either pack without being throttled or damped by intermediate springs.

- **Direct Actuation:** By bypassing the NFCP, the secondary piston ensures the high-friction pack can be engaged without pre-loading the low-friction pack, offering superior tactical flexibility in varying driving conditions.

Disadvantages:

- **Hydraulic Complexity:** Implementation requires a major overhaul of the internal hydraulic circuitry, including new galleries, high-pressure seals, and the integration of a secondary proportional control valve.

- **Increased Production Cost:** The addition of a second piston assembly and specialized valving significantly increases manufacturing time, material costs, and assembly complexity.

- **Space Constraints:** Integrating a secondary hydraulic cavity and piston assembly significantly increases the axial and radial footprint of the differential internals, challenging standard packaging limits.

Technical Summary: The "Dual-Piston" configuration transitions the LSD from a passive, load-dependent system to an active, electronically-controlled hydraulic system. By utilizing separate pistons for the NFCP and HFCP, the design offers unparalleled controllability and rigidity. However, the requirement for a split-hub assembly and a complex hydraulic manifold positions this as a high-end solution necessitating a complete redesign of the differential's internal architecture.

14.1.7 Separate Hubs with Compression Bushing (Concept 8)

Working principles: This concept introduces a decoupled hub architecture where the NFCP and HFCP are mounted on distinct hub sections, isolated by a specialized compression bushing. This allows the NFCP to rotate independently of the HFCP during the initial phase of engagement. As axial pressure increases, the bushing undergoes calibrated axial compression. Once the bushing reaches its limit, the hubs synchronize and lock together, facilitating full torque transfer through the HFCP. In other words, this concept rewrites the problem from activation of two clutch packs to another problem which is engaging two gears.

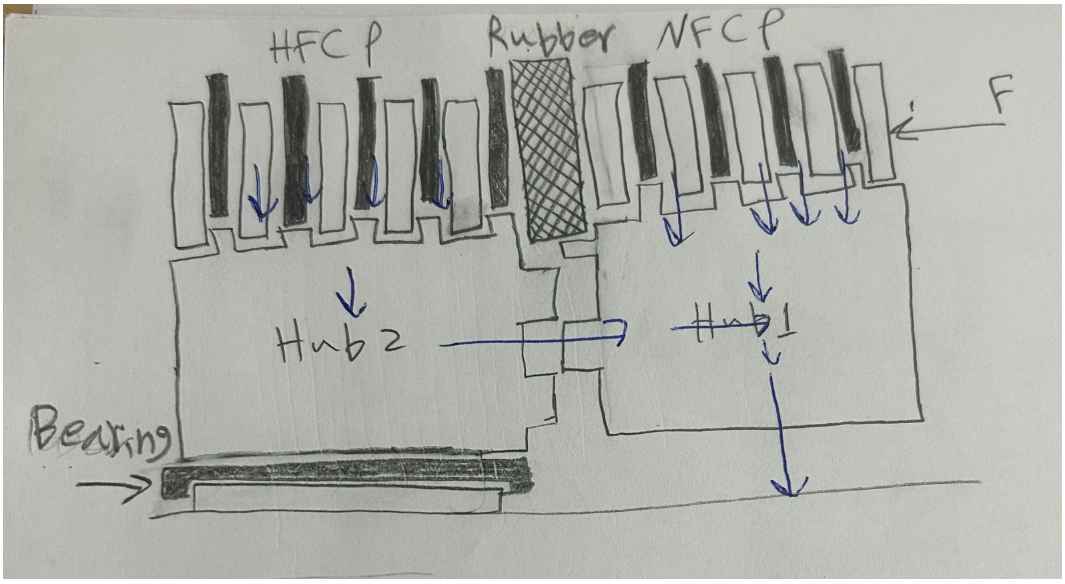

Figure 14.7: Schematic drawing Separate Hubs with Compression Bushing.

Advantages:

- **Mechanical Decoupling:** The ability for the NFCP to spin independently provides smoother engagement transitions and superior thermal management during low-load slip conditions.
- **Cost-Effective Simplicity:** Despite the split-hub design, the mechanism adds very few physical components, keeping production costs relatively low compared to active systems.
- **Broad Adaptability:** The concept is versatile and can be integrated into various LSD platforms with only minor modifications to the core housing and hub splines.

Disadvantages:

- **Synchronization Lag:** The time required for the hubs to align and synchronize can lead to a delayed engagement "hit," which may be difficult to calibrate for high-performance applications.
- **Fluid Contamination:** As the compression bushing wears, particulate matter may shed into the differential oil, potentially shortening the service life of bearings and friction interfaces.
- **Performance Degradation:** Material fatigue or permanent set (deformation) of the bushing will directly alter the engagement threshold, leading to inconsistent locking behavior over the unit's lifecycle.

Technical Summary: The ”Separate Hub” design utilizes an elastic bushing to manage the transition between friction packs. By allowing independent rotation between the NFCP and HFCP hubs, the system achieves a modular engagement feel. However, the engineering focus remains on the durability of the bushing material, as its wear characteristics are the primary factor in both oil cleanliness and the long-term consistency of the LSD functionality.

14.1.8 Nested Concentric Piston with Transmission Shafts (Concept 9)

Working principles: This design utilizes a dual-stage concentric piston assembly engineered to respond to varying hydraulic pressure levels through a sequenced stroke. The primary piston movement handles the initial engagement of the Normal-Friction Clutch Pack (NFCP). Upon a further increase in hydraulic pressure, a secondary nested element telescopically extends. This extension makes physical contact with cylindrical transmission shafts positioned strategically between the disc teeth; these shafts travel through the assembly to compress and engage the High-Friction Clutch Pack (HFCP) directly.

Advantages:

- **Instantaneous Response:** Force is derived directly from the main hydraulic actuator for both clutch packs, effectively eliminating the mechanical lag typically associated with secondary spring sets or ramp-based systems.
- **Cost-Efficient Integration:** While the piston itself is a specialized component, the overall mechanism remains relatively simple, avoiding the requirement for a secondary hydraulic circuit or complex valve blocks.
- **Design Versatility:** The architecture is sufficiently compact to be adapted for various Limited Slip Differential (LSD) housings without requiring a comprehensive overhaul of the differential casing.

Disadvantages:

- **Piston Complexity:** The manufacturing of a high-precision, multi-stage concentric piston requires exceptionally tight tolerances and advanced sealing solutions to prevent internal pressure ”cross-talk” or leaks.
- **Structural Rigidity Concerns:** Transmitting high clamping forces through small cylindrical shafts may introduce ”point-loading” stresses on the disc teeth, potentially compromising the long-term alignment and rigidity of the clutch pack.

- **Component Wear:** The contact interface between the telescopic piston elements and the transmission shafts represents a high-stress zone susceptible to galling, surface fatigue, or mushrooming over extended duty cycles.

Technical Summary: The "Nested Concentric" approach employs a telescopic piston to achieve sequenced actuation. By utilizing the piston's secondary stroke to drive transmission pins directly into the HFCP, the design achieves the performance characteristics of a dual-circuit system while maintaining the simplicity of a single hydraulic line. The primary engineering challenges lie in the precision machining of the nested piston assembly and ensuring the load-bearing cylinders do not undergo plastic deformation under peak clamping pressures.

14.1.9 Dual Hydraulic Cavity and Secondary Piston (Concept 10)

Working principles: This architecture introduces an auxiliary hydraulic cavity and a secondary piston integrated directly as a force interface between the NFCP and HFCP. Unlike passive, load-dependent systems, this design utilizes an active control strategy facilitated by a dedicated hydraulic line routed through the housing to actuate the secondary piston independently. This configuration allows the pump and control unit to modulate the engagement of each clutch pack based on real-time vehicle dynamics and sensor feedback, rather than relying on a preset spring threshold.

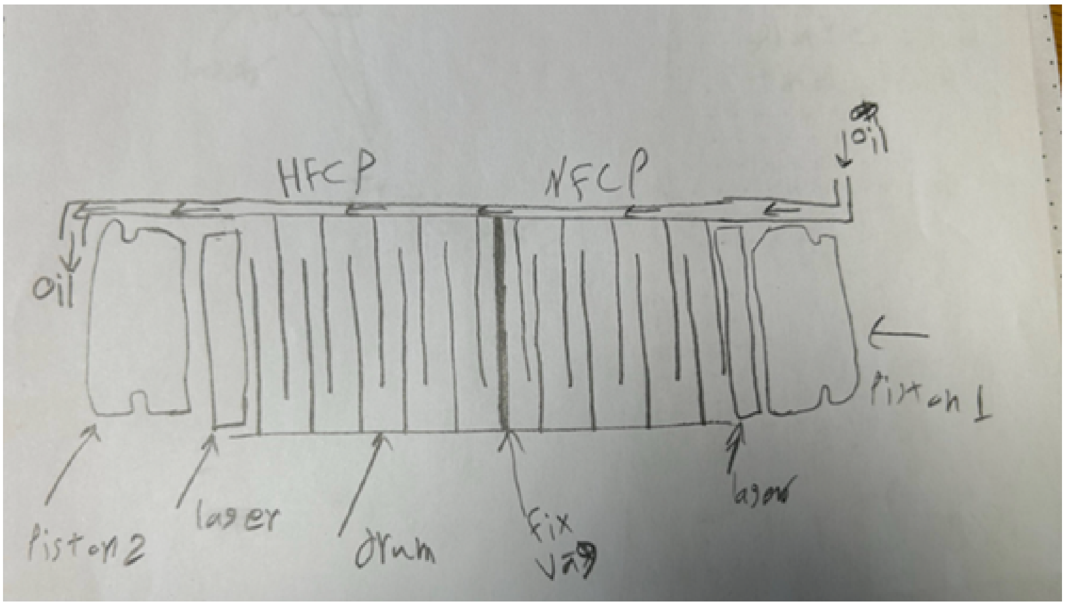

Figure 14.8: Schematic drawing of the Hydrostatic Bearing Interface concept.

Advantages:

- **Total Engagement Autonomy:** The primary benefit is the ability to control each clutch pack independently, enabling highly sophisticated torque-vectoring strategies and precision traction management tailored to specific driving modes.
- **Rapid Actuation:** By utilizing direct hydraulic pressure for both friction packs, the system achieves near-instantaneous response times compared to passive designs that require overcoming spring preloads or mechanical ramp friction.
- **Infrastructure Leverage:** The system utilizes the existing high-pressure pump and fluid reservoir, ensuring the core power source remains consistent while expanding the actuator's functionality.
- **High Scalability:** The logic of the dual-cavity actuation can be scaled and adapted to various Limited Slip Differential (LSD) sizes and torque ratings across different vehicle platforms.

Disadvantages:

- **Engineering Complexity:** Routing high-pressure hydraulic lines through rotating components, such as the differential carrier, requires specialized rotary unions or advanced fluid transfer seals. This represents a significant technical hurdle regarding sealing longevity and pressure maintenance.
- **Spatial Constraints:** The addition of a second hydraulic cavity and piston significantly increases the internal volume required, which may exceed the axial and radial dimensions of standard, mass-produced differential housings.
- **Financial Investment:** The unit cost is high due to the precision machining required for new internal fluid galleries and the addition of complex proportional control valves to the hydraulic manifold.

Technical Summary: The "Dual Hydraulic Cavity" design transforms the LSD into a fully active system. By providing a dedicated pressure path for each friction pack, the design offers the highest level of controllability and response in the selection. However, the specialized engineering required to manage fluid delivery to rotating parts, combined with the increased physical footprint, makes this a high-cost, high-performance solution that necessitates a complete redesign of the internal housing architecture.

14.1.10 Hydrostatic Bearing Interface (Concept 11)

Working principles: This concept utilizes a hydrostatic bearing as a pressure-regulated intermediary between the NFCP and the HFCP. As the hydraulic piston compresses the NFCP, a calibrated portion of the fluid pressure is diverted into a dedicated bearing assembly. Once the internal pressure within the bearing reaches a specific design threshold, it functions as a fluid-link actuator, expanding axially to transfer the clamping force directly to the HFCP. A schematic figure of this concept is shown in figure 14.9.

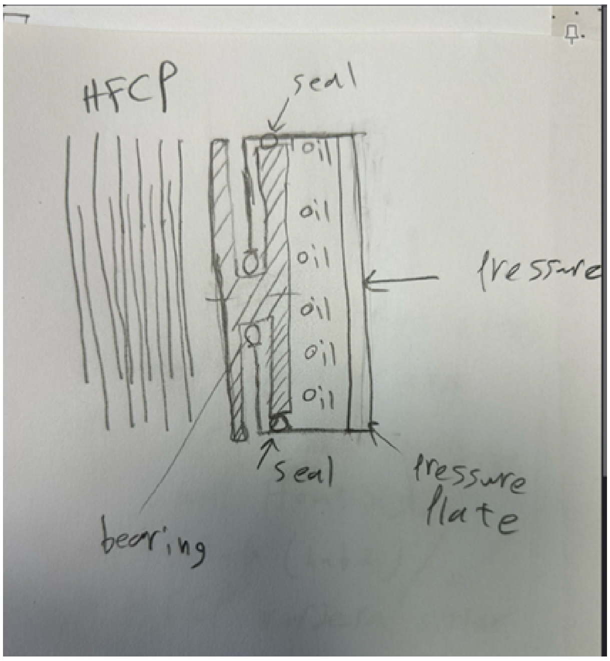

Figure 14.9: A Schematic drawing of the Hydrostatic Bearing Interface concept.

Advantages:

- **Universal Application:** The self-contained nature of the hydrostatic interface allows for integration into various Limited Slip Differential (LSD) designs without requiring massive architectural overhauls of the carrier or housing.
- **Cost-Effectiveness:** Compared to the addition of secondary electronic valves or complex nested pistons, a fluid-pressure bearing is relatively inexpensive to manufacture and maintain.
- **Simplified Assembly:** The mechanism is designed for modular mounting within the existing clutch stack, requiring minimal specialized tooling or complex assembly sequences.

Disadvantages:

- **Hydraulic Latency:** The response time may be difficult to optimize, as the system relies on physical fluid displacement and pressure buildup within the bearing chamber before the HFCP engages.
- **Spatial Claims:** Hydrostatic bearings require a specific internal volume to function effectively; finding sufficient axial space within a standard, compact differential housing remains a significant engineering challenge.

- **Pressure Calibration:** Ensuring a consistent and repeatable "switch" point between the NFCP and HFCP requires extremely tight tolerances on fluid seals and flow-control orifices to prevent premature engagement or pressure leakage.

Technical Summary: This concept employs a hydrostatic bearing as a pressure-controlled intermediary between the NFCP and HFCP. When pressure is applied to the NFCP, a portion of the hydraulic fluid is directed into the bearing assembly. Once the fluid pressure reaches a predefined threshold, the bearing expands axially and transfers the clamping force to the HFCP.

14.1.11 Flexible Bushing Mechanism (Concept 12)

Working principles: This concept features a high-capacity flexible bushing situated as a load-gated interface between the Normal-Friction Clutch Pack (NFCP) and the High-Friction Clutch Pack (HFCP). This bushing is engineered from high-durometer elastomers or reinforced polymers designed to withstand significant axial force without initial deformation. Upon reaching a critical pressure threshold, the bushing undergoes a rapid, non-linear axial compression (buckling or collapsing), allowing the entirety of the hydraulic force to be transferred directly to the HFCP for full engagement.
Advantages:

- **Architectural Simplicity:** The design is inherently straightforward, avoiding the complexities of secondary hydraulic lines, multi-stage pistons, or additional valving.
- **Ease of Integration:** The bushing can be easily positioned within existing clutch stacks with virtually no changes to the internal hub or carrier tooling.
- **Cost-Effectiveness:** The component is inexpensive to produce in high volumes compared to active hydraulic actuators or precision-machined mechanical linkages.
- **High Versatility:** This mechanism can be retrofitted or added to several different types of Limited Slip Differentials (LSDs) as a simple modular upgrade.

Disadvantages:

- **Structural Rigidity:** The inherent elasticity of the material is a primary disadvantage, potentially leading to a "soft" or "spongy" engagement feel and less precise torque modulation compared to rigid mechanical links.
- **Elastic Fatigue:** The material is subject to fatigue and thermal degradation over time. This leads to a shortened lifecycle and inconsistent engagement thresholds as the polymer's material properties shift under constant duty cycles.

Technical Summary: The "Flexible Bushing" design serves as a passive force-gate between the two clutch packs. By utilizing a high-force elastic threshold, it ensures the HFCP only engages when the system pressure is sufficient to fully collapse the bushing. While it offers a low-cost and highly adaptable solution for modular LSDs, the trade-offs include reduced system rigidity and long-term durability concerns due to the fatigue and thermal characteristics of the elastic material.

14.1.12 Concept 14: Separation ring with spiral groove

Working principles: This concept consists of a plate positioned between the NFCP and the HFCP. The plate is mounted on a spiral groove integrated into the drum. When a difference in rotational velocity between the drum and the plate is introduced, the drum rotation causes the plate to rotate relative to the groove geometry. Due to the shape of the spiral groove, this rotational motion is converted into an axial displacement of the plate. As the plate moves axially, it comes into contact with and engages the HFCP. To create the required difference in rotational velocity, a method similar to the one used in Concept 15 can be applied.

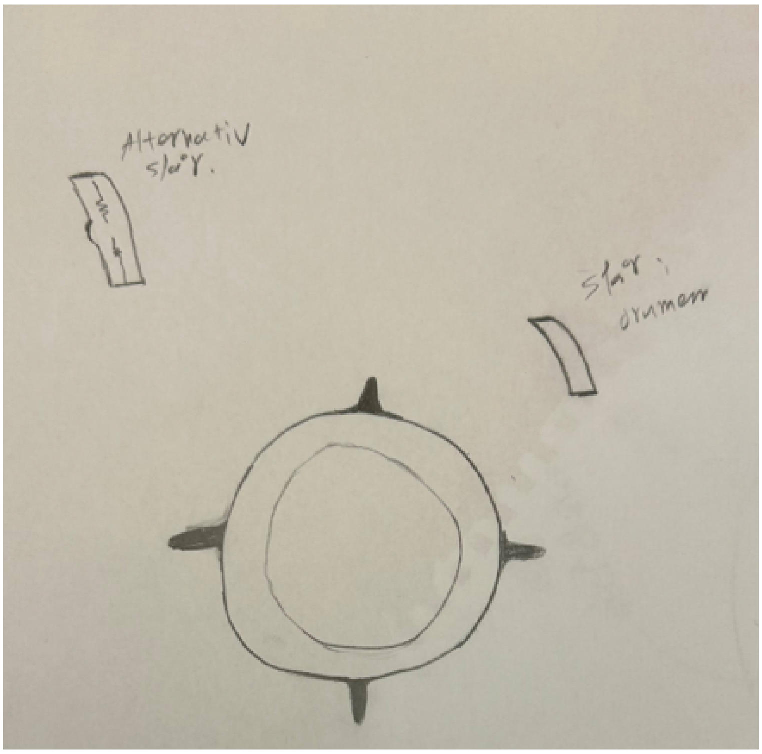

Figure 14.10: Schematic drawing of Separation ring with spiral groove concept.

Advantages:

- **Small axial distance:** The concept requires very little additional axial space, since the only necessary distance between the NFCP and HFCP is the space needed for the clutch plates.

- **Simple working principle:** The operating mechanism is relatively straightforward, making the concept easier to understand, implement, and potentially maintain.
- **Good performance and controllability:** The concept offers smooth and seamless activation/deactivation of the HFCP, which can improve overall system response and driving performance.

Disadvantages:

- **Design modifications required:** The concept cannot be implemented directly into the existing design and therefore requires multiple structural and functional changes for the housing and the drum.
- **Potential increase in manufacturing complexity:** The added components and modifications may increase manufacturing difficulty, assembly time, and production cost.

14.1.13 Stair Plate Activation Mechanism (Concept 16)

Working principles: This concept utilizes a stepped or "stair" profile machined directly into the differential drum to facilitate a robust mechanical lock between the High-Friction Clutch Pack (HFCP) and the Normal Friction Clutch Pack (NFCP). The core component is a specialized flex plate featuring triangular geometric protrusions designed to interface with the drum's keyed geometry.
Operational Logic:

1. **Axial Movement:** The hydraulic piston applies a forward force to the flex plate.
2. **Climbing Phase:** The triangular protrusions on the plate "climb" through corresponding stair-shaped openings in the drum.
3. **Rotational Engagement:** A secondary mechanism (potentially electronic) provides a horizontal/rotational shove to the plate.
4. **Mechanical Lock:** By pushing the triangular figures to the side of the "stair" opening, the mechanism creates leverage that holds the plate firmly in place, even under extreme pressure.
5. **Centering:** The rotational mechanism ensures the plate remains centered during standard piston movement to prevent premature engagement.

Advantages:

- **Positive Locking:** Provides a physical, mechanical lock rather than relying solely on friction or spring pressure.
- **High Pressure Capacity:** The stair design allows the assembly to withstand significantly higher axial forces once locked.
- **Spatial Efficiency:** The mechanism is integrated into the drum and plate geometry, making it highly space-efficient.
- **Design Continuity:** Requires only minor modifications to the overall LSD architecture.

Disadvantages:

- **Secondary Actuation:** Requires an additional rotational mechanism, which may need electrical control, increasing system complexity.
- **Structural Modification:** Necessitates precision machining of stair-shaped openings within the drum housing.

Technical Summary: The "Stair Plate" mechanism moves away from passive spring-based sequencing to a positive mechanical interlock. By using the drum as a keyed interface for the plate's triangular teeth, the system can "step" into a locked state that resists high-pressure blow-back. While it offers superior load-holding and compact packaging, the requirement for an active rotational actuator adds a layer of electronic and mechanical complexity not found in simpler bushing or ramp designs.

14.2 Appendix B - Result of the Screening and Scoring

14.2.1 The Result of the Screening

	Concepts:																
Selection Criteria	1	2	3=REF	4	5	6	7	8	9	10	11	12	13	14	15	16	17
Simplicity	0	1	0	1	-1	-1	-1	-1	0	-1	1	1	0	0	-1	-1	1
Safety	-1	-1	0	1	1	-1	1	-1	-1	-1	1	-1	1	0	0	-1	1
Size	0	0	0	1	1	1	1	0	0	1	0	1	0	1	1	1	-1
Rigidity	0	-1	0	1	1	-1	1	0	1	0	1	0	1	0	1	0	0
Repeatability	0	-1	0	0	0	0	1	-1	-1	-1	-1	-1	0	0	0	-1	0
Manufacturability	1	-1	0	-1	0	-1	-1	-1	-1	-1	0	0	0	1	1	1	1
PLUSES	1	1	0	4	3	1	4	0	1	1	3	2	2	2	3	2	3
SAMES	3	1	0	1	2	1	0	2	1	1	2	2	4	4	2	3	1
MINUSES	1	4	0	1	1	4	2	4	3	4	1	2	0	0	1	3	1
NET	-1	-3	0	3	2	-3	2	-4	-2	-3	2	0	2	2	2	-1	2
RANK	4	6	3	1	2	6	2	7	5	6	2	3	2	2	2	4	2
CONTINUE	NO	NO	yes	yes	yes	NO	yes	NO	NO	NO	yes	yes	yes	Yes	Yes	No	Yes

Figure 14.11: The result of the screening evaluation.

14.2.2 The Result of the Scoring

Selection Criteria	Key Parameters	Weight	3		4		5		7		11		12		13		14		15		16		17	
			Rating	Weighted	Rating	Weighted	Rating	Weighted	Rating	Weighted	Rating	Weighted	Rating	Weighted	Rating	Weighted	Rating	Weighted	Rating	Weighted	Rating	Weighted	Rating	Weighted
Simplicity	Number of parts	1	7		8		6		4		5		7		4		8		6		8		6	
	Modification	1	8		8		3		4		8		7		7		6		6		6		6	
	Cost	1	8		8		4		3		4		7		7		7		7		7		7	
Performance	Torque loss:	1	5		5		5		9		4		2		8		9		9		9		9	
	Activation/Deactivation Time	1	5		5		5		9		3		2		7		7		9		7		9	
	Hold Time	1	5		5		5		9		3		2		7		9		9		6		9	
Safety	Cycle Life	1	5		5		7		9		5		2		9		8		8		8		8	
	Safety Margin	1	5		5		7		9		5		2		9		5		4		5		4	
Size	Axial Length	1	5		8		6		9		6		6		4		9		9		5		9	
	Radial Length	1	5		8		6		7		7		6		7		5		5		5		5	
Rigidity	Moveable parts	1	5		7		5		6		6		7		6		7		6		7		8	
	Structural stability	1	5		7		8		6		6		3		9		8		7		8		7	
	Deflection	1	5		7		8		6		6		3		9		7		7		7		7	
Repeatability	Hysteresis	1	5		6		5		5		6		3		9		7		7		7		9	
	Fatigue of parts	1	5		5		8		5		5		3		9		7		7		7		8	
Manufacturability	Tooling change	1	5		8		5		4		4		7		8		8		8		5		8	
	Modification of critical parts	1	5		8		4		5		8		7		9		5		5		5		7	
	Realization	1	5		7		5		4		1		4		9		9		9		6		9	
NET			98		120		102		113		92		80		137		131		128		118		135	
RANK			6		4		5		2		7		6		1		2		3		2		3	
CONTINUE			no		yes		no		no		no		no		yes		no		yes		no		yes	

Figure 14.12: The result of the scoring evaluation.

14.3 Appendix C - Project time plan

14.3.1 Project plan Preliminary vs Actual

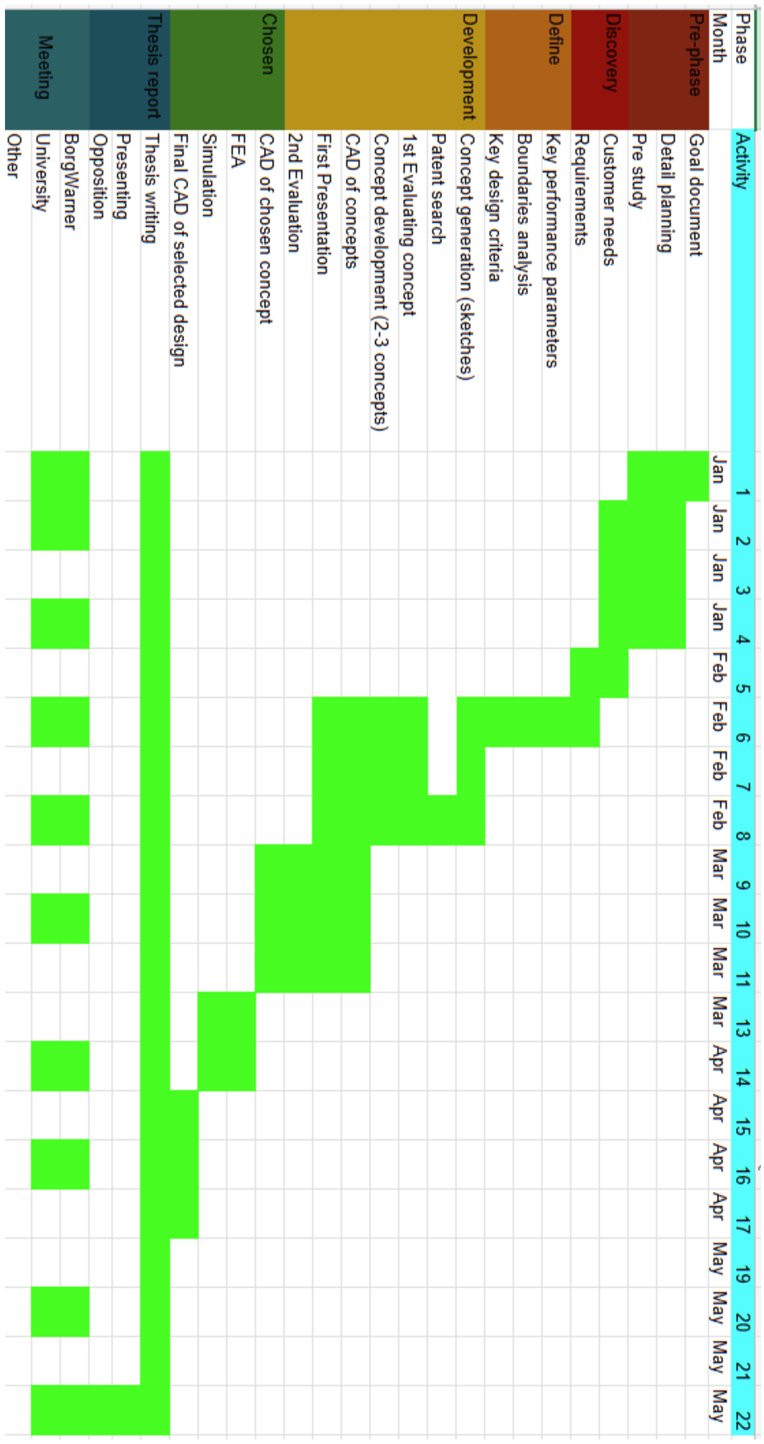

Figure 14.13: The preliminary time plan of the project

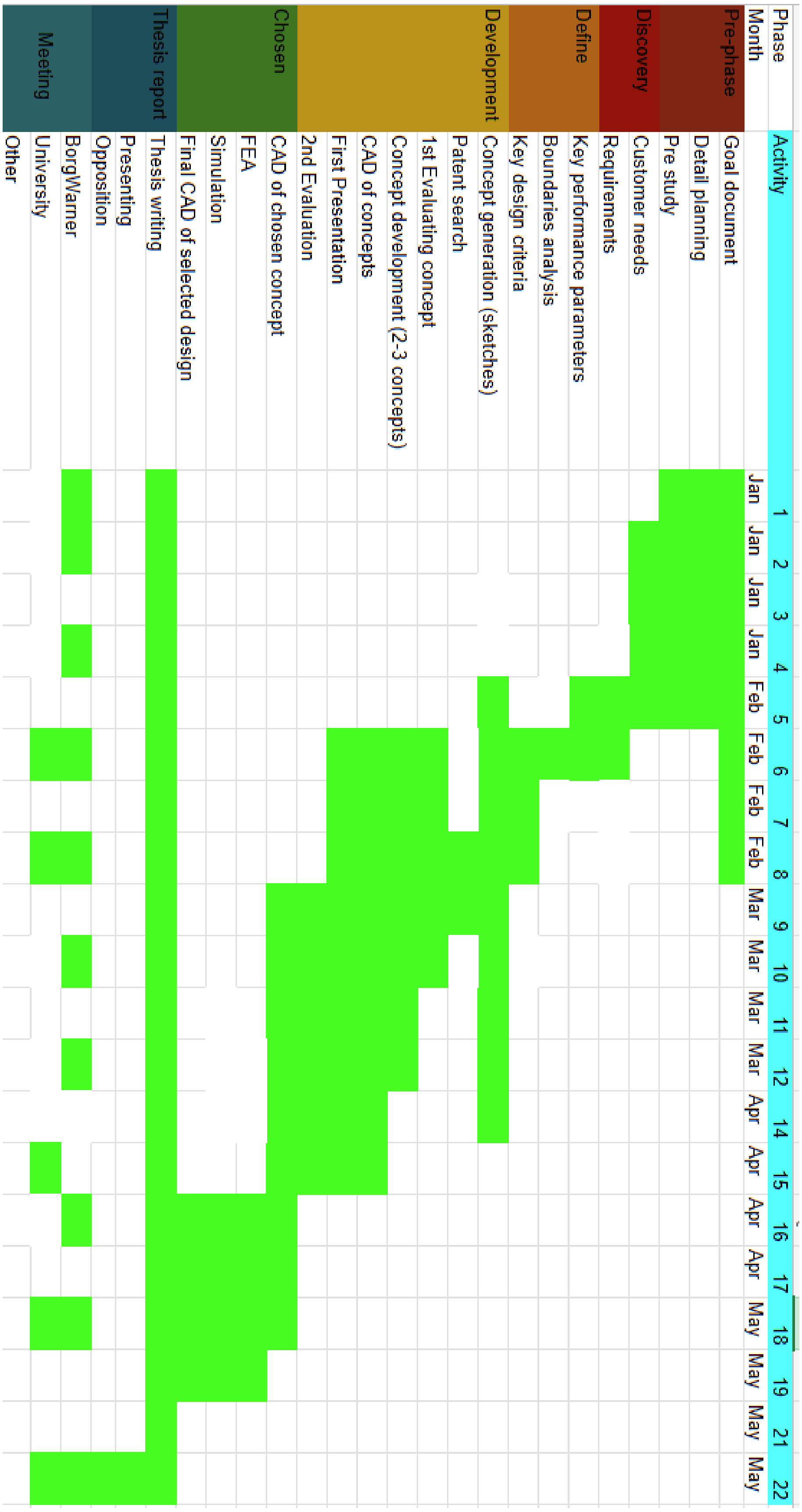

Figure 14.14: The actual time plan of the project